AN APPROACH TO DETERMINE THE THERMAL CONDUCTIVITY AND DIFFUSIVITY OF A ROCK IN SITU

By

ATA-UR-REHMAN CHOUDHARY

Bachelor of Science
University of Karachi
Karachi, Pakistan
1963

Master of Science
University of Karachi
Karachi, Pakistan
1964

Master of Science in Petroleum Engineering
University of Texas-Austin
Austin, Texas
1969

Submitted to the Faculty of the Graduate College
of the Oklahoma State University
in partial fulfillment of the requirements
for the Degree of
DOCTOR OF PHILOSOPHY
December, 1976

December 30, 1976

AN APPROACH TO DETERMINE THE THERMAL

CONDUCTIVITY AND DIFFUSIVITY

OF A ROCK IN SITU

Thesis Approved:

Roger J. Schoeppel
Thesis Adviser

W. Josh Allison

Douglas C. Kent

Herbert A. Pohl

Allen M. Rowe

Norman N. Durham
Dean of the Graduate College

ACKNOWLEDGEMENTS

I wish to express my appreciation to Dr. R. J. Schoeppel for his continual guidance in pursuing this interdisciplinary research effort and for acting as Chairman of the advisory committee.

To the other members of my committee, Dr. H. J. Allison, Dr. A. M. Rowe, Dr. H. A. Pohl and Dr. D. C. Kent, I wish to express special thanks for their guidance and invaluable suggestions during all phases of this study.

It has been my good fortune to have had many good teachers. I wish to acknowledge the role that these teachers played in helping me achieve this objective.

I would like to thank Mr. R. D. Cocanower of Western Logging Company, Mr. Foley Wright and engineering staff of Atlantic Richfield Oil Company for providing me with the pertinent data used in this study.

I wish to thank my colleagues and friends who helped me in the completion of this study, and finally, I want to express my special gratitude to members of my family for their constant encouragement, understanding, and many sacrifices during the course of my graduate studies.

TABLE OF CONTENTS

Chapter Page

LIST OF TABLES

LIST OF FIGURES

NOMENCLATURE

A	- constant, dimensionless
a	- radius of the sample from its center to the thermocouple edges, inches
B_n	- roots of the Bessel function
C, C_1, C_2	- constants, dimensionless
C_f	- specific heat at constant pressure, Btu/lb, ^oF
D	- constant, dimensionless
D_e	- depth of the well bore, ft
E	- constant, dimensionless
E_i	- exponential integral
F	- formation factor, dimensionless
G	- constant, dimensionless
G_t	- temperature gradient, ^oF/100 ft
h	- rate of sample heating Btu/hr
J_o, J_1	- first kind - zero order, and first kind - first order Bessel functions, respectively
K	- thermal conductivity of rock composite Btu/hr-ft, ^oF
K_1	- thermal conductivity of medium, water, air, oil, etc., Btu/hr-ft, ^oF
K_2	- thermal conductivity of rock solids, Btu/hr-ft, ^oF

K_{m_t} - normalized thermal conductivity of mixture (solids + liquid) Btu/hr-ft, ^{o}F

K_{m_e} - normalized electrical conductivity of mixture (solids + liquid), $(Ohm\text{-}meter)^{-1}$

K_{s_e} - normalized electrical conductivity of rock solids $(Ohm\text{-}meter)^{-1}$

K_{s_t} - normalized thermal conductivity of rock solids Btu/hr-ft, ^{o}F

M - intermediate constant $1/ft\text{-}^{o}F$

m - cementation factor, dimensionless

p_o - porosity, dimensionless

Q, Q_1, Q_2 - rate of heat flow, Btu/hr-ft

q_D - rate of heat flow, dimensionless

R_1, R_2 - thermal conductivity of rock matrix Btu/hr-ft, ^{o}F

r_w - well bore radius, ft

T_i - initial temperature, ^{o}F

T_s - stabilized temperature, ^{o}F

T_1 - temperature at time number one, ^{o}F

T_2 - temperature at time number two, ^{o}F

T_{mud} - temperature of drilling fluid, ^{o}F

T_n - normalized temperature, ^{o}F

T_o - observed temperature, ^{o}F

T_a - atmospheric temeprature, ^{o}F

T_D - temperature dimensionless

t - time, hours

t_D - time, dimensionless

t_1 - time at first temperature run, hrs

t_2 - time at second temperature run, hrs

v - density of composite rock, lbs/ft^3

W - water saturation, percentage

Z_1, Z_2 - exponential integral series expansion constants

Greek Letters

α - thermal diffusivity of rocks, ft^2/hr

ρ - density of rock, lb/ft^3

ρ_w - density of water, lb/ft^3

ϕ - porosity, percentage

CHAPTER I

INTRODUCTION

The internal thermal regime of the earth is of fundamental importance to geologists and geophysicists alike. It is ironic, however, that in spite of continued research in these fields for the last two centuries, very little is known about the geologic setting of the earth a few miles below its surface. Apparently, part of the problem can be attributed to a lack of reliable experimental data at this depth. It was, perhaps, to gain more knowledge about the subsurface thermal circumstances of the earth that Sir Charles Parsons in 1904 proposed his famous "hellfire exploration project," which involved the sinking of a shaft twelve miles into the earth at a cost of $14 million over a period of eighty-five years (1). However, it was not until the early 1960's that the rudimentary knowledge concerning the deep-seated thermal processes of the earth was first pieced together. This data which led to the formulation of supplementary theories to explain continental drift, the presence of mid-oceanic ridges, and the origin of orogenic forces, became known as a result of investigations of ocean floor movements.

Regardless of its sources of origin the amount of heat that flows from the earth's interior to its surface is relatively small as compared to the heat content received from the sun (1:20,000). The heat which flows from the earth's interior amounts to about 950×10^{15}

BTU/year (2). This heat, when bottled up, often manifests itself along zones of crustal weakness in terms of volcanic erruptions and earthquakes (1, 3). The heat flow from the earth's interior to its surface is not uniform and varies from location to location depending upon lithology and fluid content of the underlying formations. These nonuniformities, in an otherwise uniform heat flow field, have been used to help locate oil and gas reservoirs, deeply buried salt domes, and radioactive deposits (3, 4).

The increasing demand for energy, and the recent pressures stemming from public concern for the environment, have forced an all-out search for clean and economically viable alternatives to conventional fuels. One of the new alternatives is geothermal energy. However, our knowledge of potentially promising reservoirs is limited, because this field of research was hitherto ignored in favor of more readily available and more adequately explored energy resources. With the anticipated shortages of energy in the future, geothermal energy has begun to attract international attention. It is expected that by 1985, geothermal energy will have 132 thousand MW of power generating capacity for the United States alone, which will help save $19 billion annually in imported oil at current oil prices (5, 6).

Two decades ago very little was known about the ecological systems of the earth. However, with the recently increased activity in this field, new facets of the delicate ecological balance are being brought into focus. One ecological facet is the heat balance in the atmosphere surrounding the earth. Meterologists are becoming increasingly concerned about the dangers of heating or cooling the earth's atmosphere either by extraterrestrial or by earthen sources. Heat flow from the

interior of the earth to its surface influences not only the regional but also the global weather patterns through thermohaline, Ekman layer, and transoceanic currents (7). The U. S. Navy in cooperation with the U. S. Meteorological Society has recently undertaken extended research programs to help provide data on the heat flow characteristics of the ocean floor, analyses of which could help predict long term weather changes.

Thermal recovery processes involving conventional in situ combustion and nuclear subsurface explosions will play an increasingly important role in recovering oil from marginal and submarginal oil and gas reservoirs. In order to arrive at reasonably accurate recovery predictions -- to justify financial investments -- accuracy of the input data is important. Thermal conductivity and diffusivity values of the reservoir rocks used in thermal recovery calculations are often not readily available; therefore, if time prohibits experimentation, then speculation is often used in arriving at these values. If these rock properties were readily available, it could save time and expense in making accurate thermal recovery predictions.

In order to obtain earth heat flow values, regardless of the end objectives for which such a study may be used, an accurate knowledge of temperature gradients and thermal conductivities of the underlying formations is required. An early attempt to measure temperature gradients was recorded in 1664 (8). However, no record of these gradients has become available, over a broad area, until a recent AAPG sponsored project to collect and map this information for Canada, the United States, and Mexico was completed at Oklahoma State University (9). If a simple method to obtain the thermal conductivities of the

subsurface rock could be made available, this information would be of value in developing a companion map showing heat flow variations throughout North America. Such a map will be valuable not only in locating hitherto undiscovered oil and mineral resources, but also possibly in providing an example to the developing nations concerning the benefits that can be derived from such a study.

Accurate values for the thermal conductivity and thermal diffusivity of rocks are becoming increasingly important because of accuracy of prediction required in low-grade geothermal energy, ecological studies of the earth, and thermal recovery processes. Published values for these two properties of rocks are quiet diverse even for the same type of rock. A portion of this diversity is due to natural changes inherent in the rocks themselves. The lack of reliable techniques to determine these two properties is more responsible for the wide range of values than is the rock nonhomogeneity. In this study a method is presented from which thermal conductivity and diffusivity of rocks can be obtained in situ without recourse to laboratory measurements.

Definition of the Study

In most heat flow studies reported in the literature, the thermal conductivity and thermal diffusivity of rock samples were determined in the laboratory by using a variety of experimental techniques. The most commonly used instrument for measuring thermal conductivity is the "divided-bar" apparatus. Measurements with this apparatus are reproducible (within one percent) for individual samples but it is doubtful how well they are able to represent the absolute thermal conductivities of rocks in bulk. Benefield (10), for example,

obtained seventy samples from a coarse-grained, apparently petrologically uniform piece of granite and measured the thermal conductivities with a divided-bar apparatus. The thermal conductivity varied between 0.0069 and 0.101 Cal/Cm-Sec-C^{o} ($\pm$ 25% from the mean value). This variation in thermal conductivity results in heat flow calculations which are similarly inaccurate, because, often only single cores from each type of subunit within a formation are cut and their thermal conductivity evaluated for use in the heat flow calculations.

A number of other factors also influence laboratory thermal conductivity measurements. Some of these factors are discussed here to explain why experimentally measured thermal conductivities are not truly representative of the absolute thermal conductivities of rocks in situ.

Variables Affecting Thermal Characteristics of Rocks

Sample Preparation

A considerable degree of machining and smoothing is required to prepare a sample for laboratory thermal conductivity evaluation. The specimens that survive this mechanical process are invariably more coherent and less brittle. The bias introduced undoubtedly results in serious unaccountable errors in the thermal conductivity which in turn affects values of heat flow so determined.

Specimen Size

Another error in thermal conductivity measurement occurs when the specimen size is not large relative to the average size of the

individual crystals. With the divided-bar apparatus commonly used to measure thermal conductivity, individual crystals of monomineralic aggregates of high conductivity tend to short-circuit the heat flow - with the result, that the measured values may be higher than that of a geologically representative rock sample.

Sampling Procedure

Frequently, cores are lost or the depth of their recovery cannot be accurately ascertained. In such cases, it has been expedient to assume that thermal conductivity values from nearby wells are representative and proceed with the determination of the heat flux for the well. When such an approach is used in predicting heat-flow values, the inherent dangers can be imagined, no matter to what degree an educationally sophisticated guess is employed.

Another important variable encountered in sampling is that the drilled holes are seldom vertical. When a rock sample is taken by coring, it may not reflect the actual bedding plane which is most favorable for heat flow.

Habitat

It is difficult to simulate in the laboratory the natural environment which exists at depth within the earth. In the process of coring and subsequent transfer of the core to the surface, irreversible changes occur in the rock's physical characteristics as measured for example by bulk volume, porosity, permeability, and water, oil or gas saturations. These changes are reflected in laboratory-derived

thermal conductivity and diffusivity values, whose accuracy is generally accorded to be no better than $\pm$ 10-15% (11, 12).

Geologic Structure

It is not unusual to find two different published values of heat flux from the same geological location which vary by as much as 40 to 50%. For example, Hyndman and Sass (1966) reported 1.5 and 2.7 microcal/cm^2 heat fluxes for adjacent bore holes near Mt. Isa, Australia. The measurements were made in an area of steeply dipping beds of contrasting thermal conductivities. In this case, it appears the geologic structure was responsible for local variations in the heat flux as was reflected in the above measurements (11).

Some of the foregoing limitations can be resolved by using non-standard laboratory techniques, such as employing drill chips when the rock cores are not available, and/or using petrographic studies for better sample identification. However, it is virtually impossible to eliminate the numerous errors inherent in subsurface rock sampling and laboratory experimentation. It appears most logical, therefore, to attempt to develop a technique of obtaining the thermal conductivities of rocks without recourse to laboratory experimentation and subsurface rock sampling. This could be done if rock thermal conductivity and diffusivity were determined in situ. One such method to obtain the thermal properties is developed in this study.

Study Plan

There are three work phases which can be identified in this study. Each is discussed here briefly.

1. Develop a mathematical model to theoretically predict the thermal conductivity and diffusivity of a rock in situ:

In subsurface drilling, a drill bit is commonly used to penetrate the subsurface rocks. To lubricate the drill bit and to carry rock cuttings to the surface, a drilling fluid consisting of a mixture of clay, water, and other appropriate chemicals is pumped down the drill pipe. Except for the upper portions of a bore hole, the returning drilling fluid is at a lower temperature than the surrounding formation and acts as a heat sink. If circulation is stopped and the mud allowed to stand, its temperature tends to equalize with that of the surrounding rocks. The rate of this temperature-increase is time-dependent and decreases as time increases. The objective of this phase of the study is to mathematically relate this time-temperature behavior to the thermal conductivity and diffusivity of the rock surrounding a bore hole.

2. Test the mathematical model with laboratory and in situ field data:

One way to determine the validity of the mathematical model is by independently comparing its predicted conductivity and diffusivity values with those obtained by conventional methods. Variable time-temperature data of a sufficient quality to evaluate the mathematical approach was needed. After an extensive search, an oil well located in Stephens County, Oklahoma, was found for which the required basic data were available. It not only had time-temperature but also thermal conductivity and diffusivity data available as well. A number of logs had been run between 1930 and 1966 to define lithology, porosity, etc. These were obtained from the Western Logging Company and the Atlantic Richfield Oil Company, for use in this study. The objective of this

second phase of the work was to use this field data in the mathematical model to predict the in situ thermal conductivity and diffusivity. The predicted values could then be compared with the experimental (laboratory) obtained thermal conductivity and diffusivity values to help in determining the validity of the mathematical model.

3. Demonstrate the mathematical model's field applicability by constructing an electrical analog to automatically perform thermal conductivity calculations:

Analog, digital and hybrid computer technology has become very sophisticated in the last decade. Special-purpose small computers are becoming increasingly popular as the means for an instant recording, calculation, and/or relay of information. If a calculation procedure is such that it does not involve extensive storage memory, or trial and error calculations, a small special-purpose computer can quickly provide the needed information. The mathematical approach developed in this study does not require an extensive data storage in its simulation; accordingly, this appears to be an ideal situation where the thermal conductivity of subsurface rocks could be determined from time-temperature data, and recorded along with the temperature on field recorded borehole logs.

Scope of the Study

The approach presented in this study uses the in situ time-temperature data associated with rock formations to calculate their thermal conductivity and diffusivity. The time-temperature data can be easily recorded during routine logging; therefore, to apply this method no laboratory experimentation is required. Accordingly,

this approach proposes to by-pass the subsurface rock coring and sample preparation which are prerequisite to laboratory experimentation. Because of the time and effort involved, such "experimental" thermal conductivity and diffusivity values are often quite expensive. This approach, by eliminating the laboratory experimentation phase currently practiced, may potentially provide thermal property data more cheaply and expediently.

The experimentally derived thermal conductivity and diffusivity values are often inaccurate because of the bias introduced during coring, sample preparation, and because of changes in habitat of the rock specimens. This approach, by virtue of the in situ time-temperature data used in the mathematical model, potentially offers to provide thermal conductivity and diffusivity data which more realistically reflect the heat flow characteristics of rocks in situ.

It should be realized that application of the model will be limited to those cases where the transient temperature data accurately reflects the heat transfer from the formation into the well bore. For example, in cased wells, usually some cementing is done to hold the casing in place, to seal-off fresh water zones, or to prevent migration of oil and gas. Freshly poured cement undergoes exothermic reactions while setting. The heat thus released modifies the transient temperature data. This circumstance could only realistically be analyzed if the mathematical model were adjusted to account for the heat release upon chemical reaction.

Similarly measured rock face temperatures in producing oil and gas wells do not always reflect their true temperatures, because the oil and gas flowing through the rocks may be undergoing phase change.

Unless a producing well is first shut-in for an appropriate period of time -- to allow the rock formations to come into thermal equilibrium with the fluid in the well bore -- no subsequent time-temperature data should be collected; otherwise the resultant thermal conductivity and diffusivity values will be correspondingly erroneous.

In addition, the application of the approach developed in this study should be limited to those cases where time-temperature data is collected on wells drilled with water or oil base muds. Air drilled holes, for example, unless the well bore is filled with water, do not provide a good heat transfer medium for heat to flow from the formation into the well bore. As a result, time-temperature data collected on such wells may not reflect the true heat flow characteristics of the surrounding rocks.

In the end, it should be noted that in those wells which pass through active acquifer zones, water tends to first migrate horizontally and then flow vertically from the acquifer zone through the well bore into the neighboring strata. This movement of water severly influences the otherwise radial flow of heat into a well bore; hence, the reliability of time-temperature data obtained from such zones is open to question. This factor may be of significance only in open holes. For cased well bores, unless there is water migration around the casing, it can be safely neglected.

Summary

In summary, this study is to be primarily concerned with the development of an in situ method to obtain thermal conductivity and diffusivity of rocks without recourse to laboratory experimentation.

The method developed uses time-temperature data which can be easily collected by using available equipment during routine well logging. The objectives of this study involve the determination of thermal properties of rocks in situ from these data, a test to determine their apparent validity, and the developement of associated necessary instrumentation for field application. The method to be used in achieving these objectives involves the development of a mathematical model as is presented in Chapter III. In order to test the validity of the mathematical model, it will be applied in Chapter IV to a field case where experimentally obtained thermal properties were available for comparison. Equipment for possible field use in application of the technique will be presented in Chapter V.

CHAPTER II

LITERATURE SURVEY

Introduction

An early attempt to report thermal conductivities of some commonly occuring rocks was made in 1878 by a committee of the British Association for the Advancement of Science (13). Keller in 1934, proposed to use thermal conductivities of some of the commonly occuring rocks to develop heat flow patterns around Columbia, Missouri, to help locate bentonitic clay (14). At about the same time Lovering worked out a fairly comprehensive mathematical analysis of the steady and unsteady state heat flow through the earth's crust; and, this work which was published in the form of two articles, formed a basis for heat flow calculations through the use of experimentally obtained thermal conductivity and diffusivity values of rocks (15, 16).

Rock thermal conductivity and diffusivity values were obtained in the recent past by a variety of methods which can be broadly classified as the experimental, statistical, and in situ probe methods. The subject matter related to this study is mainly concerned with the statistical and in situ techniques to measure the thermal conductivity and diffusivity of rocks. A thorough survey of these techniques is, therefore, included in the literature survey. However, a brief survey of the experimental methods is also included for reference purposes.

It is difficult to thoroughly cover the background literature for an approach of the type presented in this study because it uses the independently recorded time-temperature data as an input into a mathematical model to obtain thermal conductivity and diffusivity of rocks. It seems appropriate, however, that a survey of the temperature sensing tools and temperature recording systems be included to help emphasize the necessity for accurately recorded time-temperature data as a prerequisite for determining representative thermal conductivity and diffusivity values of rock formations.

Experimental Techniques

In the 1930's and early 1940's, the most commonly used apparatus to measure thermal conductivities was a modified form of the apparatus used by Lodge in 1878 to measure the thermal conductivities of insulations (17). In this apparatus, because of design limitations, vaseline or glycerine had to be used on the specimens to insure an efficient heat transfer from heater to the rocks. Since the rock specimens were porous, these viscous substances tended to occupy some of the pore space and thus changed their measured thermal conductivities. Birch and Clark (12) used a slightly different design and by using helium and hydrogen to surround the rock specimens eliminated the earlier practice of using vaseline or glycerine to obtain a more efficient transfer of heat from the heater to the rock sample. Excellent discussions of modifications and improvements in the apparatus design from 1950 - 1973 are given by Birch (18), ASTM Special Publication No. 217 (19), Zierfus (20), Kunii and Smith (21), by a number of authors in the Apparatus Section of the 8th Conference on Thermal

Conductivity, Purdue, (1968) (22), and by Thomas, Frost and Harvey (23).

Sass and his co-workers pioneered in determining thermal conductivities of rocks from drilling chips by packing them in a plastic cell and filling the surrounding space with water (24, 25). In comparison with core samples, this method eliminates the possible sources of error due to machining and sample preparation. However, because of assumptions made (of rock continuity between chips, degree of compaction, changes in composition, etc.), the validity of the thermal conductivity values so obtained may be questioned.

Ever since Lord Kelvin coined the term "thermal diffusivity" for "thermometric conductivity" as used by Maxwell (26), it has been commonly used in transient heat flow studies. Experimentally, it can be obtained by dividing the thermal conductivity of a substance by its density and heat capacity. However, several methods are available in the literature, where by substituting the experimental data into equations describing transient heat flow under successive sets of conditions, thermal diffusivities of various substances may be obtained. One such method was presented by Sommerton, et al. (27). This method consisted of heating a long cylindrical sample of a rock with a constant increase in temperature. Sample edge temperatures and differential temperatures were constantly measured, and by substituting this data into the unsteady heat-flow equation described below, thermal diffusivity values were calculated.

$$T = T_o + h\left(t - \frac{a^2 - r^2}{4\alpha}\right) + \frac{2h}{a\alpha} \sum_{n=1}^{\infty} e^{-\alpha B_n^2 t} \left[\frac{J_o (r B_n)}{B_n^3 J_1 (a B_n)}\right]$$

where

t = time

h = rate of heating the sample

T = temperature at a radius r

T_o = initial temperature

a = radius of the sample from its center to the thermocouple edges

r = radius $a \geq r \geq 0$

α = thermal diffusivity

J_o = first kind, zero order Bessel function

J_1 = first kind, first order Bessel function

B_n = roots of the Bessel function: $J_o (a B_n) = 0$

In summary, the results obtained from the experimental methods were accurate when duplicated on the same sample; however, because of a number of factors which affect the samples in their preparations, change in habitat, etc., irreversible changes in the specimens are introduced that cannot be accounted for by the experimental method. To avoid these problems a number of statistical correlations have been attempted by workers in the area. Some of these correlations are discussed next.

Statistical Correlations

Petrophysical properties of rocks have been used in the last two decades to obtain thermal conductivity values by means of statistical correlations. The most commonly used petrophysical properties for correlation purposes are porosity, water saturation and formation factor. Some of the correlations describing the relationship between these properties and the thermal conductivity of rocks are presented in this section.

It is difficult to envision a general correlation between the thermal conductivity and electrical conductivity of rocks because of the salinity of the fluids saturating the rocks. The salinity of the fluids saturating the rocks tends to short-circuit electrical flow, and as a result the rock's true electrical conductivity is predominantly indicative of its fluid electrical properties. However, a series of statistical correlations was found in the literature whereby thermal and electrical conductivities could be approximately correlated. These interesting correlations are presented in the suceeding sections.

Thermal Conductivity, Porosity, and Water Saturation Correlations

In order to avoid complicated and time-consuming experiments, soil chemists turned their attention to developing petrophysical correlations between thermal conductivity, water saturation, and porosity. Meridith (28) has given an excellent account of contributions from a variety of sources dating as far back as 1892 as applied to the thermal conductivity of dispersions. Some of these correlations, when applied to insulations, give poor to fair results (29). None of these techniques has been used to obtain thermal conductivities of rocks, -- perhaps because not only does the determination of rock matrix properties involve lengthy experimentation; but also the rock compositions are seldom uniform and matrix thermal conductivities vary from one sample to another, due to a variety of compositions which depend upon their modes of deposition.

Zierfus and Van-Der Vliet (30) conducted a series of experiments to determine thermal and petrophysical properties of different types

of rocks. From trends indicated by cross plots of this data they obtained a third-degree polynominal which correlates thermal conductivity, formation factor, and porosity. Their final equation was

$$\log_{10} FK = A + B\phi + C\phi^2 + D\phi^3$$

where

F = formation factor

K = thermal conductivity

ϕ = porosity

A, B, C, and D = constants determined by regression analysis

The above equation gives predictions which vary by as much as $\pm$ 50% from the values used in the development of the correlation. The equation is of limited significance to the present study as it is valid only for highly porous samples (porosity more than 25%) and for those cases where the composition of the matrix has not been changed drastically. Such cases are rare, of course, because it is rather unusual to have sedimentary rocks of the same composition in two different geologic locations.

Horai and Seiya (31) studied the effect of water saturation on thermal conductivity. Although their studies were mainly concerned with soft sediments and not with conventional rocks, the final form of their equation correlating matrix and fluid properties with the thermal conductivity is presented here.

$$K = K_1 \frac{3 - 2(1 - v)\ (1 - K_1/K_2)}{3K_1/K_2 + (1 - v)\ (1 - K_1/K_2}$$

where

K_1 = thermal conductivity of medium (water, air, etc.)

K_2 = thermal conductivity of rock solids

K = thermal conductivity of composite

$v = \rho/P_a - \rho_w (1/w - 1)$

ρ = apparent density

P_a = porosity

ρ_w = density of water

w = percentage concentration of water

Assad and Sommerton (32) measured thermal conductivities of about two hundred samples and developed an empirical correlation which includes not only porosity but also the thermal conductivities of the rock matrix and the fluid. The final form of their equation was:

$$K = R_1 \left(\frac{R_2}{R_1}\right)^{C\phi}$$

where

K = thermal conductivity of composite

R_1 = thermal conductivity of rock matrix

R_2 = thermal conductivity of saturating fluid

C = empirical constant $\simeq 1$

ϕ = porosity

This simple equation gives fairly accurate values for the thermal conductivities when porosity, rock matrix thermal conductivity, and fluid-thermal conductivity are accurately known. However, determination of rock matrix thermal conductivity requires involved and

time-consuming experimentation preceded by tedious procedures to sample the rock formations by coring. The scope of this equation is limited unless the individual fluid and rock matrix properties are already available and no experimentation is needed to determine them.

Diment and Robertson (33) used a new approach to correlate thermal conductivity with the amount of residual solids in limestone and shale samples after they were treated with hydrochloric acid. The correlation is poor. The approach is significant, nonetheless, because the residual solids reflect the absence of porosity of the sample.

Recently, another correlation between thermal conductivity, clay content, and porosity was reported by Rijswick Shell Laboratories (34). This approach is highly empirical; moreover, procedures to determine the clay content of a rock sample are even more complicated than the actual experimentation needed to measure the thermal conductivity. The applicability of this approach, therefore, appears to be limited.

Thermal and Electrical Conductivity Correlation

Direct correlations between thermal and electrical conductivities of metals were developed by Wiederman, Franz, Lorenz, Fermi, and Dirac (35). Archie, Kilmer and Wyle casually mentioned the possibility of a relationship between rock thermal and electrical conductivities; however, McDonald (36) made the first direct reference to the existence of a correlation between thermal and electrical conductivities. Meridith (28) in 1964 performed experiments for the first time to establish a correlation between thermal and electrical conductivities of soils. This approach was followed by Hutt and Berg (29) in 1968. Their final correlations were as follows:

$$K_{me} = \frac{3K_{se} K_{mt}^{1/3} (1 - K_{st}) + (K_{mt} - K_{st}) (1 - K_{se})}{3K_{mt}^{1/3} (1 - K_{st}) - 2(K_{mt} - K_{st}) (1 - K_{se})}$$

$$K_{me} = \frac{\ell n\, K_{st} (1 + 2K_{se}) + \ell n K_{mt} (K_{se} - 1)}{\ell n\, K_{st} (1 + 2K_{se}) - 2\ell n K_{mt} (K_{se} - 1)}$$

$$K_{me} = 1 - \frac{\ell n\, K_{mt}^{m}}{\ell n\, K_{st}}$$

where

K_{me} = normalized electrical conductivity of mixture (solids + liquids)

K_{se} = normalized electrical conductivity of solids

K_{mt} = normalized thermal conductivity of mixture

K_{st} = normalized thermal conductivity of solids

m = cementation factor

Hutt and Berg (29) experimentally determined the various quantities required in the above equations and compared the calculated thermal conductivities with the experimentally determined values. In a few samples the percentage difference from the experimental values was as much as 116% -- although most of the samples gave thermal conductivity values between $\pm$ 25%. The above equations correlating thermal and electrical conductivity are highly empirical and represent the results achieved through the use of statistical models. Moreover, in order to use these equations, it is necessary that rock-matrix properties be known, and these need to be determined experimentally.

In Situ Probe Methods

In view of the errors introduced during measurement, as described in Chapter I, it has always been thought that the intermediate error introducing steps between sampling and experimentation could be avoided if the rock thermal conductivity and diffusivity were determined in situ. A German physicist named Schleiremachen first proposed such a method in 1833 (37). However, it was not until the early 1950's that improvements were made in the thermal diffusivity probes (38, 39, 40, 41). Excellent discussion of the so-called probe methods to measure thermal diffusivities is given by Jaeger (42) and De-Vries and Peck (43), and more recently by Prats and Brian (44).

A schematic diagram of a typical in situ measuring probe is shown in Figure 1. The probe consists of a heater, enclosed inside a stainless steel sheath, and one or more thermocouples embedded at predetermined distances and insulated from the heater by a ceramic insulator. The length and diameter of a probe affect its sensitivity therefore, a brief listing and description of associated dimensional and material factors influencing accuracy of a probe is of interest here as follows:

1. probe diameter
2. probe length to diameter ratio
3. thermal properties of the probes (stainless steel as compared to copper sheaths; epoxy, as compared to solder fillers, etc.)
4. location and type of sensor (thermocouple or thermistor)
5. type of heater

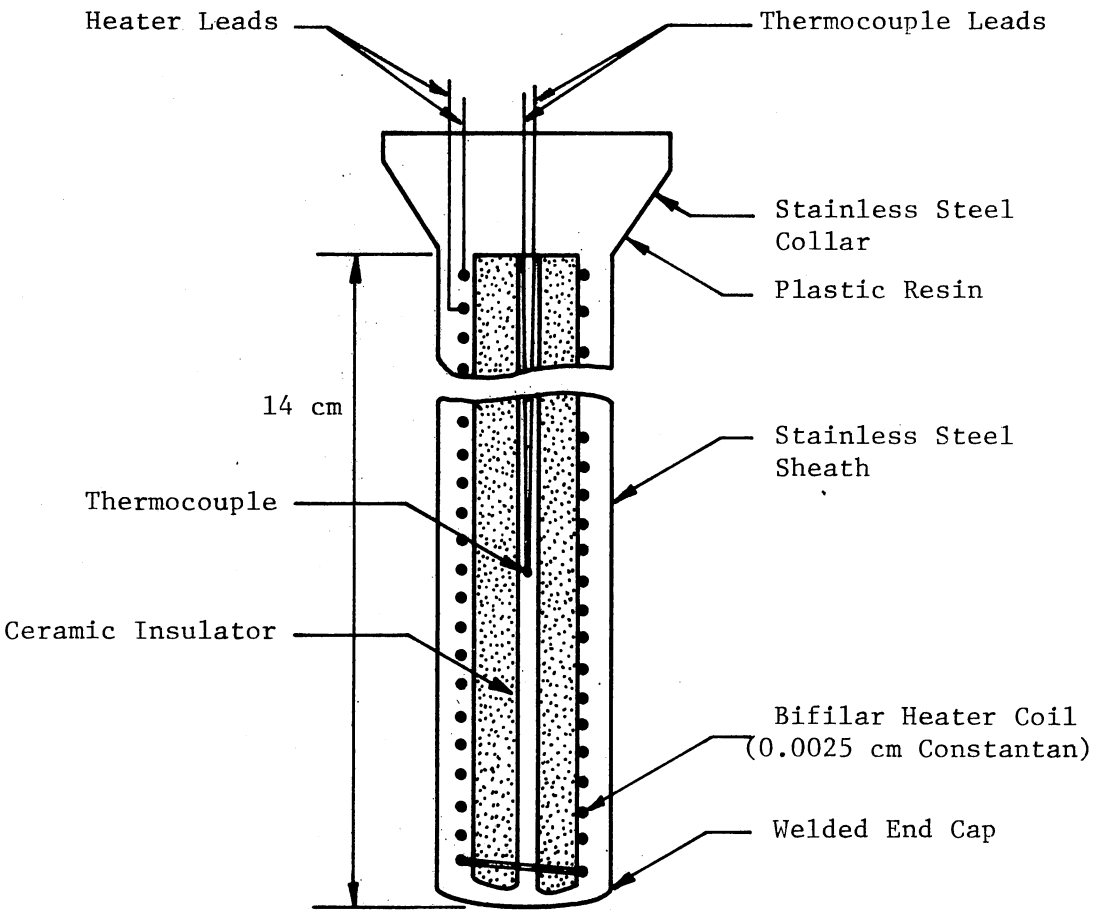

Figure 1. Schematic Diagram of a Thermal Probe

Several attempts were made in the past to standardize the probes, and it has been found that a probe length of 28.0 cm with a length-to-diameter ratio of 48, having inside and outside diameters of 5.85 and 6.35 mm, respectively, with a heater resistance of 92 ohms, gives fairly good results in recording temperature values to be used in the calculation of the thermal conductivities (26).

An effective probe is somewhat of a compromise between good mechanical strength and low thermal mass, between fundamental accuracy of design requirements and low cost. It should be so constructed that the temperature-rise developed in the order of twenty minutes should not exceed $5^{o}K$. From a thorough survey of the probes described in the literature it seems that very few probes possess the qualities of design and accuracy required to give accurate in situ thermal conductivity predictions (26).

Temperature Sensing Tools

It is appreciated that the accuracy of any technique for determining the in situ thermal characteristics of rocks surrounding a bore hole depends on the accuracy of temperature-sensing and recording devices used in the measurement of temperature in a bore hole. Therefore a survey of the various instruments used in subsurface temperature logging appears to be in order.

There are three basic temperature-sensing tools currently being used in industry (45).

Single Element Tool

This tool (Figure 2) contains a single-sensing thermistor element,

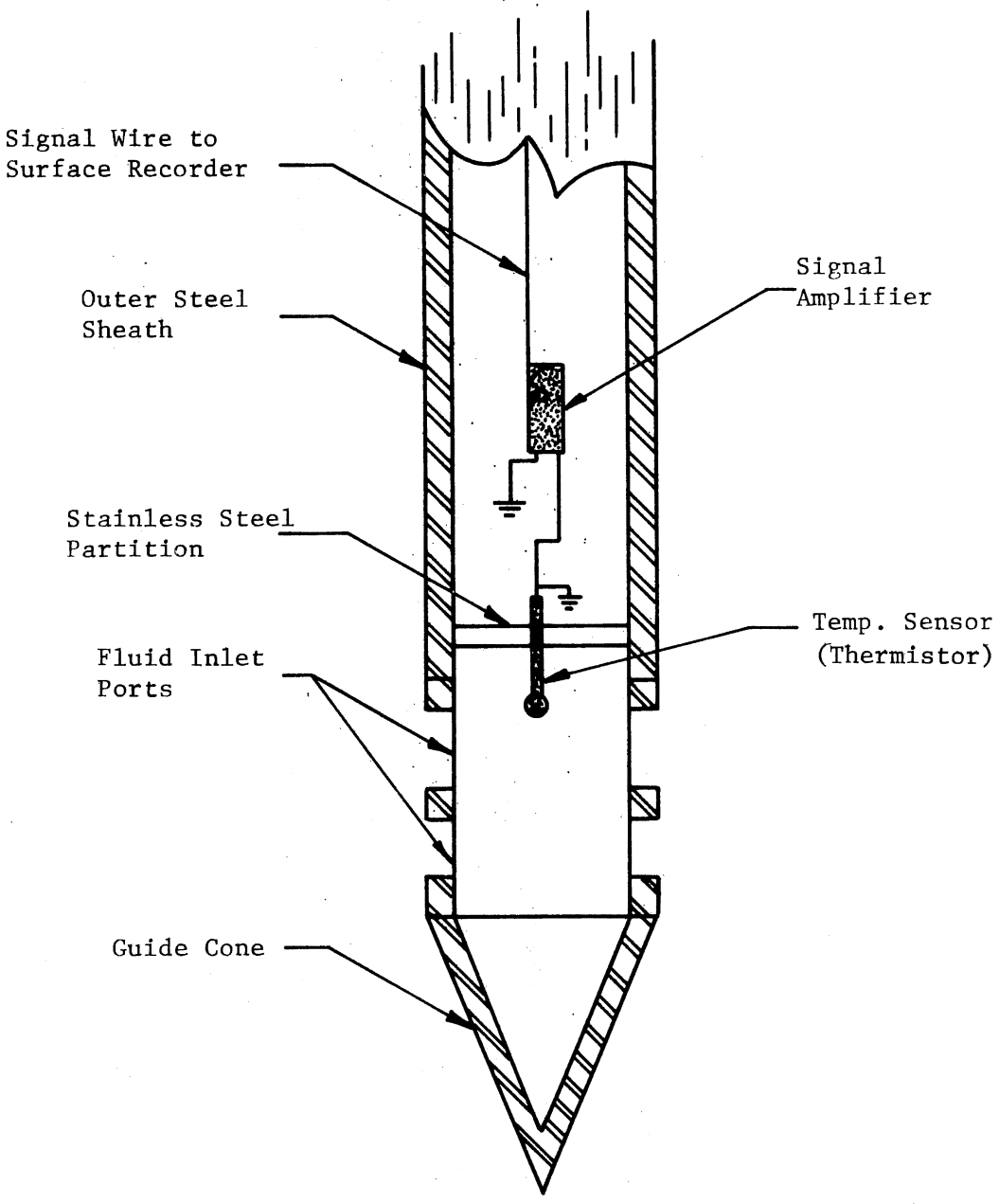

Figure 2. Schematic Diagram of a Single-Element Tool

calibrated and designed in such a way as to detect and transmit the actual down-hole temperature to the surface where it is recorded as a function of the depth.

Because of a high thermal lag, this tool is incapable of sharp definition of temperature interfaces. Total transition from one temperature to another is accordingly averaged over a long vertical interval, thereby losing the one desirable characteristic of a temperature log, i.e., sharp boundary delineation.

Dual Element Tool

This tool as shown schematically in Figure 3 utilizes two sensing-elements physically separated by a known distance. Both of these elements detect the absolute temperatures of the fluid at their respective depths. The signals are passed on to the surface. The signal from this tool along with that from another single element tool enables a sharp delineation in temperature and is the most commonly used tool in temperature logging today.

Memory Circuit Tool

This tool combines the advantages of the dual-element tool with the single-element simplicity of design as shown in Figure 4. In application, the sensing element at a preselected time interval takes the temperature reading and sends it to a memory circuit, where it is compared with a reference signal and the difference transmitted to the surface for recording.

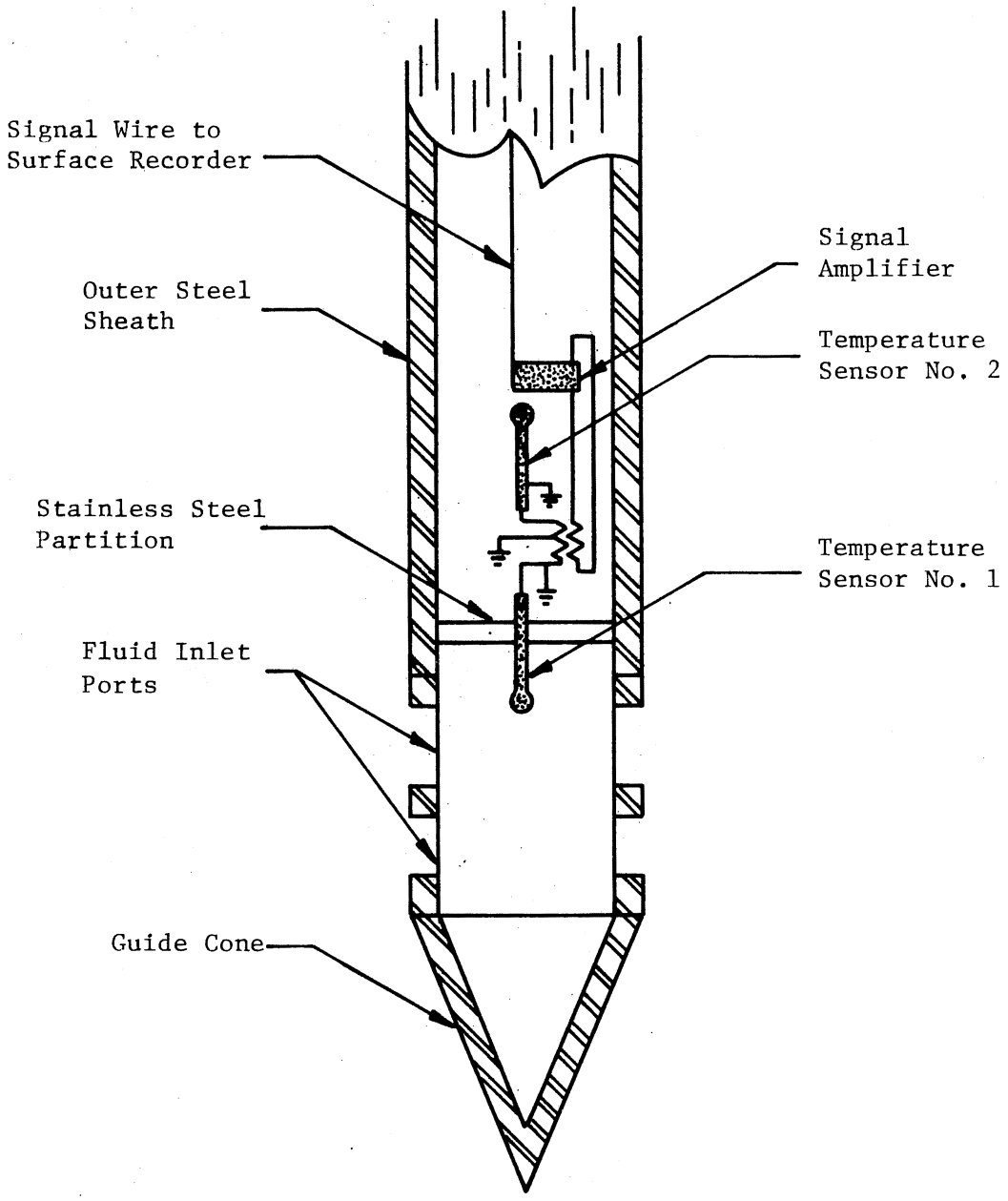

Figure 3. Schematic Diagram of a Dual-Element Tool

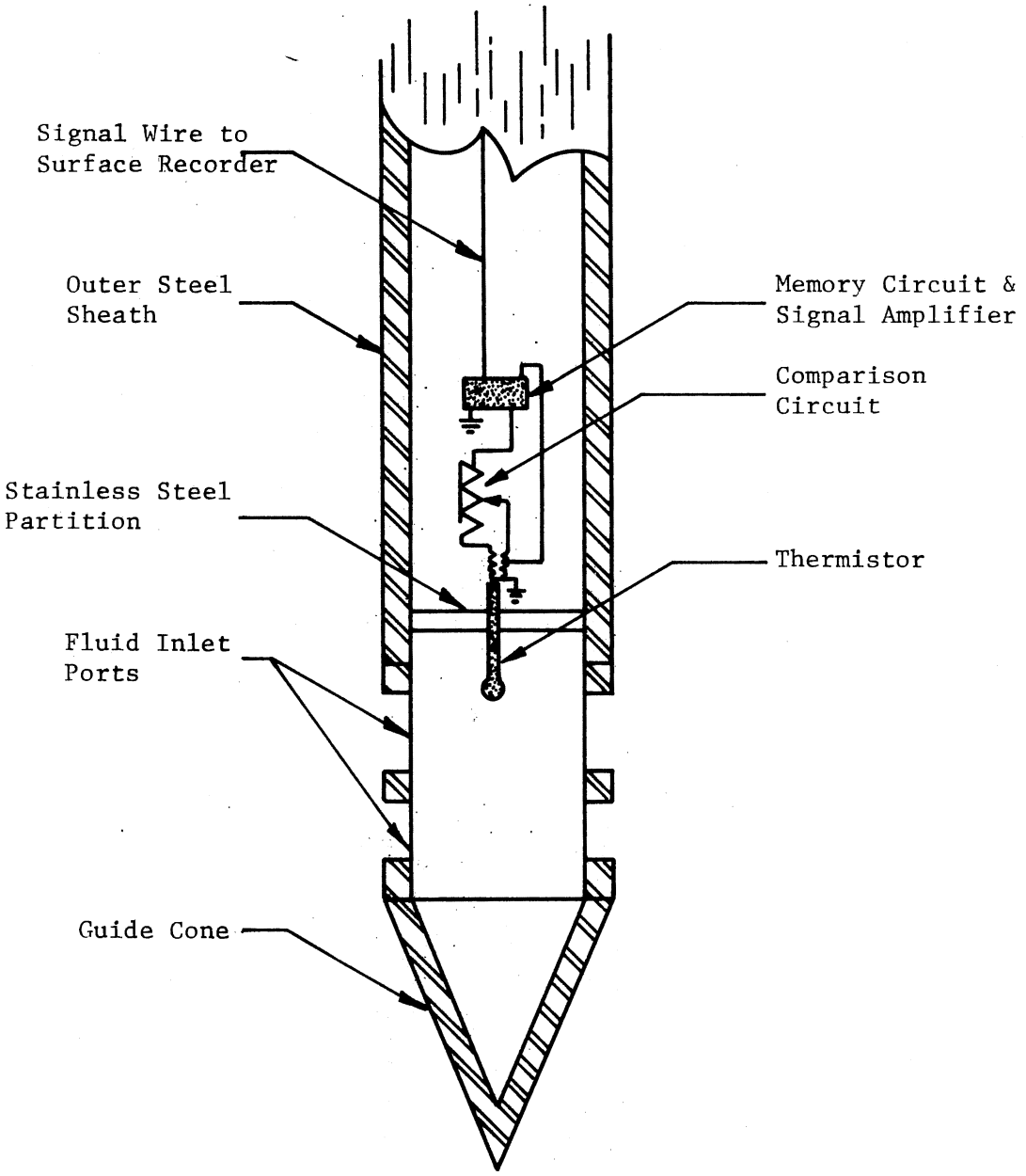

Figure 4. Schematic Diagram of a Memory Circuit Tool

Temperature Recording Systems

The amplified and corrected signal from the temperature sensing element is directed to the surface for temperature recording. It seems appropriate to discuss the temperature recording systems currently used in the industry to evaluate the degree of accuracy that can be expected for a temperature sensing and recording unit as a whole. Two types of temperature recording systems are currently being used by the temperature logging industry: the analog recording systems and the digital recording systems. A brief discussion of each of these systems is presented here as follows:

Analog Recording Systems

Analog recording systems use a time-constant circuitry wherein the depth correlation is determined by the logging speed. For a large temperature increase, as is common in deep well temperature logging, the time constant circuitry tends to average the response -- more so towards the surface than at a depth. Also, because of an increased noise due to relatively faint signals, the lower temperatures recorded for depths near the surface may be grossly in error.

Digital Recording Systems

These systems take the discrete incremental variations in the signal from the logging tool and calibrate it with the thermistor resistance, which is directly proportional to changes in the relative or absolute temperatures as the case may be. The size of the increment can be adjusted; thereby, a very small variation in temperature

can be recorded. Once an incremental change in temperature is digitized, it is recorded along with the depth on magnetic tape. It is common practice to convert this signal into an analog response for simultaneous strip-chart recording.

In modern subsurface temperature recording, digital recording systems are the heart of an increased accuracy in temperature recording. The digital system is very accurate and thus eliminates drawbacks inherent in electronic conversions. A schematic diagram of the recording system along with accessories is shown in Figure 5.

Summary

From the above survey of the experimental and statistical methods of obtaining the thermal properties, it can be seen that most of these methods have limitations of experimentation, repeatability, and accuracy. They not only give erroneous results but also are expensive and time consuming.

The probe methods are currently being used in oceanography and were an integral part of the Apollo 10 program to determine the thermal characteristics of moon rocks in situ. These methods require repeated experimentation to obtain reliable data for a very short interval of the well bores, and therefore are quite expensive for the purposes of heat flow calculations through the earth's crust.

Literature survey of the temperature sensing tools and recording systems shows that small variations in temperature can be easily recorded. As will be discussed further under accuracy considerations, these variations accurately reflect the nonhomogeneities of the underlying formations. A method capable of calculating the thermal

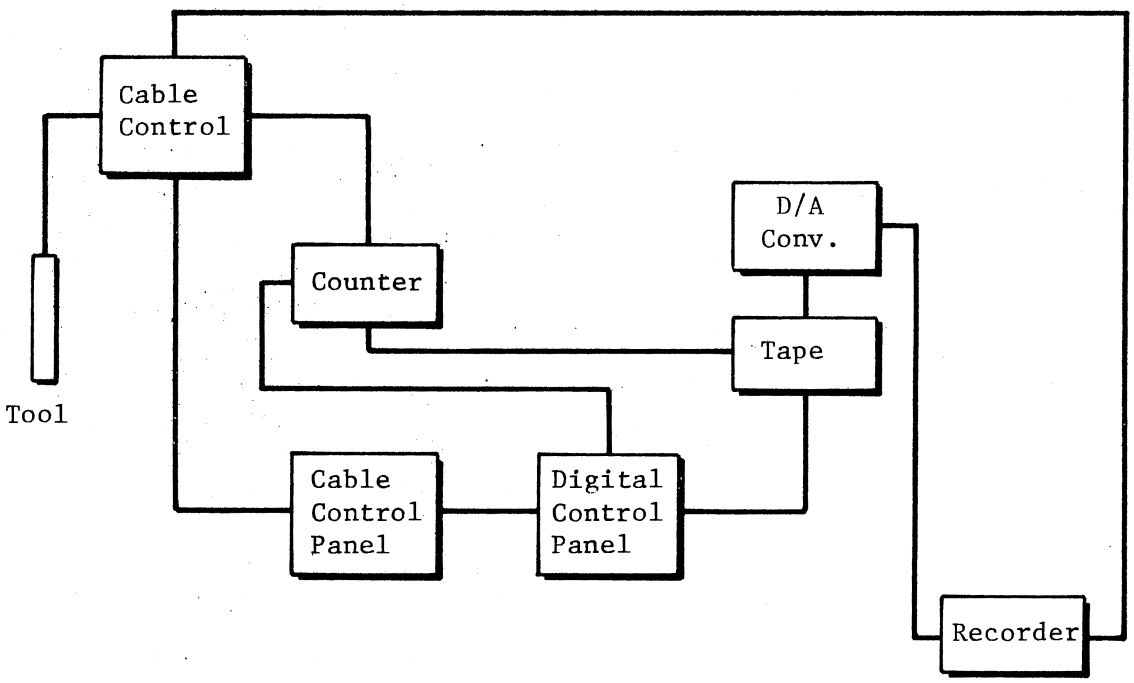

Figure 5. Schematic Diagram of a Typical Temperature Logging System

properties of rocks in situ by using accurately recorded time-temperature data is presented in this study. This method eliminates the experimentation required by the methods currently available in the industry, and it is hoped that this study will contribute to the technology in this field.

CHAPTER III

DESCRIPTION OF THE MATHEMATICAL MODEL

Introduction

One of the objectives of this research is to devise a technique for measuring the thermal properties of rocks in situ. To accomplish this task a mathematical model of the transient temperature buildup in a well bore surrounded by rock formations is developed. The development of the model is based upon energy balance techniques. The resultant equations are manipulated numerically to obtain the thermal conductivity and diffusivity of a rock. The model eliminates laboratory experimental errors as described in Chapter I by using in situ time-temperature data.

In order to abstract a complex system into a meaningful mathematical model, a series of assumptions have been made. These assumptions are presented in this chapter along with a description of the model in order to clarify its potential application. The objective behind the assumptions is to exclude the irrelevant and to focus on the relevant; therefore, the validity of the assumptions and their possible significance is also discussed in this chapter.

Description of the Physical Model

The temperature of the earth increases continually with depth,

and this variation is commonly termed the geothermal gradient. Geothermal gradients for different regions of the world have been determined by using temperature measurements taken inside the bore holes which have come into thermal equilibrium with the surrounding formations.

The thermal equilibrium of a well bore is disturbed if the fluid contained in it is replaced by a fluid of comparatively lower temperature. This process of circulation (by pumping the drilling fluid down the drill pipe and up the annular space between the formation and the outside wall of the drill pipe) establishes a heat sink in the lower portions of the well bore causing heat to flow from the formation to the well bore. If, after an appropriate period of circulation, the pumping is stopped and the fluid in the well bore allowed to remain undisturbed, its temperature increases at a rate varying with time and the thermal properties of formations adjacent to the well bore. The nature of the temperature changes taking place at various depths are illustrated in the temperature logs of two wells as shown in Figures 6 and 7. From these figures it can also be noted that the rate of tempearture increase obviously varies with the type of rock encountered at different depths in the same bore hole.

The effect of formation thermal properties on overall temperature increase is more clearly shown in Figures 8 and 9, where the "normalized" temperature is plotted against depth. The normalized temperature is defined as:

$$T_n = T_o - (T_a + G\, D_e)$$

where

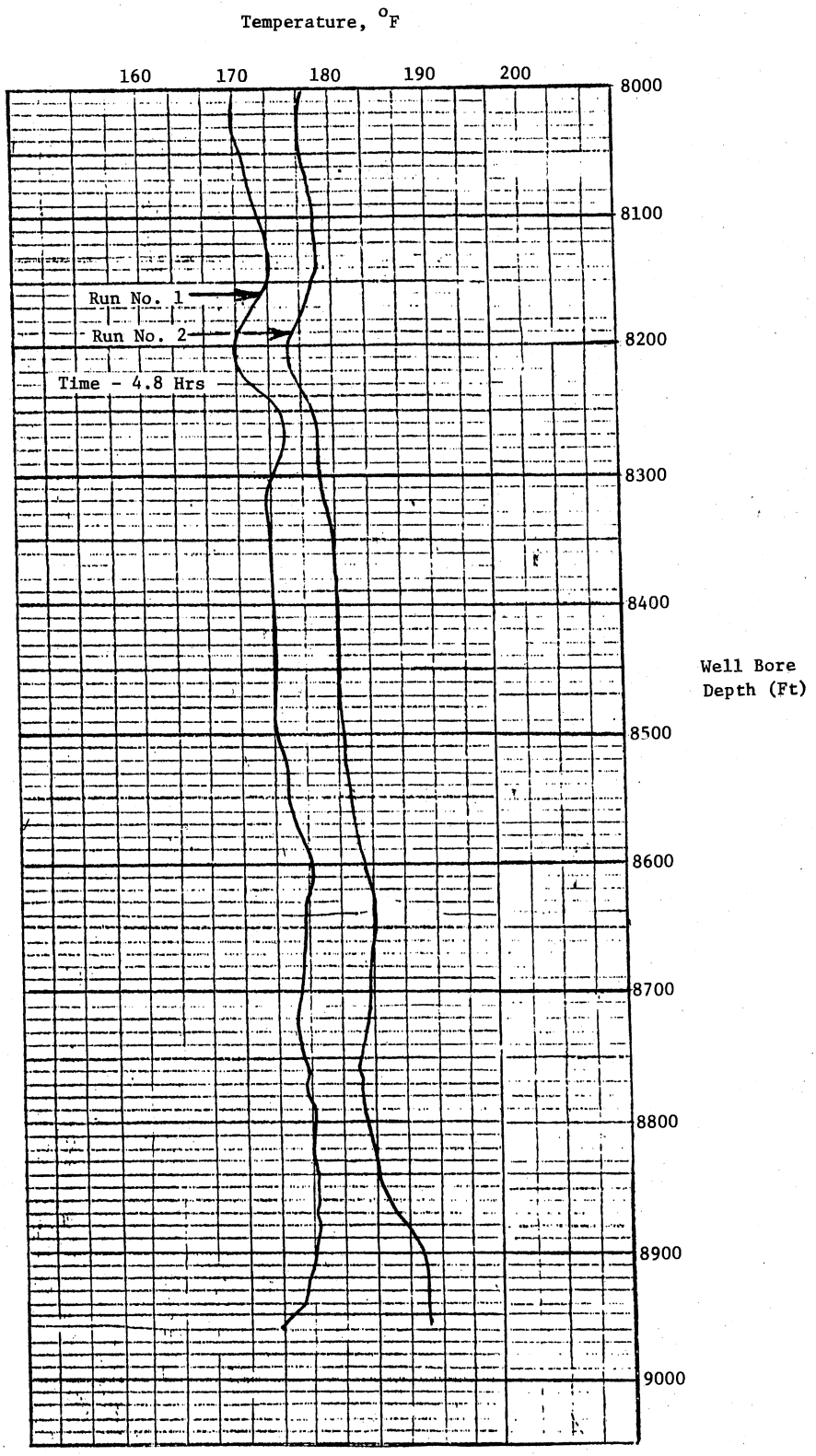

Figure 6. Temperature Buildup as a Function of Time for a Test Case in Montana (46)

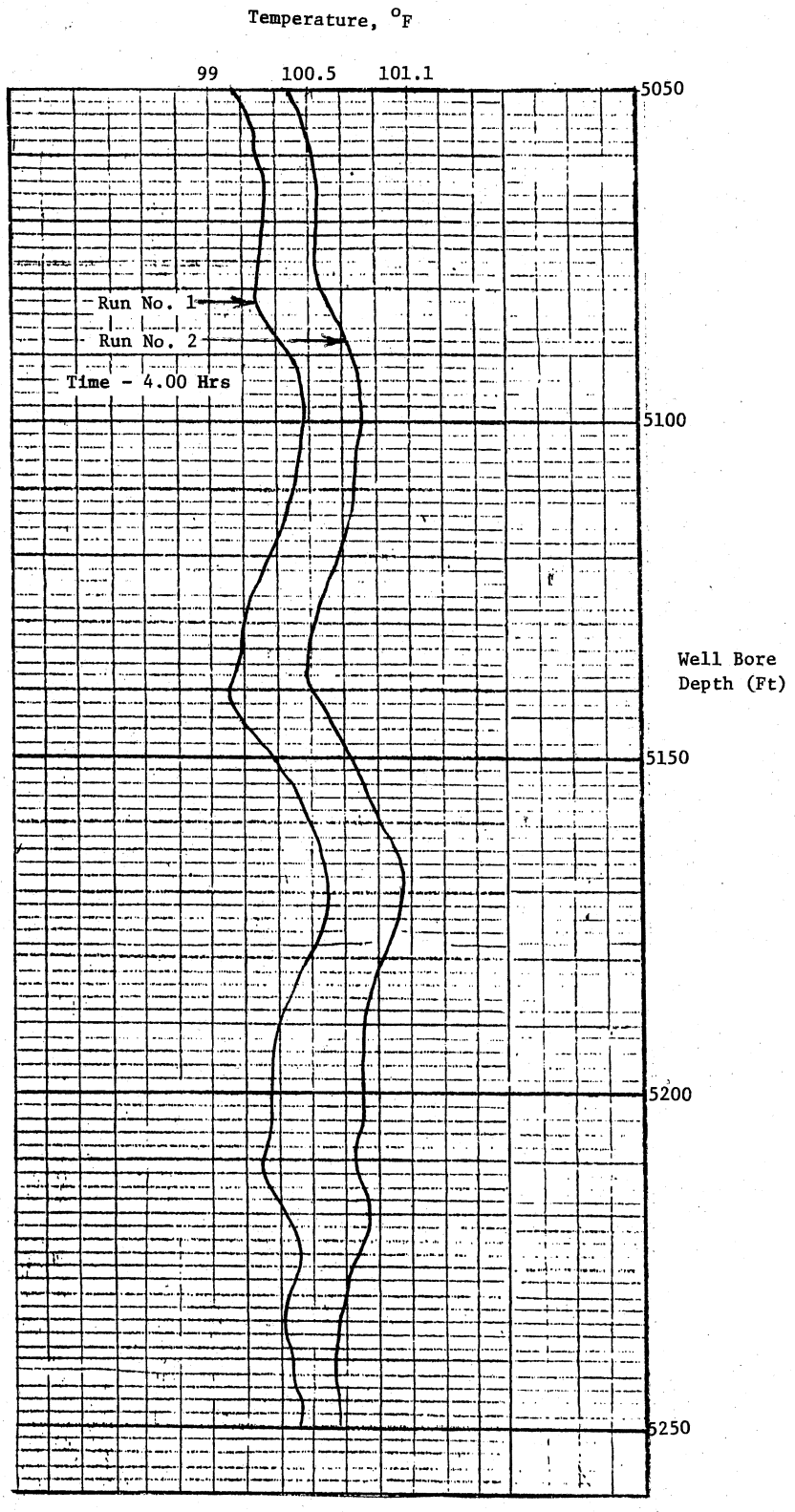

Figure 7. Temperature Buildup as a Function of Time for a Test Case in Oklahoma

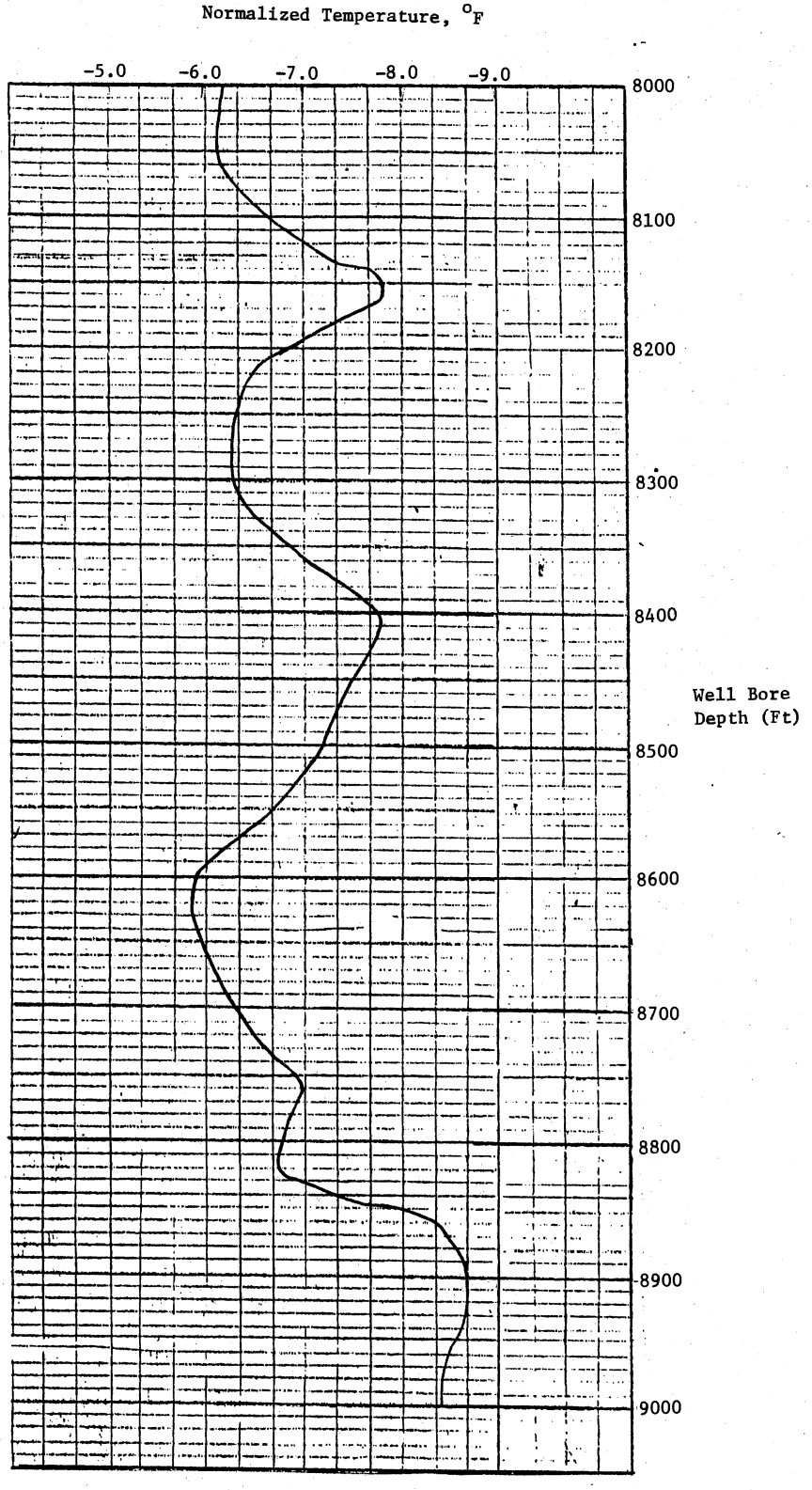

Figure 8. Normalized Temperature vs. Depth for the Montana Test Case

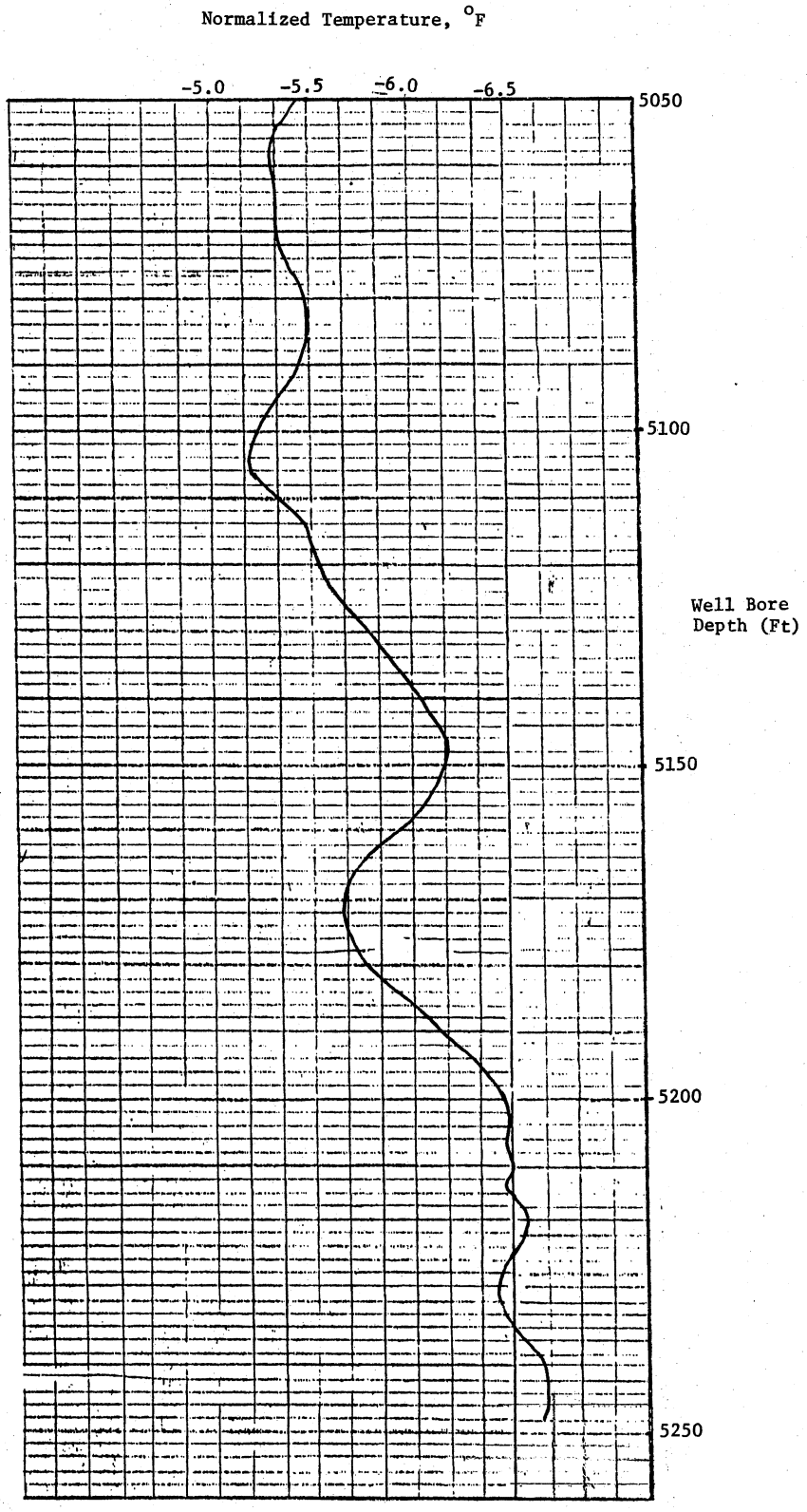

Figure 9. Normalized Temperature vs. Depth for the Oklahoma Test Case

T_n = normalized temperature

T_o = observed temperature

T_a = average annual ambient temperature

G = temperature gradient

D_e = depth

Variations in the normalized temperature appear to reflect the lithology as can be seen by correlating these plots with the logs presented in Figures 10 and 11 for the same intervals. Such variations appear to be due to the thermal characteristics of rocks as they exist in their natural habitat.

Development of the Mathematical Model

The temperature buildup as shown in Figures 8 and 9 is used as a basis for the physical model to be simulated mathematically. A basic equation describing this transient flow of heat from the formation into the well bore can be represented in cylindrical coordinates by the diffusivity equation as:

$$\frac{1}{r}\frac{\partial}{\partial r}\left(K_r r \frac{\partial T}{\partial r}\right)+\frac{1}{r^2}\frac{\partial}{\partial \theta}\left(K_\theta \frac{\partial T}{\partial \theta}\right)+\frac{\partial}{\partial z}\left(K_z \frac{\partial T}{\partial z}\right)=\rho C_f \frac{\partial T}{\partial t} \qquad (3.1)$$

where

T = temperature

r = radial distance

ρ = formation density

C_f = specific heat of the formation

K = thermal conductivity of the formation

t = time

r, θ, z = cylindrical coordinates

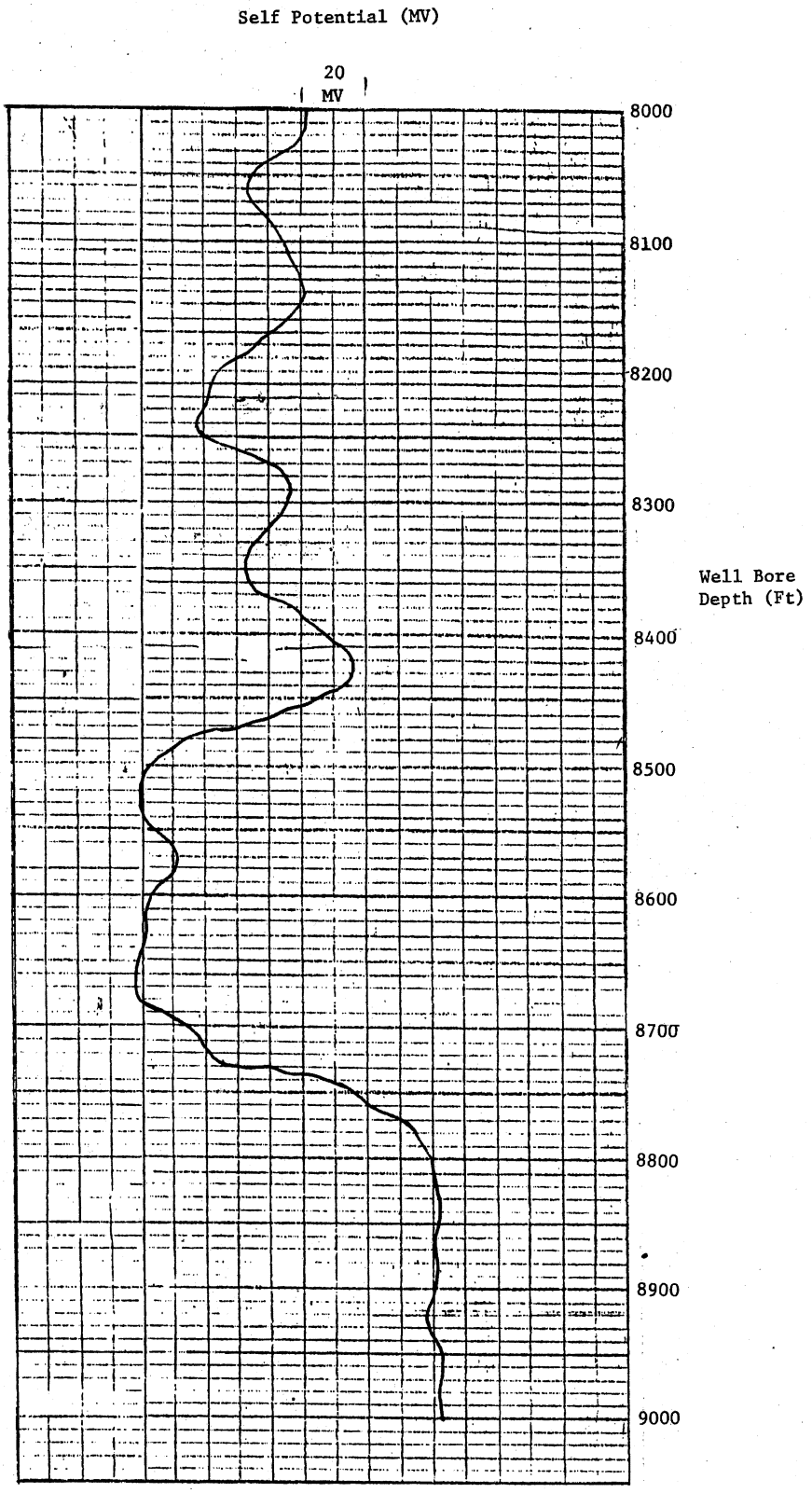

Figure 10. Self Potential vs. Depth for the Montana Test Case

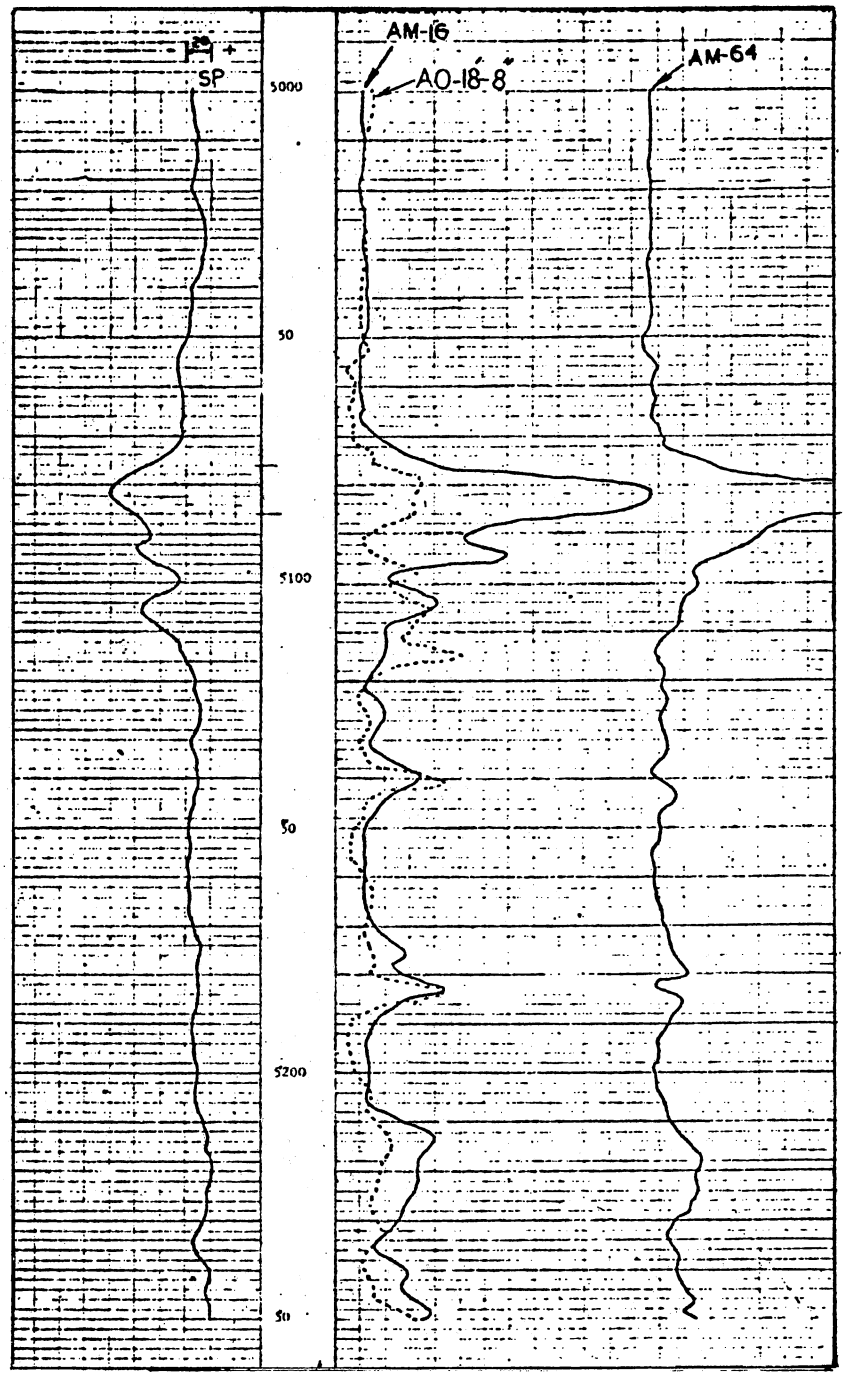

Figure 11. Electric Logs for the Test Case in Oklahoma

Assuming the formation to be isotropic, the equation can be reduced to:

$$\frac{\partial^2 T}{\partial r^2} + \frac{1}{r}\frac{\partial T}{\partial r} + \frac{1}{r^2}\frac{\partial^2 T}{\partial \theta^2} + \frac{\partial^2 T}{\partial z^2} = \frac{\rho C_f}{K}\frac{\partial T}{\partial t} \qquad (3.2)$$

Assuming further that the temperature gradient in the vertical direction is negligible in comparison to that in the horizontal direction, then the above equation reduces to:

$$\frac{\partial^2 T}{\partial r^2} + \frac{1}{r}\frac{\partial T}{\partial r} = \frac{\rho C_f}{K}\frac{\partial T}{\partial t} \qquad (3.3)$$

A number of numerical and Bessel function solutions to Equation 3.3 exist in the literature by which temperature of a rock formation can be predicted as a function of time. The accuracy of prediction of these solutions, however, depends upon the length of time for which the heat flow from the formation into the well bore is recorded. For this study temperature buildup extending over relatively longer periods of time is available. Lord Kelvin proposed an exponential integral solution to predict temperature buildup as a function of time extending over long periods of time. This solution which has been quoted by Jaeger et al., Carslaw and Jaeger, Ingersol and Zobel among others (47, 48, 49) is presented next.

Appropriate boundary conditions to describe the physical model are:

$$T_{(r)}\Big|_{t=0} = T_s \qquad (3.4)$$

$$T_{(t)}\Big|_{r=\infty} = T_s \qquad (3.5)$$

$$Q\Big|_{r=r_w} = -2\pi K r_w \left.\frac{\partial T}{\partial r}\right|_{r=r_w} \tag{3.6}$$

Equation 3.6 can be rearranged as:

$$\frac{Q}{2\pi K} = -\left(r \frac{\partial T}{\partial r}\right)_{r=r_w} \tag{3.7}$$

For a well bore radius to be vanishingly small as compared to the size of the heat reservoir Equation 3.7 can be expressed as:

$$\lim_{r \longrightarrow 0} r \frac{\partial T}{\partial r} = -\frac{Q}{2\pi K} \tag{3.8}$$

To change the partial differential Equation 3.3 to a total differential equation the similarity transformation as proposed by Matthews and Russel (50) is used as follows:

$$y = \frac{\rho C_f r^2}{4Kt} \tag{3.9}$$

From the above transformation, expressions for partial derivatives in Equation 3.3 can be derived as:

$$\frac{\partial T}{\partial r} = \frac{dT}{dy}\frac{\partial y}{\partial r} = \frac{2\rho C_f r}{4Kt}\frac{dT}{dy} \tag{3.10}$$

$$\frac{\partial T}{\partial t} = \frac{dT}{dy}\frac{\partial y}{\partial t} = -\frac{\rho C_f r^2}{4\pi t^2}\frac{dT}{dy} \tag{3.11}$$

$$\frac{\partial^2 T}{\partial r^2} = \frac{\partial}{\partial r}\left[\frac{2\rho C_f r}{4Kt}\frac{dT}{dy}\right] \tag{3.12}$$

or

$$\frac{\partial^2 T}{\partial r^2} = \frac{2\rho C_f}{4Kt} \frac{dT}{dy} + \frac{2\rho C_f r}{4Kt} \frac{\partial \left(\frac{dT}{dy}\right)}{\partial r} \tag{3.13}$$

Equation 3.13 can be further expanded as:

$$\frac{\partial^2 T}{\partial r^2} = \frac{2\rho C_f}{4Kt} \frac{dT}{dy} + \frac{2\rho C_f r}{4Kt} \left[\frac{d \left(\frac{dT}{dy}\right)}{dy} \frac{\partial y}{\partial r} \right] \tag{3.14}$$

Substituting for the expression in parenthesis, Equation 3.14 can be described as:

$$\frac{\partial^2 T}{\partial r^2} = \frac{2\rho C_f}{4Kt} \frac{dT}{dy} + \frac{2\rho C_f r}{4Kt} \left[\frac{2\rho C_f r}{4Kt} \frac{d^2 T}{dy^2} \right] \tag{3.15}$$

By substituting Equations 3.10, 3.11, 3.12 and 3.15 into Equation 3.3, it can be expressed as:

$$\frac{2\rho C_f}{4Kt} \frac{dT}{dy} + \frac{2\rho C_f}{4Kt} \frac{2\rho C_f r^2}{4Kt} \frac{d^2 T}{dy^2} + \frac{1}{r} \frac{2\rho C_f r}{4Kt} \frac{dT}{dy} + \frac{\rho C_f}{K} \frac{\rho C_f r^2}{4Kt^2} \frac{dT}{dy} = 0 \tag{3.16}$$

By using the definition of similarity transform as described by Equation 3.9, Equation 3.16 can be simplified as:

$$\frac{1}{2} \frac{dT}{dy} + y \frac{d^2 T}{dy^2} + \frac{1}{2} \frac{dT}{dy} + y \frac{dT}{dy} = 0 \tag{3.17}$$

By combining the first, third and fourth terms, Equation 3.17 can be expressed as:

$$y \frac{d^2T}{dy^2} + \frac{dT}{dy} (1+y) = 0 \tag{3.18}$$

To simplify Equation 3.18 assume $T' = \frac{dT}{dy}$ (3.19)

Upon substituting Equation 3.19 into Equation 3.18 it can be written as:

$$y \frac{dT'}{dy} + (1+y) T' = 0 \tag{3.20}$$

Separation of variables, and upon integration Equation 3.20 can be expressed as:

$$\ell n\, T' = - \ell n\, y - y + C \tag{3.21}$$

Upon rearranging, Equation 3.21 can be expressed as:

$$T' = \frac{dT}{dy} = \frac{C_1}{y} e^{-y} \tag{3.22}$$

or

$$2y \frac{dT}{dy} = 2C_1 e^{-y} \tag{3.23}$$

The initial and boundry conditions of Equations 3.4, 3.5, 3.6 can be expressed in terms of similarity transform as follows:

$$T_{(r)}\Big|_{t=0} = T_s \tag{3.24}$$

$$T_{(t)}\Big|_{r=\infty} = T_s \tag{3.25}$$

$$\lim_{y \longrightarrow 0} \quad 2y \frac{dT}{dy} = -\frac{Q}{2\pi K} \tag{3.26}$$

By comparing Equations 3.26 and 3.23, values of integration constant can be obtained as:

$$C_1 = -\frac{Q}{4\pi K} \tag{3.27}$$

Upon substitution of Equation 3.27 into Equation 3.22 one gets:

$$\frac{dT}{dy} = -\frac{Q}{4\pi K} \frac{e^{-y}}{y} \tag{3.28}$$

Upon integration of Equation 3.28 and interchanging integration limits it can be written as:

$$T = \frac{Q}{4\pi K} \int_y^\infty \frac{e^{-y}}{y} dy + C_2 \tag{3.29}$$

An exponential integral is defined as:

$$-E_i(-y) = \int_y^\infty \frac{e^{-y}}{y} dy \tag{3.30}$$

By substituting value of exponential integral as defined in Equation 3.30 one gets:

$$T = -\frac{Q}{4\pi K} E_i(-y) + C_2 \tag{3.31}$$

Upon applying boundary conditions of Equation 3.25 and substituting the value of y into Equation 3.31, it can be expressed as:

$$T_s - T = -\frac{Q}{4\pi K}\left[E_i\left(-\frac{\rho C_f r^2}{4Kt}\right)\right] \tag{3.32}$$

Upon rearranging, Equation 3.32 can be written as:

$$T - T_s = \frac{Q}{4\pi K}\left[E_i\left(-\frac{\rho C_f r^2}{4Kt}\right)\right] \tag{3.33}$$

In the literature Equation 3.33 is often expressed in terms of dimensionless parameters as:

$$T_D = \frac{q_D}{2}\left[E_i\left(-\frac{1}{4t_D}\right)\right] \tag{3.34}$$

where

$$T_D = \frac{T_i - T_s}{T_s} \tag{3.35}$$

$$q_D = \frac{Q}{2\pi K T_s} \tag{3.36}$$

$$t_D = \frac{Kt}{\rho C_f r^2} \tag{3.37}$$

E_i = exponential integral

T_i = measured temperature, i=1,2,3...=number of temperature runs

T_s = stabilized formation temperature, ^oF

Q = rate of heat flow, BTU/Hr-Ft

K = rock thermal conductivity, BTU/Hr-Ft-^oF

t = time, hours

ρ = density of the formation, lbs/Cu Ft

r_w = well hole radius, Ft.

C_f = specific heat of the formation, BTU/Lb-^oF

By using the principle of superposition for a single well in an infinite heat reservoir and for one drawdown and one buildup in temperature as shown in Figure 12, Equation 3.33 can be written as:

$$T_D = \frac{q_D}{2}\left[E_i\left(-\frac{1}{4t_{D_1}}\right) - E_i\left(-\frac{1}{4t_{D_2}}\right)\right] \qquad (3.38)$$

Thermal Conductivity Determination

Equation 3.38 developed above forms a basis for the determination of thermal conductivity. Jaeger (47), Ingersoll and Zoebel (48) have shown that the exponential integral in Equation 3.38 can be further expanded as follows:

$$-E_i(-x) = \int_X^\infty \frac{e^{-r}}{r}\, dr$$

$$= -0.57722 - \ell nx + x - \frac{x^2}{2(2!)} + \frac{x^3}{3(3!)} \cdots \qquad (3.39)$$

$$\cdots \frac{(-1)^{n+1} x^n}{n(n!)}$$

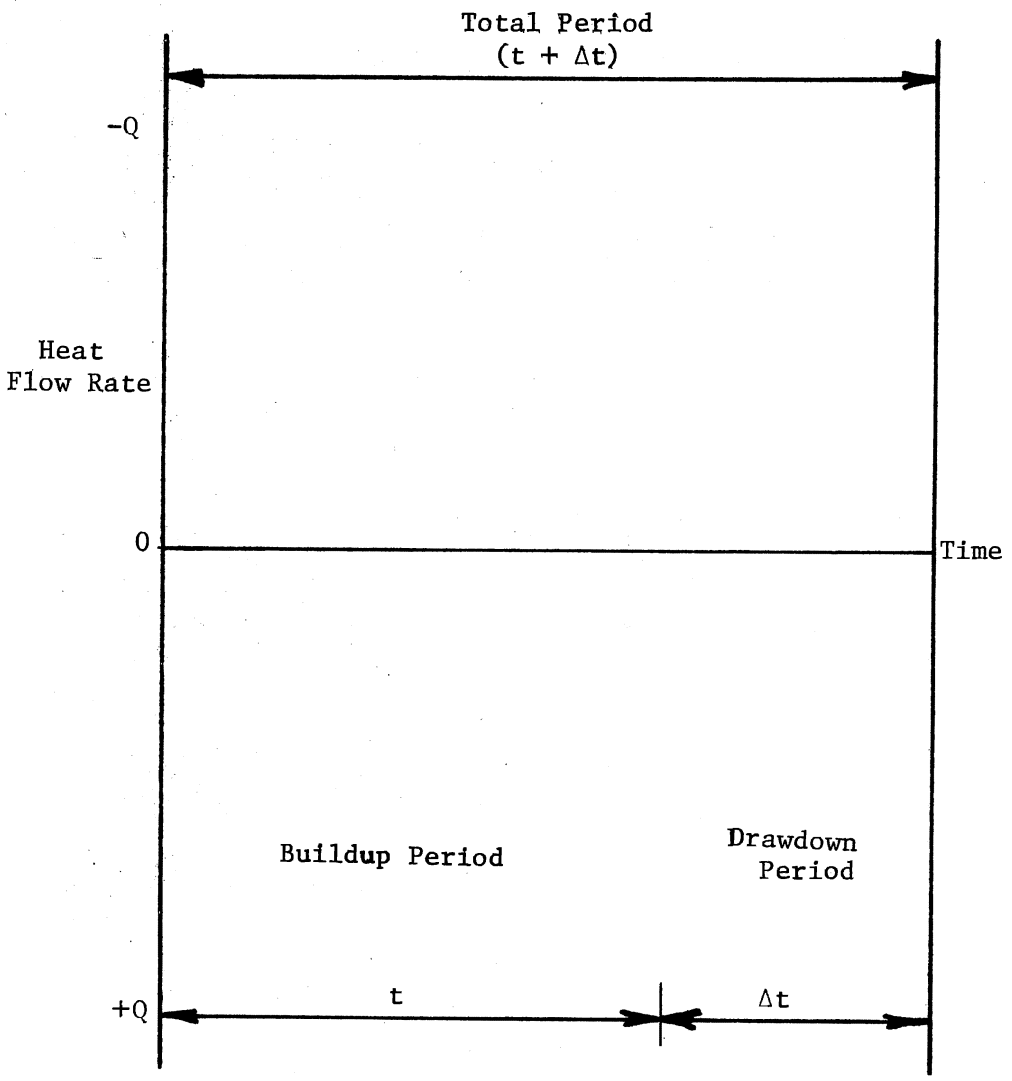

Figure 12. Schematic Representation of a Temperature Buildup and Drawdown in a Well Bore

When the argument $x = 1/4t_D$, the Kelvin solution becomes

$$-E_i(-1/4t_D) = -0.57722 - \ell n\ (1/4t_D) + 1/4t_D - \frac{(1/4t_D)^2}{2(2!)} + \frac{(1/4t_D)^3}{3(3!)} \cdots \tag{3.40}$$

When $x \leq 0.016$, then $t_D > 25$, the first two terms contribute more than 99.75 percent of the overall value of the E_i function. Then, for all practical purposes, the functional solution can be expressed as:

$$-E_i(-1/4t_D) = \ell n\ t_D + 0.80907. \tag{3.41}$$

Substituting Equation 3.41 into 3.38 gives

$$T_i - T_s = \frac{Q}{4\pi K}(-\ell n\ t_{D_1} - 0.80907 + \ell n\ t_{D_2} + 0.80907) \tag{3.42}$$

$$= \frac{Q}{4\pi K} \ell n \frac{t_{D_2}}{t_{D_1}} \quad . \tag{3.43}$$

Substituting for t_{D_1} and t_{D_2} in Equation 3.43 and rearranging gives Equation 3.44

$$T_i - T_s = \frac{Q}{4\pi K} \ell n \left(\frac{\Delta t}{t + \Delta t}\right) \tag{3.44}$$

An analogous form of Equation 3.44 has been used in fluid flow through porous media for more than a decade to obtain permeability and stabilized formation pressures for a producing zone. Equation

3.44 has been used to obtain the stabilized formation temperature "T_s" by Timko and Fertle and recently by Dowdell and Cobb (51, 52). For those cases where circulation times are not very large, Equation 3.44 gives stabilized formation temperatures accurate to within $\pm$ 2% when compared with the measured static formation temperatures (52). Since stabilized formation temperature is obtained by extrapolating the T_i vs. $\ell n\ (\frac{\Delta t}{t+\Delta t})$ plot as shown in Figure 13, the slope of the straight line will equal to

$$M = \frac{Q}{4\pi K} \tag{3.45}$$

Since the heat lost from the formation is equal to the heat gained by the drilling fluid in the well bore, the rate of heat flow can be calculated if two temperature values at two different time periods are available. Knowing the rate of heat flow and the slope, the thermal conductivity value can be calculated from Equation 3.45.

Equation 3.44 forms the mathematical basis for the computation of the "apparent" thermal conductivity of rocks in situ. Information needed to apply the above model is temperature at two different times and associated mud and bore hole characteristics. A series of calculations were carried out by using the time-temperature data collected from an oil well in Stephens County, Oklahoma, by using the above approach. Results of the calculations are presented in Chapter VI of this study and a step by step computational procedure is shown in Appendix B, Table V.

Thermal Diffusivity Determination

In conductive heat flow situations involving short time periods,

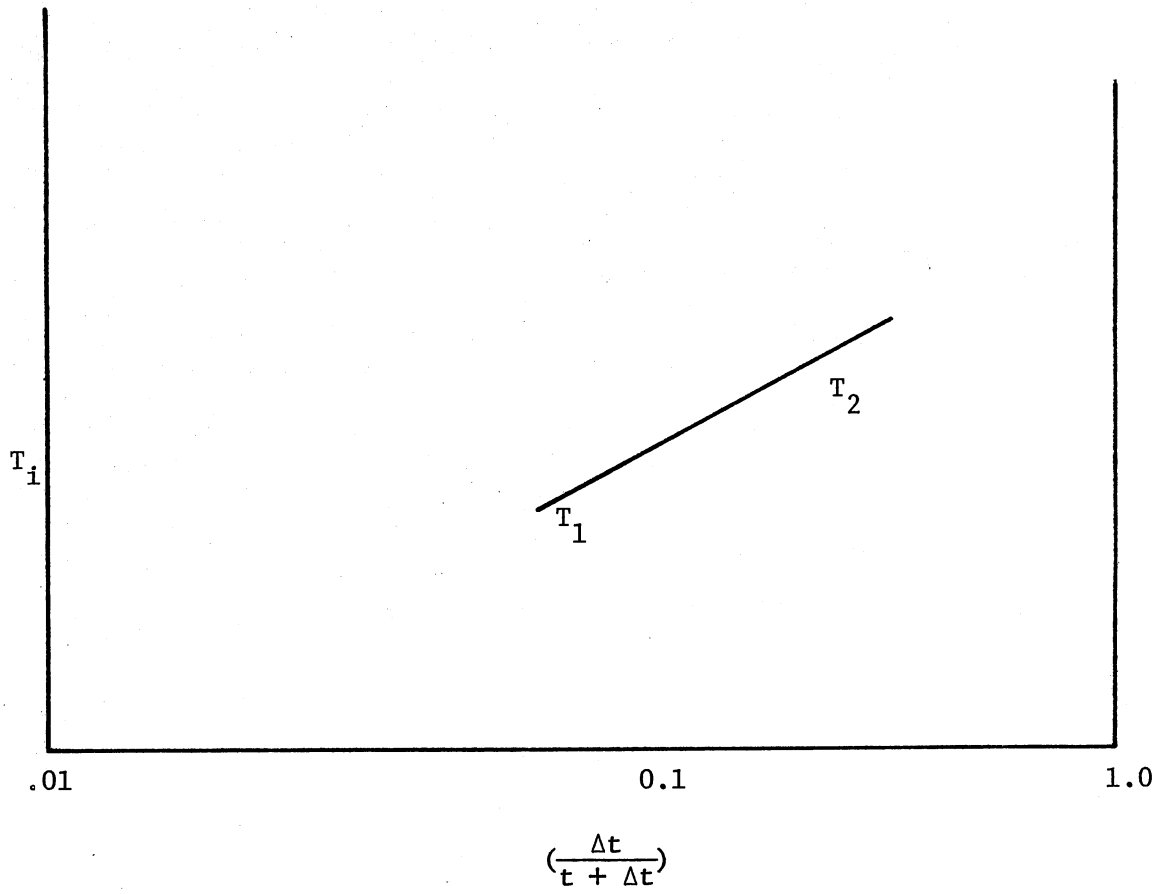

Figure 13. Semilogarithmic Time Ratio vs. Temperature Plot

the thermal diffusivity instead of the thermal conductivity more accurately accounts for the transient-temperature behavior of rocks. This property can be calculated from thermal conductivity if density and specific heat of the rocks are also known. Since this data is normally available through laboratory measurements, an alternate scheme which has been found to be valuable in predicting the thermal diffusivity values of rocks is presented here. This method is an extension of the in situ thermal conductivity evaluation technique described previously and a detailed description of the technique is presented below starting with an equation similar to Equation 3.12.

The temperature T at time t and at a distance r is given by Carslaw and Jaeger (52) as:

$$T = \frac{Q}{4\pi K} \int_{X}^{\infty} e^{-u} u^{-1} du + C \tag{3.46}$$

which according to Equation 3.33 is equivalent to

$$\Delta T = \frac{Q}{4\pi K} E_i \left(- r^2/4\alpha t\right) \tag{3.47}$$

For this study, temperature at different time periods are available; therefore, these temperatures can be described in terms of a series of euqations of the type as Equation 3.47. For two temperatures at two different times the equations will be

$$\Delta T_1 = \frac{Q_1}{4\pi K} E_i \left(- r^2/4\alpha t_1\right) \tag{3.48}$$

$$\Delta T_2 = \frac{Q_2}{4\pi K} E_i \left(- r^2/4\alpha t_2\right) \tag{3.49}$$

Assuming that the thermal conductivity does not change appreciatively with temperature over time interval and by dividing Equation 3.49 by Equation 3.48 one gets:

$$\frac{\Delta T_2}{\Delta T_1} = \left[Q_2 E_i\left(-\frac{r^2}{4\alpha t_2}\right)\right] \Big/ \left[Q_1 E_i\left(-\frac{r^2}{4\alpha t_1}\right)\right] \tag{3.50}$$

Representing $r^2/4\alpha t_1$ and $r^2/4\alpha t_2$ by Z_1 and Z_2 respectively and substituting into 3.50 gives

$$\frac{\Delta T_2}{\Delta T_1} = \frac{Q_2 E_i\ (Z_2)}{Q_1 E_i\ (Z_1)} \tag{3.51}$$

The exponential integral can be expanded in series form as

$$E_i\ (-Z_1) = 0.57722 + \ell n Z_1 - Z_1 + \frac{Z_1^{\,2}}{2(2!)} - \frac{Z_1^{\,3}}{3(3!)} + \ldots \tag{3.52}$$

Similarly

$$E_i\ (-Z_2) = 0.57722 + \ell n Z_2 - Z_2 + \frac{Z_2^{\,2}}{2(2!)} - \frac{Z_2^{\,3}}{3(3!)} + \ldots \tag{3.53}$$

Substituting for Z_1 and Z_2 into Equation 3.51 gives

$$\frac{\Delta T_2}{\Delta T_1} = \frac{Q_2[0.57722 + \ell n(r^2/4\alpha t_2) - (r^2/4\alpha t_2) + (r^2/4\alpha t_2)^2 / 2(2!) - (r^2/4\alpha t_2)^3 / 3(3!) + \ldots]}{Q_1[0.57722 + \ell n(r^2/4\alpha t_1) - (r^2/4\alpha t_1) + (r^2/4\alpha t_1)^2 / 2(2!) - (r^2/4\alpha t_1)^3 / 3(3!) + \ldots]} \tag{3.54}$$

By using the nomograph of Figure 34 and knowing the temperature runs at two different times, the only unknown of Equation 3.54 (α) can be easily obtained. A series of calculations using this approach were performed on the field data and the results obtained are presented in Chapter VI. A step by step computational procedure is shown in Appendix B, Table VII.

Significance of Assumptions

In the previous section, a mathematical model was developed to simulate unsteady state temperature buildup of the fluid contained in a well bore. The development of the model involved the following assumptions:

1. Heat flow primarily occurs in the radial direction.
2. The formation surrounding the bore hole is thick and homogeneous.
3. Heat transfer in the well bore is primarily by conduction.
4. The dimensionless time variable (t_D) is greater than 25.
5. Applicability of the boundary conditions.

This section will examine the significance of these assumptions in the order listed above and also investigate their influence on the accuracy of the model.

Heat Flow Primarily in the Radial Direction

During circulation of a well bore a fluid is pumped down the drill pipe out through the bit, and up the annular space between the drill pipe and the formation. The rate of heat flow into or out of the well bore depends upon the temperature difference

between the well bore fluid and the surrounding rock, and the rock thermal properties. Since the process of circulation disturbs temperature in the vicinity of the rocks, and the drilling fluid usually exits from the drill bit at a lower temperature than the surrounding formation, a heat sink is established in the lower sections of a well bore. The primary path of heat flow is, therefore, in the radial direction. Hence, after the circulation ceases, the assumption that heat flow occurs primarily in the radial direction appears to be justified for an investigation of that portion of the bore hole where the annular fluid temperature is substantially less than the rock temperature.

Formation Thick and Homogeneous

During temperature buildup, heat flow might occur across adjacent beds because of differences in their thermal properties. This effect is comparable with the adjacent bed effect in electric logging. However, if the bed is thick, then the adjacent bed effect will be limited primarily to the boundaries of the formations and the temperature buildup towards the center of the bed will not be affected.

Sedimentary rocks, because of their mode of deposition, often have non-homogeneities. For the purpose of this study it is assumed that the formation is homogeneous and isotropic.

Negligible Convection in the Well Bore

Bentonitic clays are commonly used as one of the major constituents of the drilling muds. These clays possess hydrophilic properties and, moreover, because of residual charges on the clay

particles, the clay suspension forms a gel by interlocking of the particles. This gel restricts a free movement of water molecules. As a result when the temperature buildup is allowed to take place for a long time (more than 24 hours), the convection effect begins to appear, especially in large diameter holes (D > 10"). For relatively short buildup times, this effect is small and therefore can be safely neglected.

Dimensionless Time Greater Than 25

In deriving Equation 3.41 from Equation 3.40 it was mentioned that the assumption of dimensionless time greater than twenty-five leads to a simplification of the original equation. In order to show the influence of this assumption on the accuracy of the model, response by using the E_i function approach for various values of dimensionless time is plotted as Curve A in Figure 14. An analogous plot, using the logarithmic approach for various values of dimensionless times is plotted as curve B. From a comparison of these two curves, it can be seen that for a dimensionless time greater than 25 the corresponding values are practically the same.

Applicability of Boundary Conditions

In order to solve Equation 3.3 to obtain Equation 3.32, the following initial and boundary conditions were used:

$$T = T_s \text{ at } t = 0 \text{ for all } r \tag{3.55}$$

$$T = T_s \text{ as } r \to \infty \text{ for all } t \tag{3.56}$$

$$T = T_{mud} \text{ at } r = r_w \text{ for all } \Delta t \tag{3.57}$$

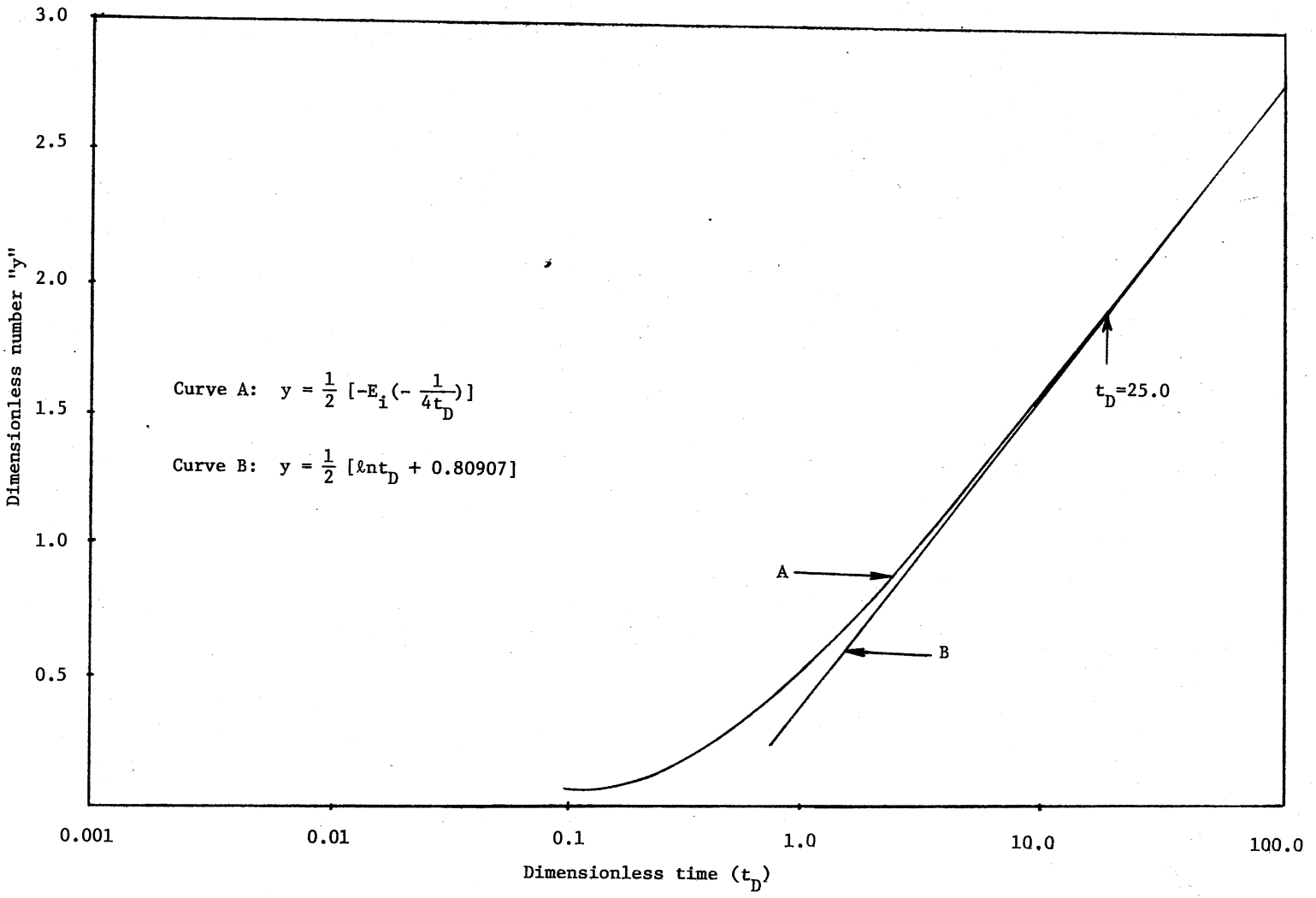

Figure 14. Comparison of Exponential Integral and Logarithmic Response

Equations 3.55 and 3.56 are the initial and final boundary conditions respectively. These two equations define the range of measured well bore temperatures as a function of time, and dictate that the measured temperatures approach equilibrium formation temperatures at an infinite distance away from the well bore as the time passes. Boundary condition 3.30 dictates that during the circulation time, temperature gradient in the reservoir remains constant, and that the temperature in the bore hole against the formation remains equal to that of the mud temperature. Temperature gradient in the formation, however, is a function of time and over prolonged periods of time will change drastically resulting in a change in the rate of heat flow from the formation into the well bore. For circulation times which are not very long, it has been shown that the assumption that the mud temperature is equal to the formation temperature, and that the temperature gradient in the formation remains constant is satisfied (52).

Summary

In summary this chapter includes a description of the physical model followed by its mathematical simulation to obtain the thermal properties of rocks in situ. Significance of the assumptions made in the development of the mathematical model was discussed with a view to explain under what conditions this model can be applied to a physical situation. In the next chapter those errors which could influence the results of this model resulting from inadequacy of the input data are discussed.

CHAPTER IV

INPUT DATA

Introduction

Input data needed for the mathematical model primarily consists of temperature as a function of time recorded against depth in a well bore. The other parameters e.g. well bore radius, weight of the drilling fluid, etc., can be obtained accurately from logs. The accuracy of the results predicted by the mathematical model will, therefore, depend to a great degree upon how accurately the temperature data in the well bore reflects the heat flow conditions in situ. A number of factors can influence the temperature build up in a well bore. Some of the relatively more important factors affecting a temperature data collection effort are presented in this chapter under accuracy considerations.

In the light of discussion of the accuracy consideration, suitability of the experimentally collected data used in this study is evaluated by systematically considering factors that might affect its accuracy. A procedure was developed to smooth the raw experimental data before inputing it to the mathematical model. Smoothing techniques and other discussions related to the analysis of the input-data along with accuracy considerations are also presented in this chapter.

Accuracy Considerations

A temperature data collection effort inside a well bore can be influenced either by the inaccuracies inherrent in the temperature sensing devices and/or by the circumstances which affect the heat flow conditions around the well bore. Both of these aspects of temperature measurement in a bore hole are discussed as follows:

Sensitivity of Temperature Logging Tools

A variety of temperature logging tools (e.g. single-element temperature gradient tool, dual-element differential delta tool and memory circuit differential tool), are currently being used in the industry. Invariably all of these logging tools use platinum resistance thermometers in their temperature sensing elements. The platinum resistance thermometers are capable of recording temperatures to within $\pm$ 0.1^{o}F of the temperature being measured and are very accurate (53, 54). Since the sensing devices transfer temperature to the surface in the form of a low voltage signal, resistance of the wire which transmits the signal to the surface recording systems becomes important -- especially so in temperature logging of deep wells. A variety of temperature compensating devices which use a manual input for the wire resistance, and an automatic feed from the logged depth indicator, compensate for the loss in electrical signal. Since the logging cables are properly insulated, the temperature variations inside the bore hole do not appear to significantly influence accuracy of the temperatures measured.

In addition to the sensitivity of the temperature measuring devices, the temperature logging speed also influences the accuracy

of the recorded temperatures. If a well bore was logged at too high a speed, the temperature log does not show variations in lithology along the bore hole. It has been found that temperature logging speed should correspond with the SP logging devices. Perhaps that is why the two devices are often used together (55, 56, 57).

Influence of the Bore Hole Condition

Type of fluid produced from a pay zone, condition of the well bore and characteristics of the drilling fluids along with the lithological uncertainties of the drilled formations combine to introduce a number of variables which effect the temperature logs. Some of the resulting manifestations in the form of water migration in the well bore, oil and gas production, and casing and cementing of the well bore, are discussed here to give an idea as to what sources of error would be avoided in obtaining accurate temperature values for a bore hole.

Effect of Oil and Gas Production

When an oil reservoir is tapped, part of the gas dissolved in oil comes out of solution and escapes into the well bore. It changes the temperature in the immediate vicinity of the bore hole because of Joule-Thompson cooling. Effect of flowing gas on the bore hole temperature can be seen from two temperature runs made on a gas producing well after and before shut-in as shown in Figure 15 (56, 57). The shut-in temperature varies from as much as $29^{o}F$ to $4^{o}F$ from the flowing gas temperature. This sudden temperature change was used in the past to help locate gas producing zones and detection of gas-oil contact in thick producing zones.

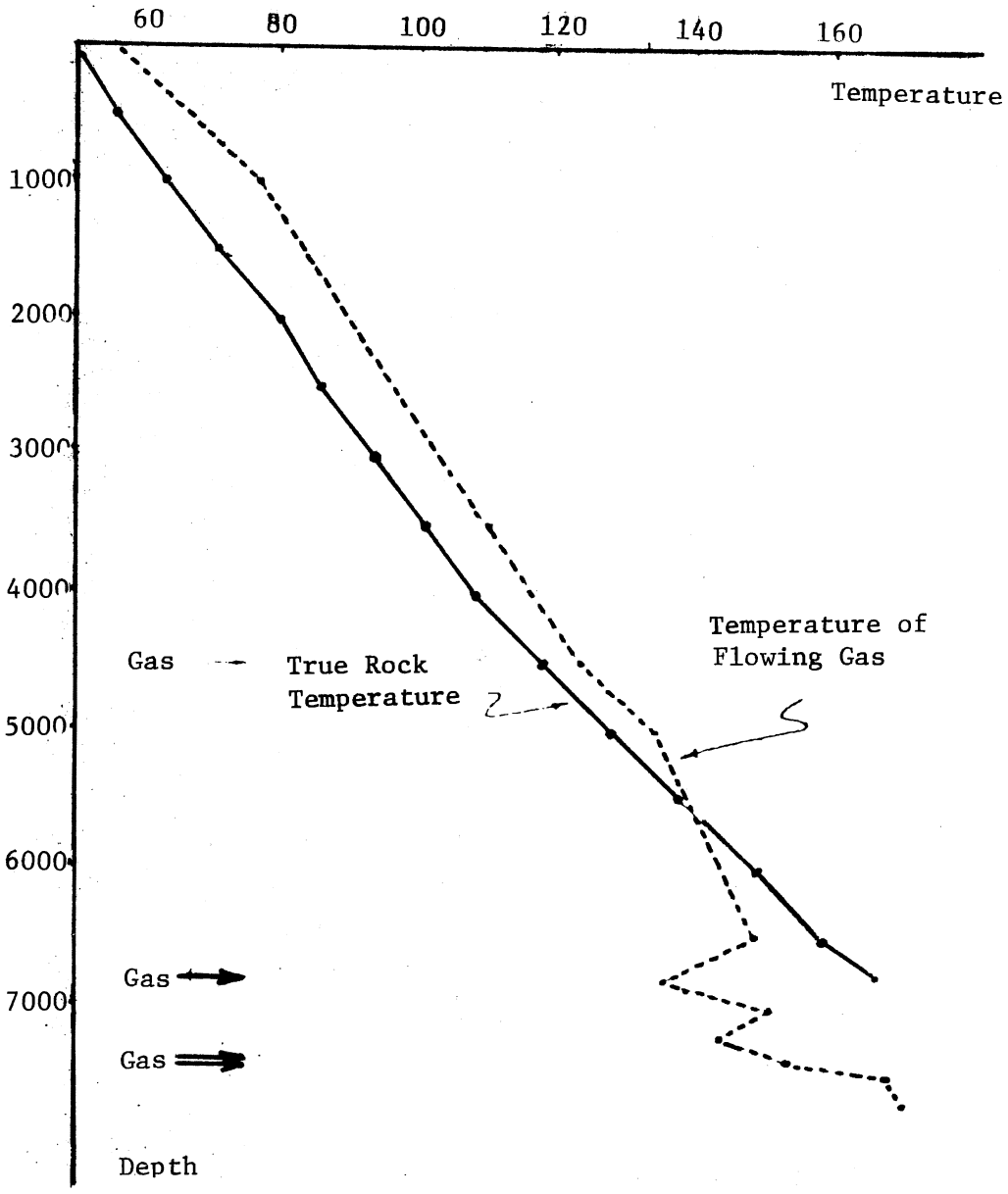

Figure 15. Effect of Gas Production on Temperature Surveys

Effect of Water Migration in the Bore Holes

It has often been observed that active water influx from a formation into the well bore changes its temperature. A good example of this effect is shown in Figure 16. Three temperature surveys of a well in West Virginia are presented. The first run was made immediately after drilling to the terminal depth. The second run was made two hours after the first run, and the third run was made about two hours after the second run. The second and the third runs show the same temperature at 3026 feet, but above that the temperature of the well bore is incoherent. This unusual effect was attributed to water migration at 3026 feet from the formation into the well bore, and was remedied by selectively plugging the water-bearing formation.

Effects of Casing

The temperature variations indicative of lithology are still present when the temperature survey is repeated after casing an open hole. This effect is attributed to the much higher thermal conductivity of the casing steel as compared to that of the surrounding rock; therefore, heat flows freely from the formation and casing interface into the well bore. A good example of temperature indicating lithology is presented in Figure 17. In this figure two temperature surveys are shown; one before the casing and the second after the casing was run. Various characteristics of the temperature log in the first survey can be easily distinguished in the second survey.

Effect of Cementing on Temperature Surveys

In modern well completion procedures a portion of the well bore

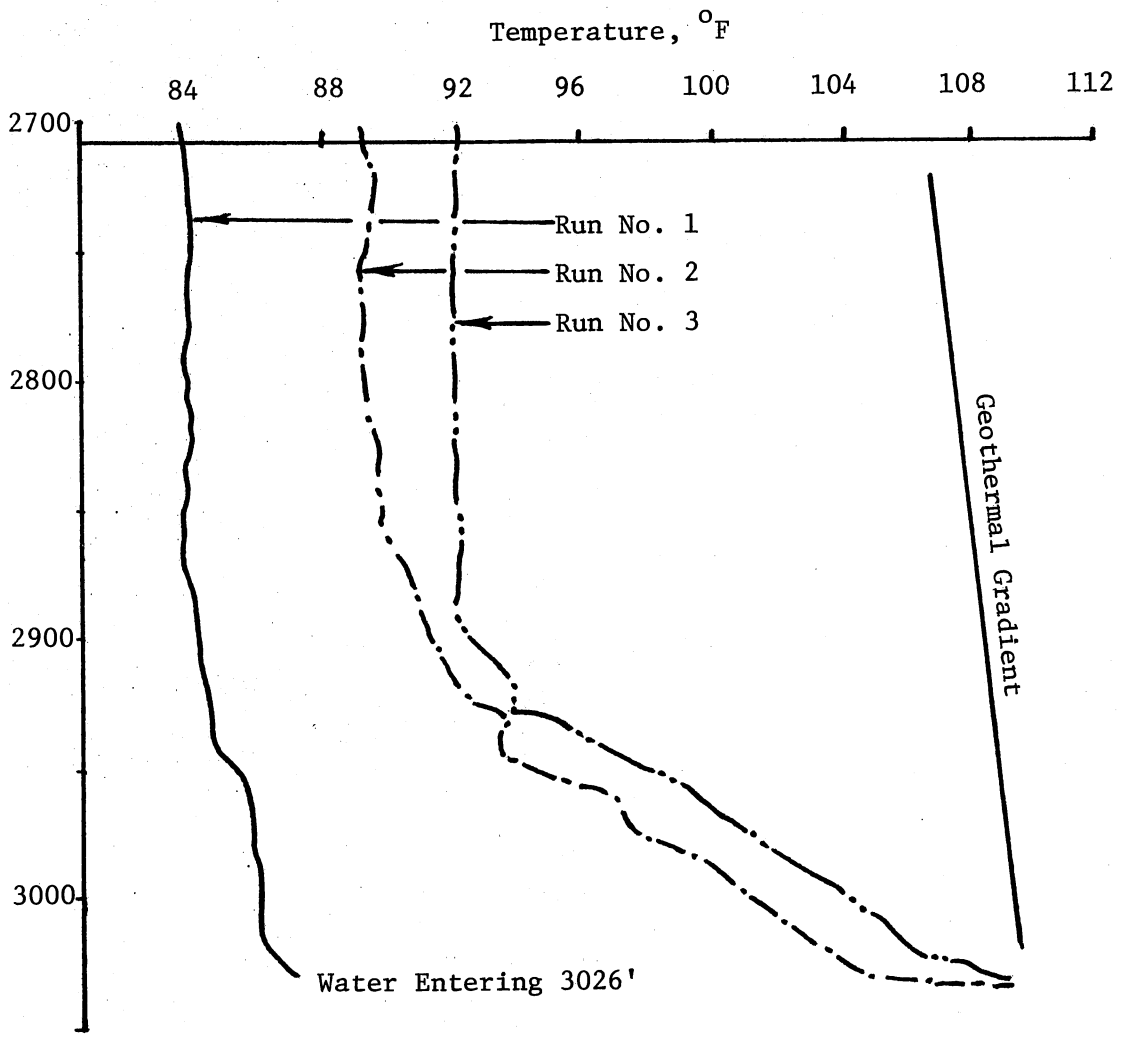

Figure 16. Effect of Water Migration on Temperature Surveys (54)

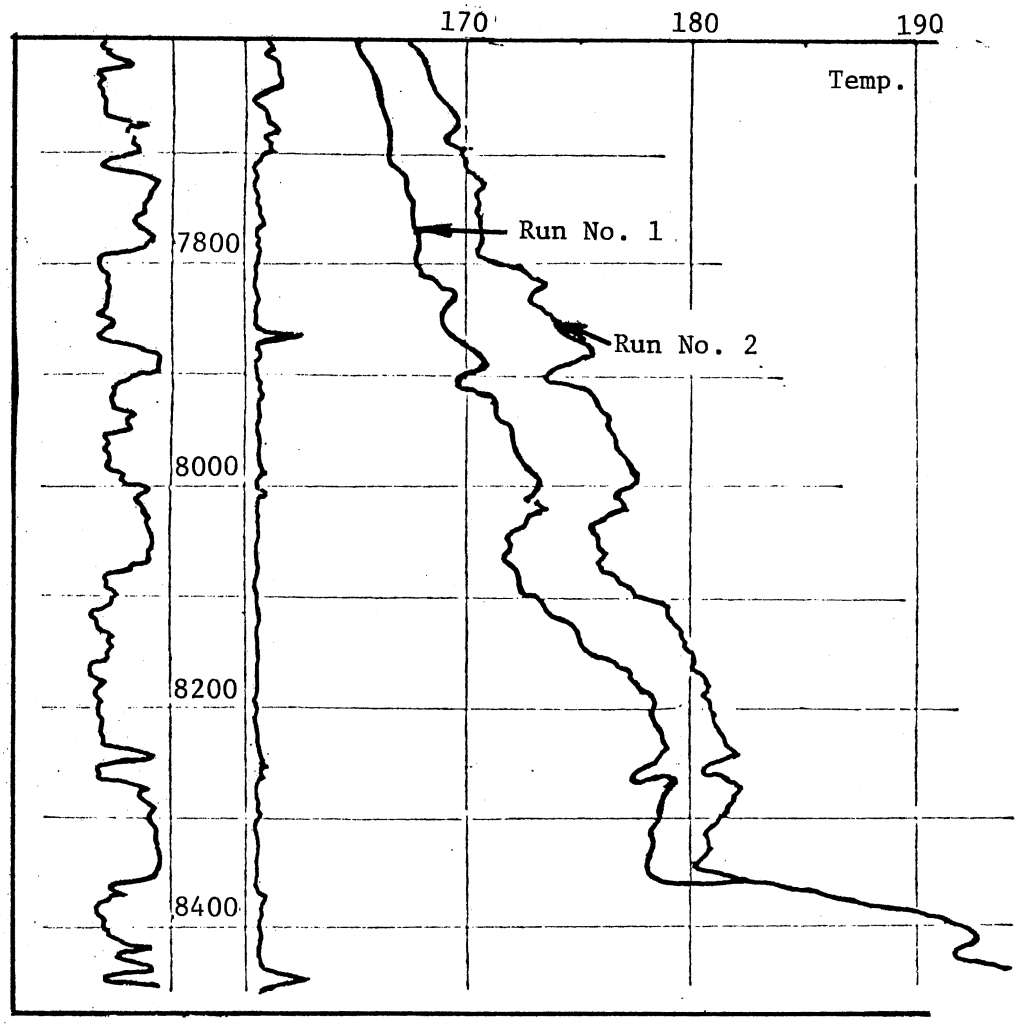

Figure 17. Effect of Casing on Temperature Surveys

is cemented to exclude water-bearing formation, to protect the producing formation, and to control the flow of oil and gas from the formation into the well bore. A good example of effect of cementing on temperature surveys is shown in Figure 18. In this figure two temperature runs are shown. The first run was made immediately after cementing the well bore and the second run after circulating the well for about five hours. The setting of cement is an exothermic process, and as a result the temperature in the immediate vicinity of the cement is severely modified. Temperature surveys in old wells, where this temporary effect has dissipated, reflect more the properties of the surrounding lithology than the cement. Moreover, Portland cement has thermal conductivity values in the range of 1 to 2 x 10^{-3} cal/cm-C^{o}-sec. which is very close to that of sandstone. Therefore, the effects due to cementation can be safely neglected unless the well has been very recently completed.

Presentation and Analysis of Input Data

In order to obtain meaningful results from the mathematical model presented in Chapter III, a series of temperature runs in a well bore as a function of time are needed. The results from the mathematical model, however, need to be checked to ascertain their accuracy. Experimental thermal property data is therefore also needed to complete this study. The data needed for this study is not collected as part of a routine logging practice. As a result of an extensive literature survey a well was located in Stephens County, Oklahoma where time-temperature and thermal property data were available. This data was used by the Western Logging Company

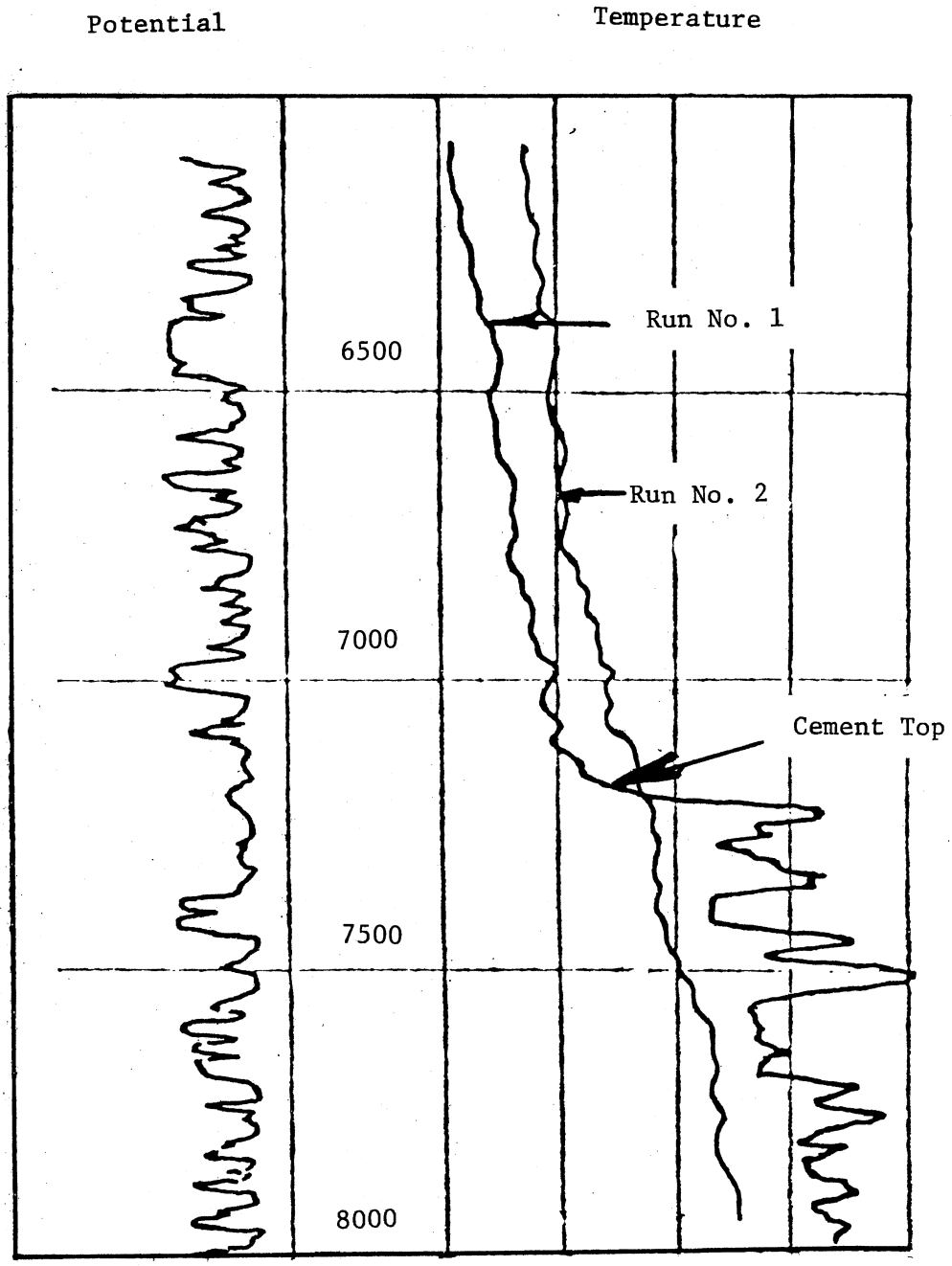

Figure 18. Effect of Cementation on Temperature Surveys

in predicting the static temperature profiles on a separate lithology study for the same interval. This data along with other logging data collected by the Atlantic Richfield Oil Company is presented in this chapter.

Presentation of Input Data

The input data was collected on Humphry Unit No. 65 well, East Velma Field, Stephens County, Oklahoma. A brief history and geology of the oil field is presented here (59, 60, 61).

Production History and Geologic Environment of the East Velma Oil Field

The East Velma Field is located in the T-1S, R4W and T-2S, R4W, Stephens County, Oklahoma as can be seen from the structural map of the oil field presented as Figure 19. This field was discovered in July 1917 by the Texas Oil Company and the discovery well's oil production was from a shallow Permian sand. There was no pipeline outlet until 1920, and development of the oil field was very insignificant. However, since then, about 110 wells have been drilled to tap the mineral resources of this field. About ten years ago this field was abandoned because of lack of production. Recently a water flooding operation has been started on this field to recover part of the residual oil in place.

Oil production in the East Velma Field is obtained from rocks of Permian, Pennsylvanian, Mississipian and Ordovician ages. The large and faulted Velma structure is located near the southern limit of the Anadarco Basin where originally 7,000 feet of the massive

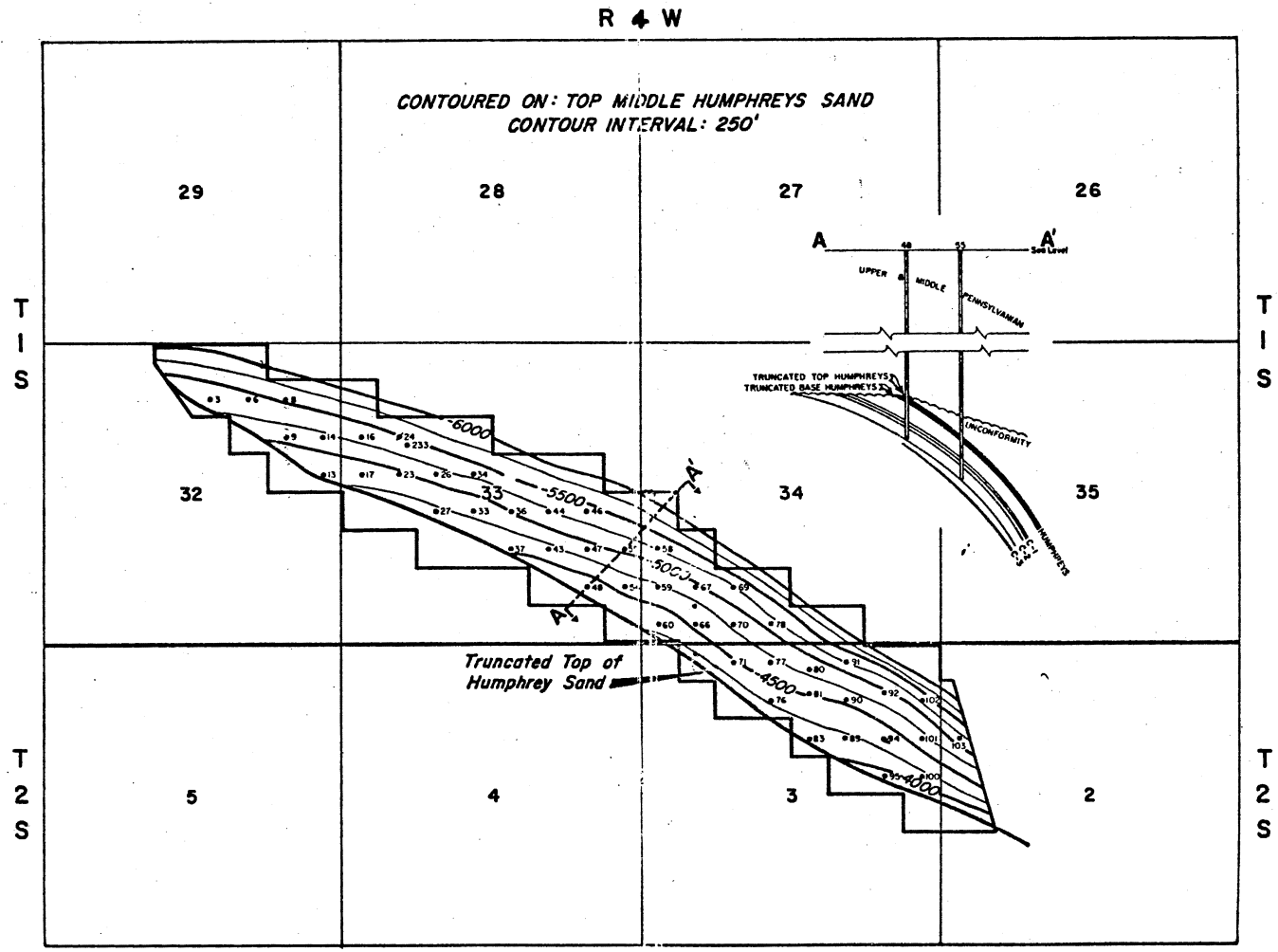

Figure 19. Structural Map of Stephens County, Oklahoma

Pennsylvanian strata were deposited. These strata were subjected to uplift, folding, and faulting in post-Morrow and post Hoxber times. Subsequently the structures formed were truncated by erosion and covered by more than 1,000 feet of predominately red sand stone and shale of Permian age. These sediments have arched into a pronounced mapable subsurface structure as can be seen from Figure 19.

Drilling Data on the Humphry Unit #65 Well

The Humphry Unit #65 well is located in East Velma Field, Stephens County, Oklahoma at NW-NW-NW sec. 3, TWP-2S, RGE-4W. It was drilled to a depth of 5350 feet and tested. The well showed very low production and was abandoned. Later on the well was used as a boundary well to mark the East Velma Oil Field. Other pertinent data on the well is shown in Table I. The 250 foot interval from 5000 feet to 5250 feet is to be evaluated in detail.

Well Log Data on the Humphry Unit #65 Well

SP and electric logs were run in the well bore when it was originally drilled. These logs which are presented in Figure 20 show that the bore hole penetrated through the so-called shale shaker, in which the thin limestone and sand beds are wedged in between the predominately shale setting. Porosity logs were not run originally on the well. A porosity log on an adjacent well, after the common datum for the two wells was matched, is presented in Figure 21 for the same interval. The porosity log shows predominantly low porosity with interbedded streaks of porous zones.

TABLE I

LOCATION AND DRILLING DATA ON HUMPHRY UNIT #65 WELL

Field	East Velma
County	Stephens, Oklahoma
Location	NE.NW.NW Sec-3, TWP-2S RGE-4W
Terminal Depth	5350'
Logged Interval	5000' - 5250'
Density of Drilling Fluid	70.2 pounds/cu ft
Specific Heat of Drilling Fluid	0.8335 Btu/pound
Drill Bit	NX. Diamond
Method of Drilling	Rotary
Drilling Fluid	Water, Clay and Other Chemicals
Temperature Buildup Time Before Run #1	10 Hours
Bore Hole	Open Uncased
Size of Drill Bit	9 7/8"
Casing	Surface Casing To Protect Fresh Water Sand

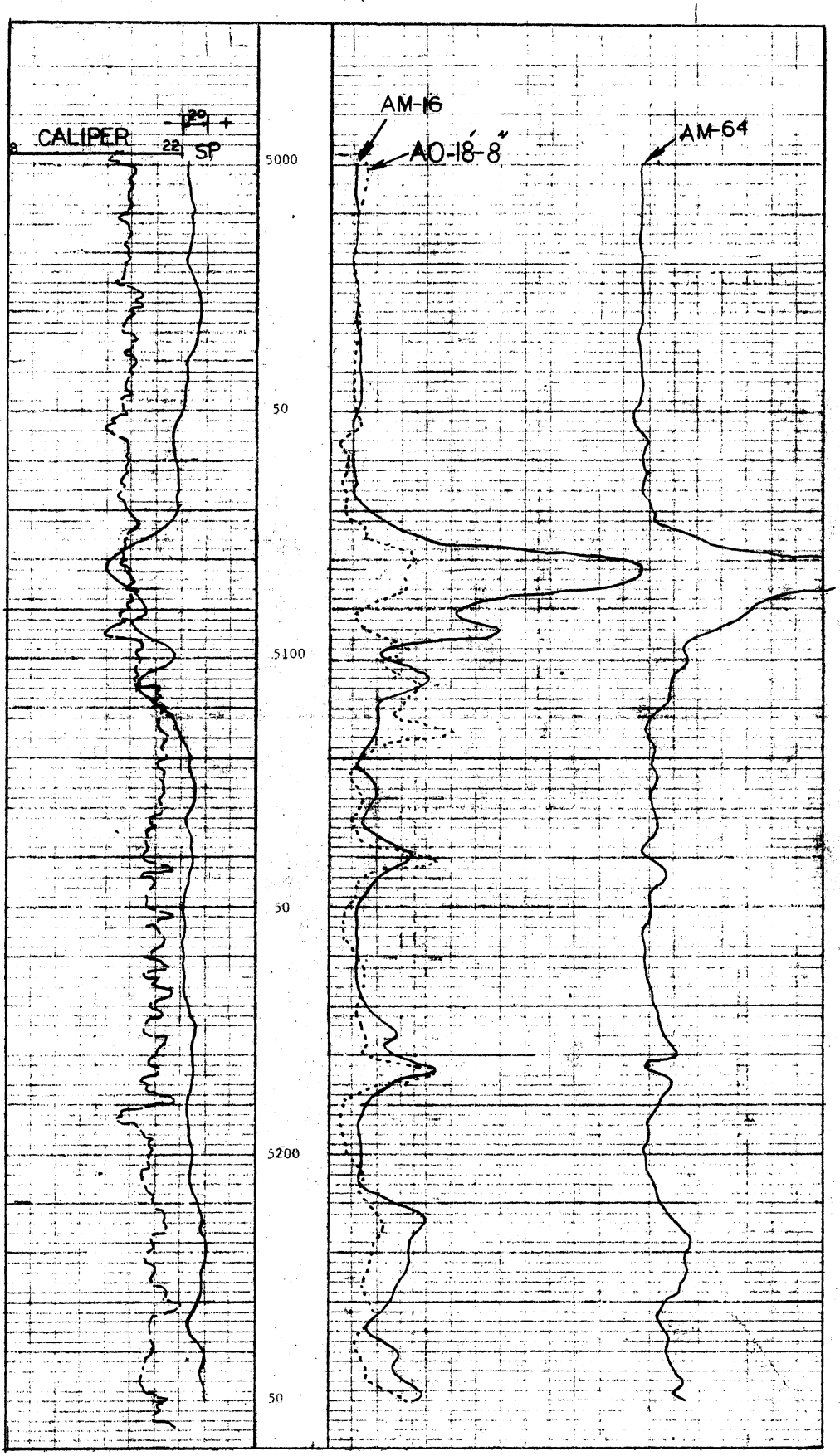

Figure 20. Electric Logs for Humphry #65 Well

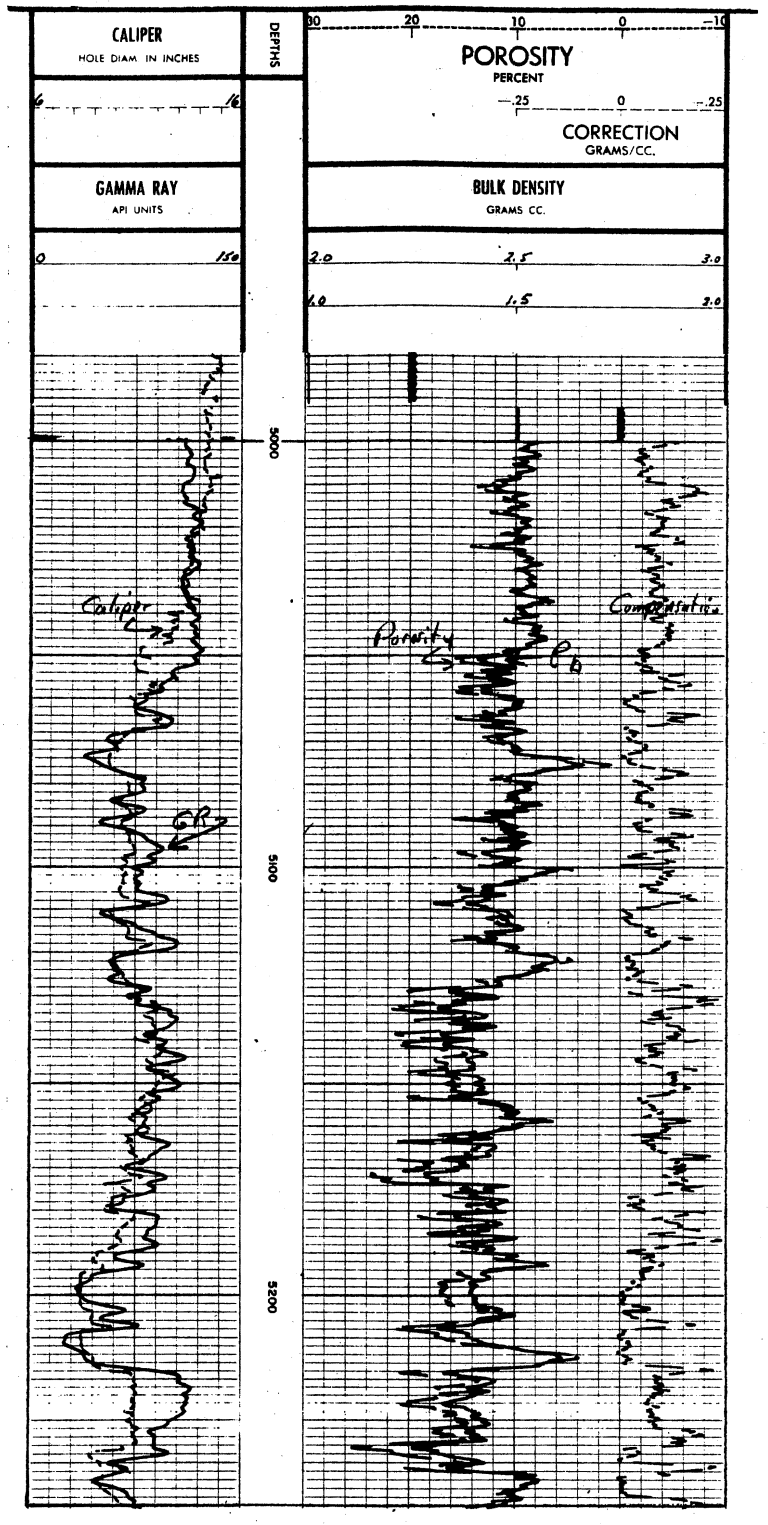

Figure 21. Porosity Log for Humphry #65 Well

This porosity setting describes fairly well the shallow subsurface geology of the area.

In Figure 22, time-temperature data for well #65 Humphry sand East Velma Field is presented. The first temperature run was made at 8:00 p.m. after the well was allowed to stand undisturbed for ten hours, and the subsequent runs were made at 8:30 p.m., 10:00 p.m., 12:00 a.m., 2:00 a.m., 4:00 a.m., and at 6:00 a.m. respectively. The temperature runs were made with a digital two-element tool, and appropriate corrections were made to compensate for wire resistance to obtain correct temperature response. Platinum resistance thermometers were used in sensing temperature in the bore hole, and the speed of the logging tool was controlled to obtain an accurate temperature recording.

Thermal Conductivity and Diffusivity Data

In Figure 23 experimental and interpolated thermal conductivity data for the 250-foot interval is presented. Experimental thermal conductivity values were obtained from cores which were in turn obtained by the use of a side corer, from the formation at preselected locations. The cores were then machined, polished and cut to size, and used in divided-bar apparatus to obtain thermal conductivity values. By comparing the depths at which these cores were taken with the well bore depths on the SP log, thermal conductivity values for the intermediate intervals were "interpolated." The interpolated and experimental thermal conductivity values are also tabulated in Appendix B, Table VI.

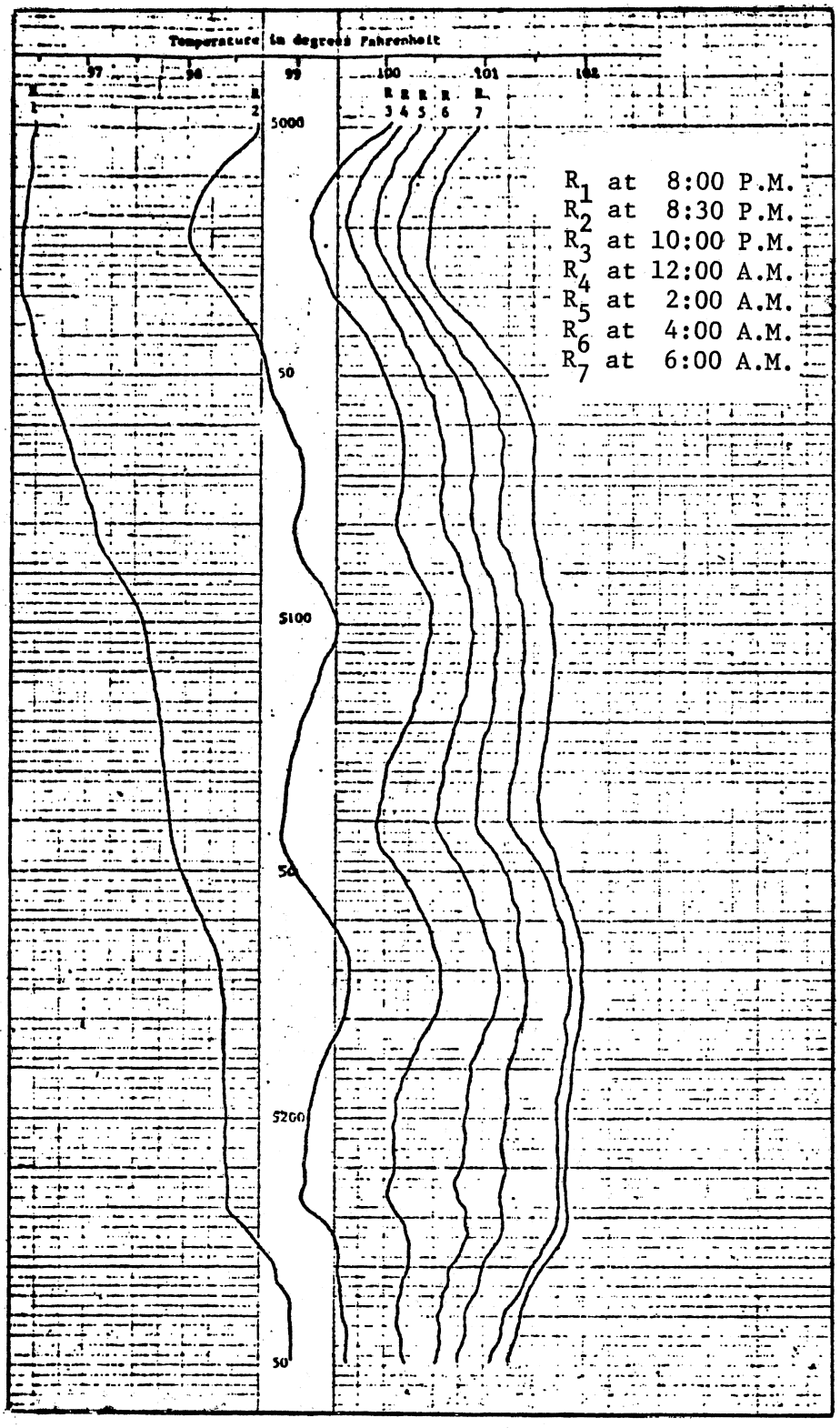

Figure 22. Experimental Time-Temperature Data for Humphry #65 Well

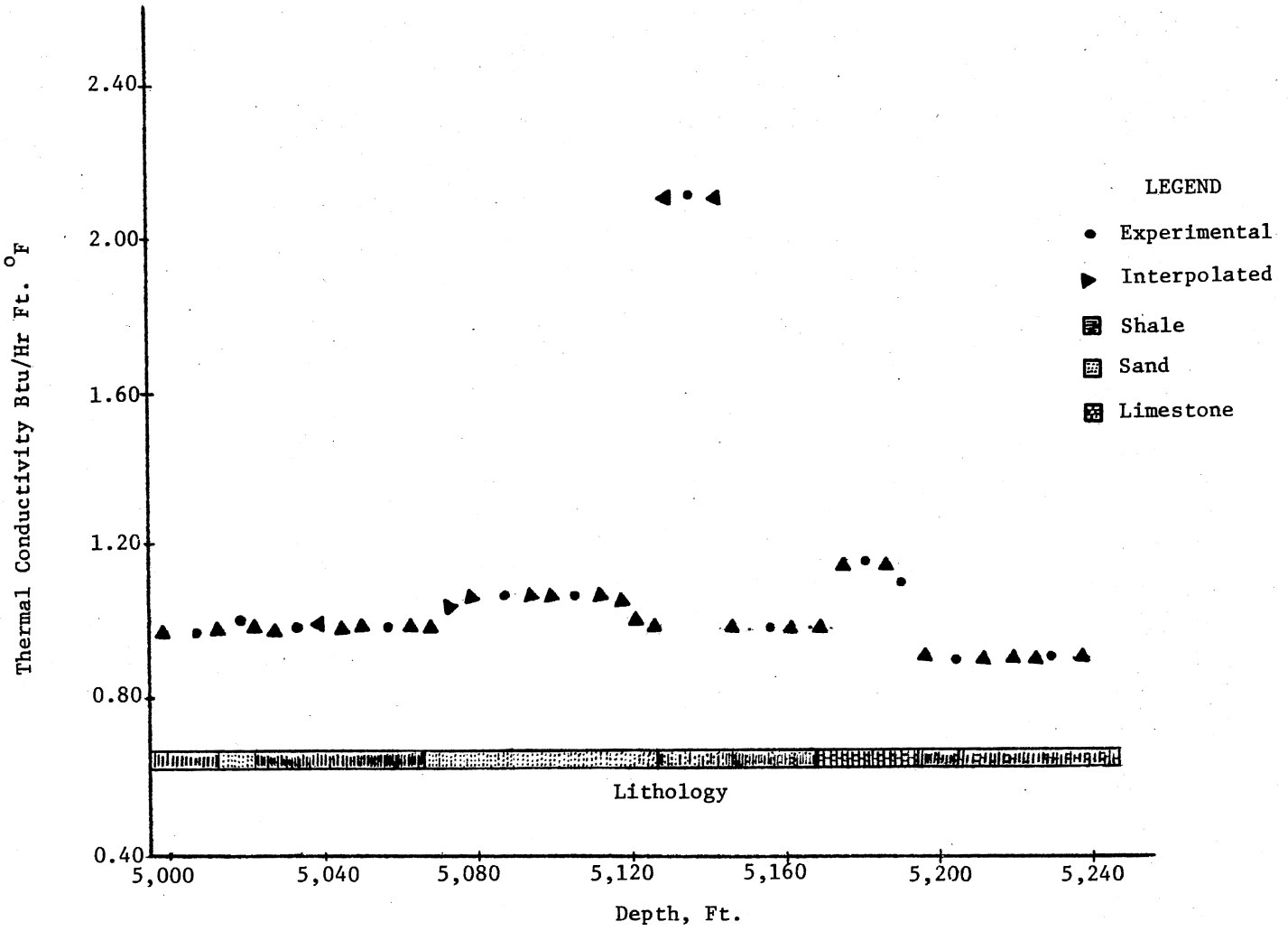

Figure 23. Experimental and Interpolated Thermal Conductivity Data for Humphry #65 Well

In Figure 24, experimental and interpolated thermal diffusivity data for the 250 foot-interval is presented. The experimental thermal diffusivity values were obtained by dividing the experimental thermal conductivity values by the product of density and specific heat. The thermal diffusivity values for the intermediate intervals were interpolated with reference to SP log by comparing the logged depth with the cored depth. The experimental and interpolated thermal diffusivity values are also tabulated in Appendix B, Table VII.

Analysis of Input Data

Under Accuracy Considerations, a number of factors which can influence the well bore temperature values were discussed. The temperature data collected for the Humphry #65 well was analyzed in the light of this discussion to evaluate its accuracy. From well logs presented here the following observations were made regarding the conditions in the well bore.

1. The electrical logs show that the formation under study is a tight formation with a predominantly low porosity.
2. The well is a dry well.
3. There is no evidence of water migration into the well bore.

The above observations show that the data being used in this study is not affected by any of the factors which commonly influence the temperature logging efforts as discussed under Accuracy Consideration.

Correction Procedure for Input Data.

In experimental heat transfer studies a number of authors have noted that frequently the time-temperature values are not accurately

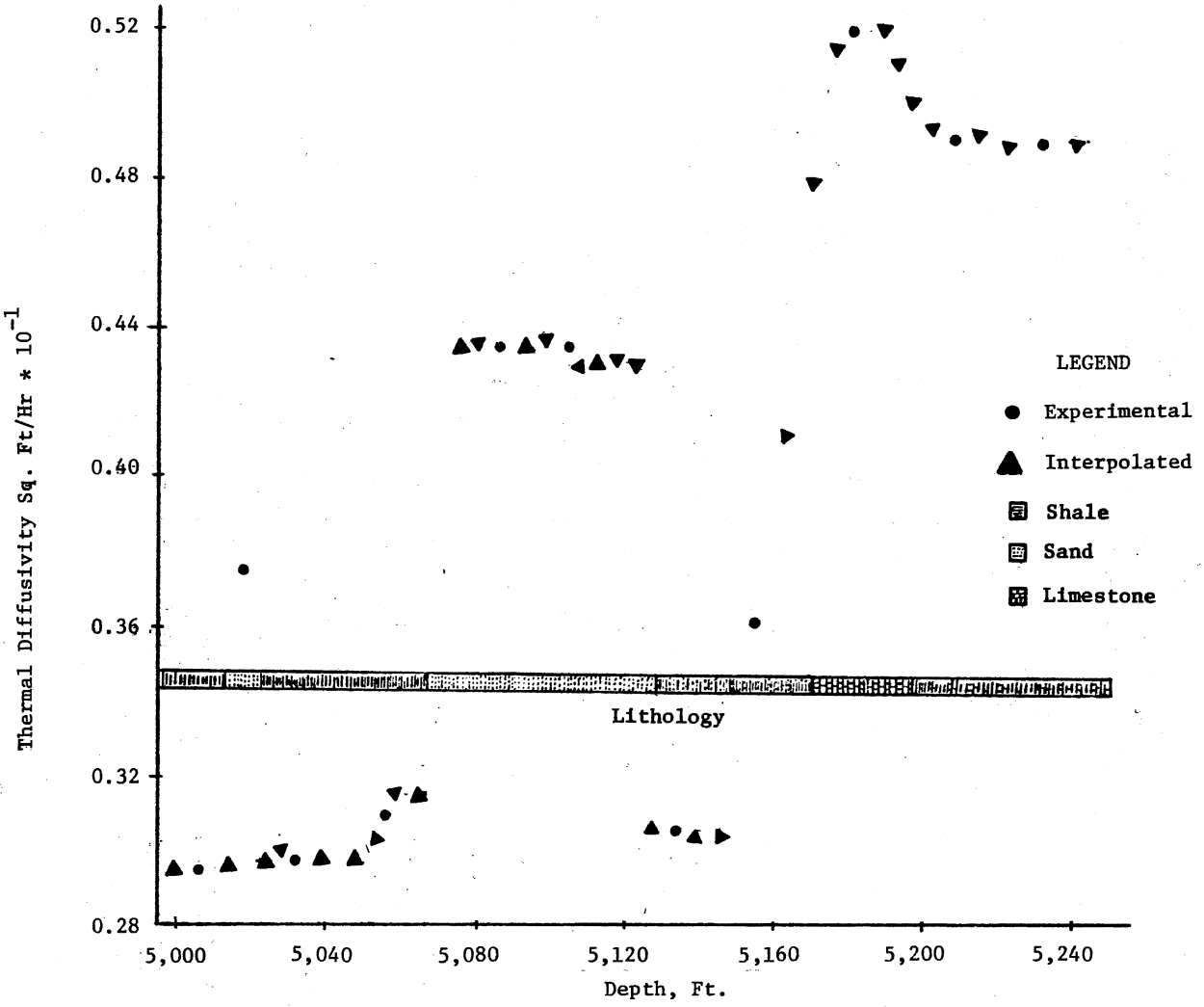

Figure 24. Experimental and Interpolated Thermal Diffusivity Data for Humphry #65 Well

recorded. Therefore, minor errors in data collection influence the accuracy of the calculated thermal conductivity values (63). As a preliminary check, it has often been found useful to make a semilogrithmic time-temperature plot for the experimental data. If the trend in the experimental data is such that it can be fit into a straight line, then often a curve fit program is used to smooth the data. A semilogarithmic plot of time vs. temperature was made for the experimental data used in this study as shown in Figure 25. From the general trend in data it can be seen that variation in the experimental values is around a straight line.

To determine the best fit for the values a computer program was developed by which the experimental data could be smoothed. The approach used takes the recorded time-temperature data at the various intervals and expresses it in terms of an equation of the type

$$y = C_1 (x) + C_2$$

By the standard least squares method the summation to be minimized is

$$\sum_{i=1}^{m} (C_1 (x) + C_2)^2 \longrightarrow \text{minimum}$$

Differentiating partially with respect to C_1 and C_2 results in two linear simultaneous equation

$$m\, C_2 + C_1 \Sigma x_i = \Sigma y_i$$

$$a \Sigma x_i + \ell n \Sigma x_i^2 = \Sigma x_i \Sigma y_i$$

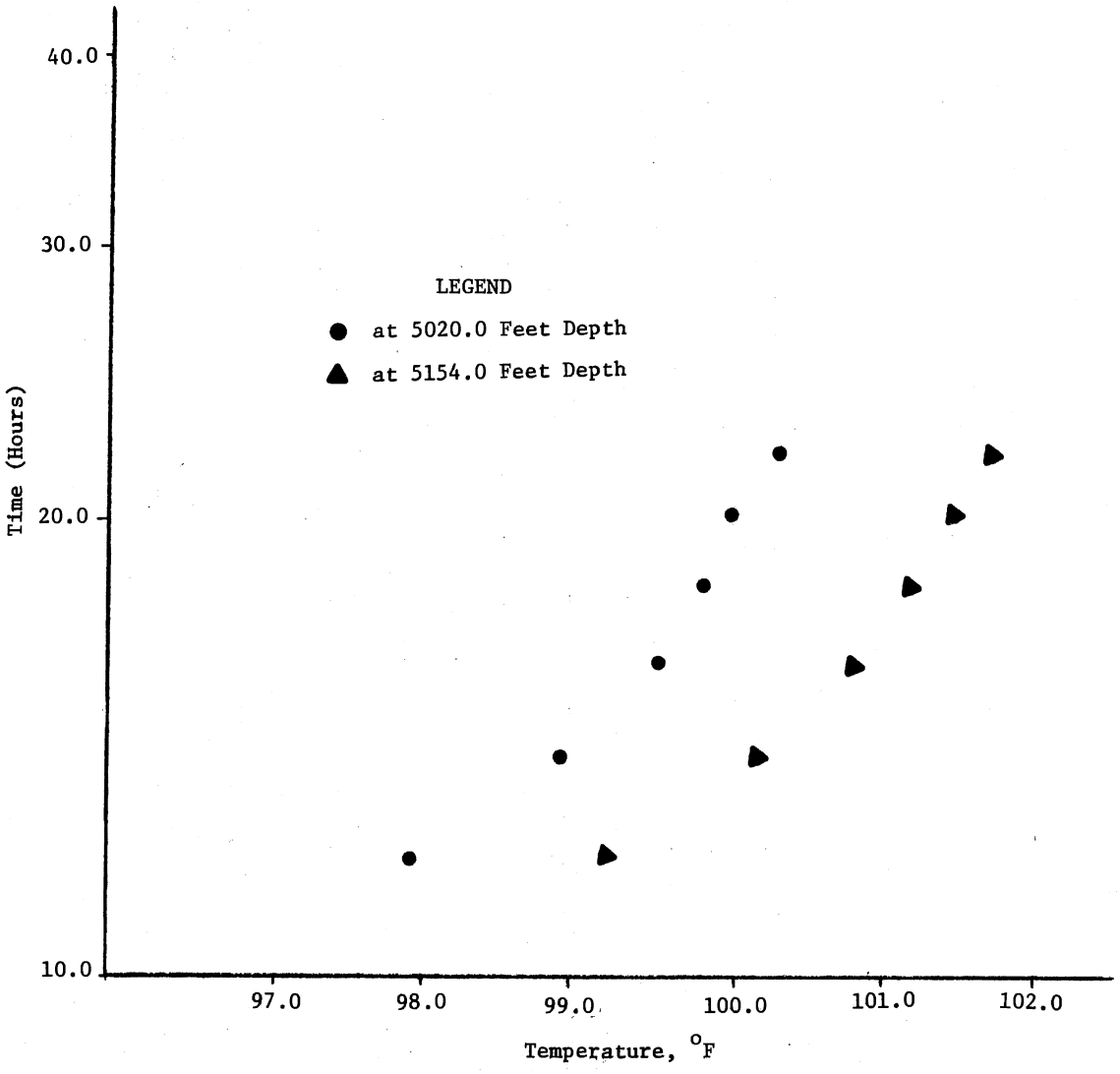

Figure 25. Semilogarithmic Time vs. Temperature Plot for Humphry #65 Well

These equations were solved by Gaussian elimination technique and the coefficients C_1 and C_2 were printed out to be used in predicting time and temperature values at desired intermediate intervals.

Summary

A variety of factors influence accuracy of the temperature logs, i.e. sensitivity of the temperature measuring elements, speed of temperature logging, water migration, oil and gas production, cementation, etc. All of these factors are discussed in this chapter and, where possible, field examples are included to show how these factors affect the recorded temperature. From the discussion it is concluded that temperature recordings from recently cemented wells, oil and gas producing wells and wells showing water migration should not be used in the thermal conductivity and diffusivity calculation as presented in this study.

The data used in this study is evaluated in the light of discussion on accuracy considerations and since this well is drilled into a relatively tight formation and is a non-producing well it is concluded that the recorded temperature data is suitable for use in the mathematical model. Temperature, SP, electric, porosity, and thermal property data for a 250-foot interval in the Humphry #65 well is presented and a correction procedure is described to prepare the raw temperature data to be used in the study.

CHAPTER V

DEVELOPMENT OF THE ELECTRONIC ANALOG

Introduction

Aids to calculation like abacus have been used from remote times. Since the latter half of the 17th century, use of such devices have become increasingly popular. The primitive desk calculator, which was originally designed by Pascal in 1642, has been used in one form or another for the last three centuries. In the last three decades electronic analog, digital, or hybrid computers have almost completely replaced the conventional calculator. Charles Babbage and Lord Kelvin, the original contributors, could have hardly guessed the revolutionary nature of crude devices which they used to make arithmatic calculations. These devices went unnoticed for almost a century and in 1939 IBM and Harvard University jointly brought the ideas of Babbage into existance in the form of a small computer called Harvard Mark-1. In the last two decades there have been an explosive growth in the development of computers. Improvements in the usage and manufacture of integrated circuits have brought the computer technology within reach of the lay man through the use of pocket calculators.

In the scientific and engineering related industries, small special purpose computers are extensively used to make difficult and time consuming calculations. These computers have become

an integral part of instrumentation used in collecting and relaying scientific and engineering information. If a calculation procedure is iterative, and does not require an extensive storage capacity, a special purpose computer is extremely well suited to perform the calculations.

The approach presented in this study does not require an extensive memory and data storage capacity. This appears to be an ideal situation where thermal conductivity data could be handily recorded along with the temperature data in the field in a matter of minutes. In this chapter, development of such an analog is presented. The objective of this development is to provide a basis for possible field application, describe the required hardware, and show the accuracy of its operation. If warranted, this analog could be developed into an instrument capable of measuring the thermal conductivities of rocks in situ. If the proposed analog were integraded into a temperature logging system, as proposed in Figure 26, it would allow the simultaneous logging of bore hole temperature and adjacent rock thermal conductivity.

Development Considerations

The first step in the development of an electronic analog of a mathematical model is to describe various mathematical operations by a flow chart. A flow chart for thermal conductivity simulation is presented in Figure 27. In the development of this flow chart a number of symbols were used. These have been standardized in the analog industry. A list of symbols commonly used is presented in Table II.

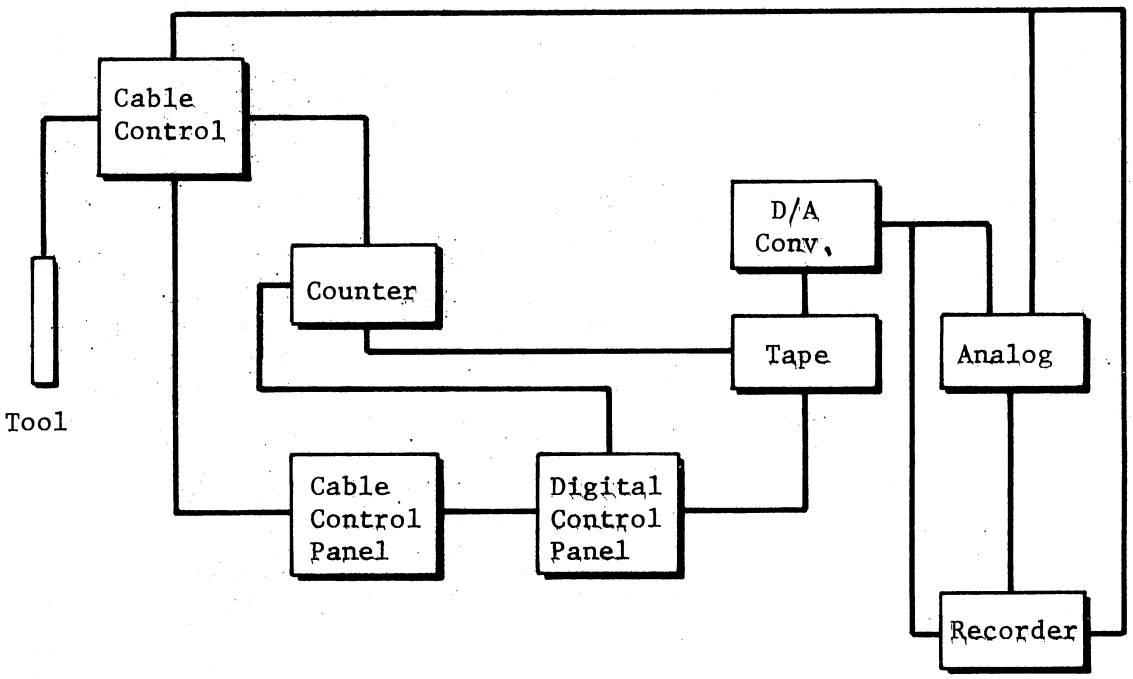

Figure 26. Proposed Schematic Diagram for a Temperature Logging System

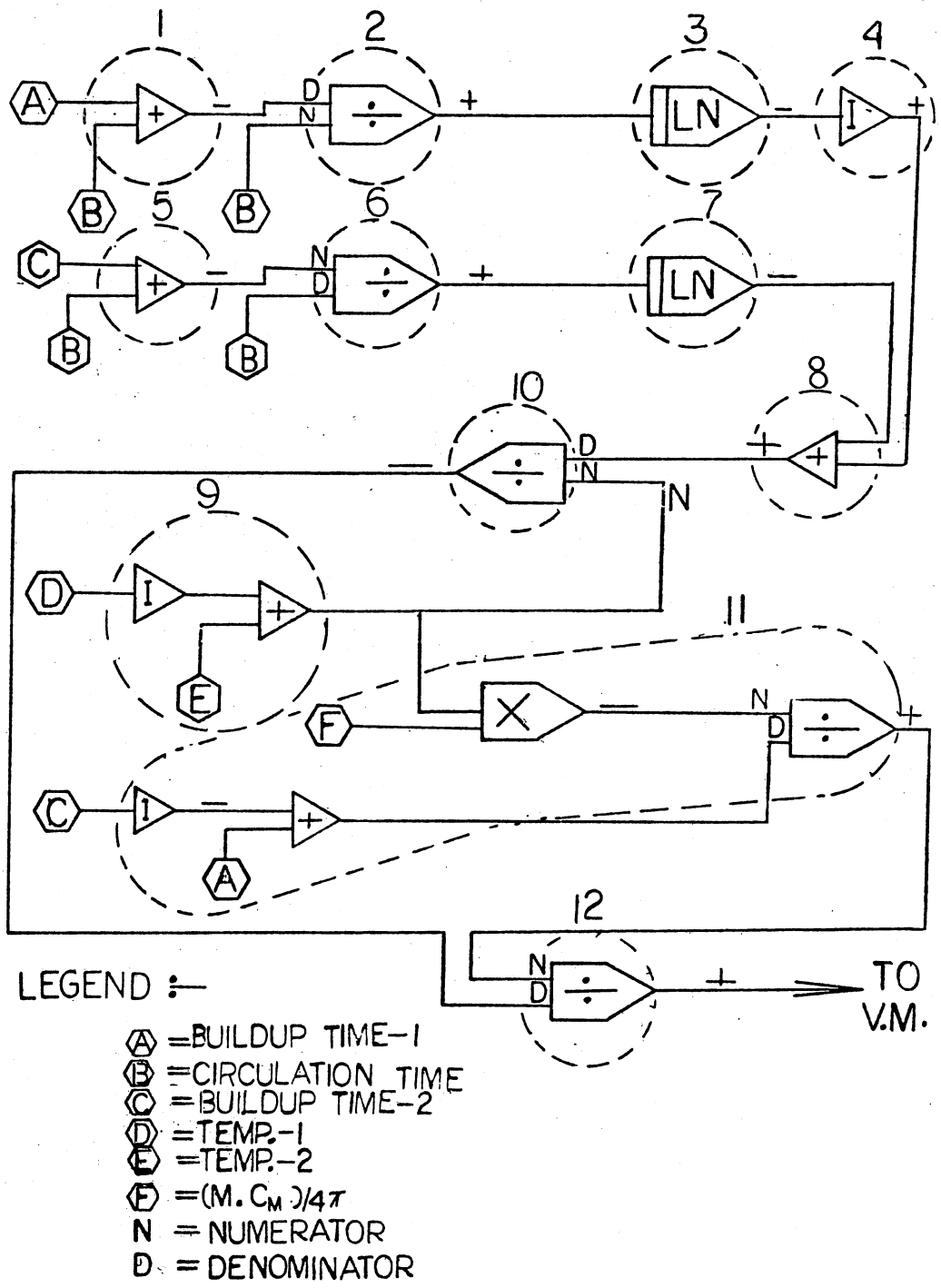

Figure 27. Flow Diagram of the Electronic Analog

TABLE II

GRAPHIC SYMBOLS FOR ANALOG COMPUTERS

SYMBOL	DESCRIPTION
	ANALOG SIGNAL LINE
	DIGITAL (COMMAND) SIGNAL LINE
	CONNECTION NO CONNECTION
N	TERMINAL, TRUNK LINE, ADDRESS POINT
a 10, b 5, c 1 → X	ADDER : $X = -(10a + 5b + c)$
a 1 → X	INVERTER : $X = -a$
a 1, b 2, μ → X	HIGH-GAIN OPERATIONAL AMPLIFIER : $X = -\mu(a + 2b)$ (μ NORMALLY $10^5 - 10^6$)
e(t), a 1, b 2, c 5, d → X	INTEGRATOR : $X = X - \int_0^t (a + 2b + 5c)\,dt$ WHEN $e = 1$ $X = -d$ WHEN $e = 0$
a, b 1 5, C → X	TRACK-STORE : $X = -(5a + b)$ WHEN $C = 1$ $X = X$ WHEN $C = 0$
a, P → X	POTENTIOMETER : $X = Pa$ $(0 \leq P \leq 1)$
a, b → X	MULTIPLIER : $X = -ab$
a, b, D, N → X	DIVIDER : $X = -b/a$
a, F( ) → X	FUNCTION GENERATOR : $X = F(a)$
a, b → c	COMPARATOR : $c = 1$ WHEN $(a + b) \geq 0$ $c = 0$ WHEN $(a + b) < 0$
a → c	LOGIC INVERTER : $c = 1$ WHEN $a = 0$ $c = 0$ WHEN $a = 1$
c, a → X	DIGITAL/ANALOG SWITCH : $X = a$ WHEN $C = 1$ $X = 0$ WHEN $C = 0$

The first step in the determination of thermal conductivity is the calculation of the slope of the semilogarithmic time-temperature graph of the type presented in Chapter II, Figure 13. To obtain the slope a number of sequential calculations need to be performed. These are illustrated as steps 1 - 10 in the flow chart of Figure 27. A discussion of each step follows.

In step one of the flow chart, circulation and buildup times were added by using a unit-gain amplifier. In this case, the voltage output from the amplifier is negative. This change in sign upon passing through the amplifier is dictated by the hardware (amplifier) and, as will be shown in subsequent steps, can be used to advantage if a subtraction instead of an addition needs to be made. In step two, a division is needed to calculate $\Delta t/(t+\Delta t)$. The division process utilized several amplifiers and resistors, the details of which will be presented in the section on hardware development. The voltage output from step two is negative. Since output voltage from the previous step was negative, after division, the voltage sign becomes positive. In step three, the natural logarithm of the output value from step two is obtained by using a function generator. Since the resultant value from the natural log function generator is negative, an inverter is used to obtain a positive output. Steps one, two and three are then repeated in steps five, six and seven to determine the natural log of the time ratio at a subsequent time t_2. In step eight a subtraction is performed and in step nine the temperature difference is obtained by using a summer along with an inverter. In step ten the slope is calculated by using the resultant voltage values from steps eight and nine.

In steps eleven and twelve of the thermal conductivity calculations, the slope as calculated by the flow chart steps 1 - 10 is manipulated to yield the thermal conductivity. This is accomplished by calculating the rate of heat flow as described in step eleven using time, well bore and mud parameters, and by dividing the slope calculated in steps 1 - 10 by the rate of heat flow, etc., as shown in step twelve. A resultant positive value is obtained for the thermal conductivity by using the positive output from the unit-gain amplifier. The output voltage from step twelve is then taken to a digital voltmeter where it is recorded for reference purposes.

Development of Analog Hardware

Preparation of the flow chart as described in the previous section was the first step taken in developing the electronic analog. In this section equipment and techniques used to develop hardware to perform the flow chart calculations are presented.

Description of the Equipment

For this study an analog computer model TR-48 manufactured by Electronics Associates, Inc. was used. The TR-48 is ideally suited to simulate problems where the number of amplifiers required is less than 48. It is a general purpose, solid state, medium size computer and is ideal for presenting laboratory demonstrations. It has a variety of components to perform mathematical manipulations, each component having input and output terminals on a prepatch panel which can be connected by using banana (or bottle) plugs and patch cords. This computer is of modular design. If desired, additional modules

can be added to the prepatch panel to increase the capacity of the computer. Because it is of modular design, the TR-48 analog computer tends to minimize patching clutter because fewer patch cords are needed in panel patching. The front panel of TR-48 consists of three sub-panels:

1. The monitoring and control panel (Figure 28)
2. The prepatch panel (Figure 29)
3. The attenuator panel (Figure 30)

The Monitoring and Control Panel. This panel is located to the extreme left in the main panel and contains control, power switches and instruments to monitor the operations of the computer. This panel also has display instruments which consist of a small oscilloscope, a digital voltmeter with a number of settings, a regular multirange voltmeter to show the rate of computation, and a push button signal selector system. By manipulating the controls on this panel, the potentiometer, the attenuators and other modules can be engaged or disengaged. If desired, it has provisions to allow a complete physical removal of the prepatch panel to allow patching of the panel at a more convenient location.

The Prepatch Panel. The prepatch panel is composed of a series of modules representing input, output and manipulation ports for forty-eight amplifiers, fifty-two potentiometers, four diode function generators, six multipliers, four comparators and a number of integrators. The input and output ports for the modules are gold coated to reduce signal impedance. By connecting these ports with bottle plugs and patch cords, a systematic mathematical manipulation can be exercised. Moreover, the patch cords have been designed to provide

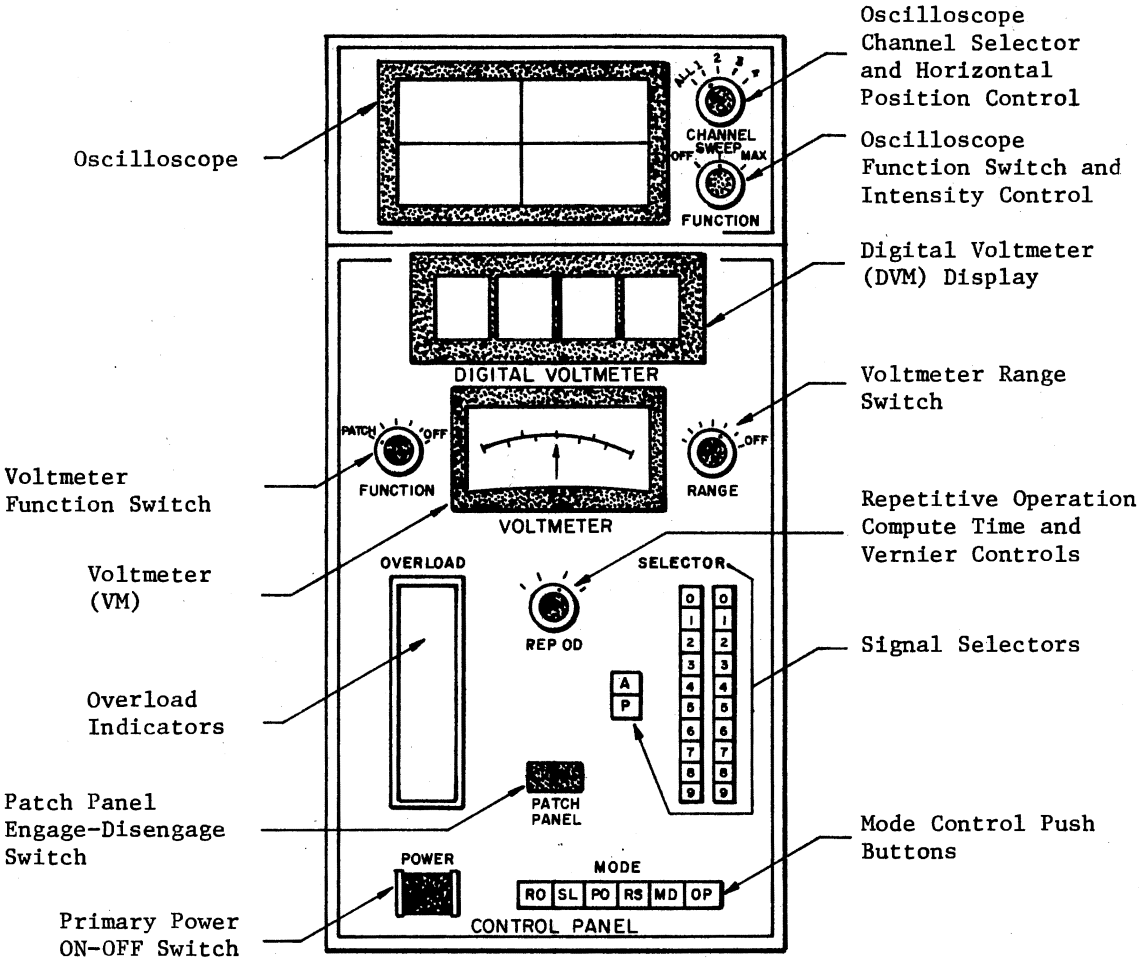

Figure 28. Monitoring and Control Panel for TR-48 Analog Computer

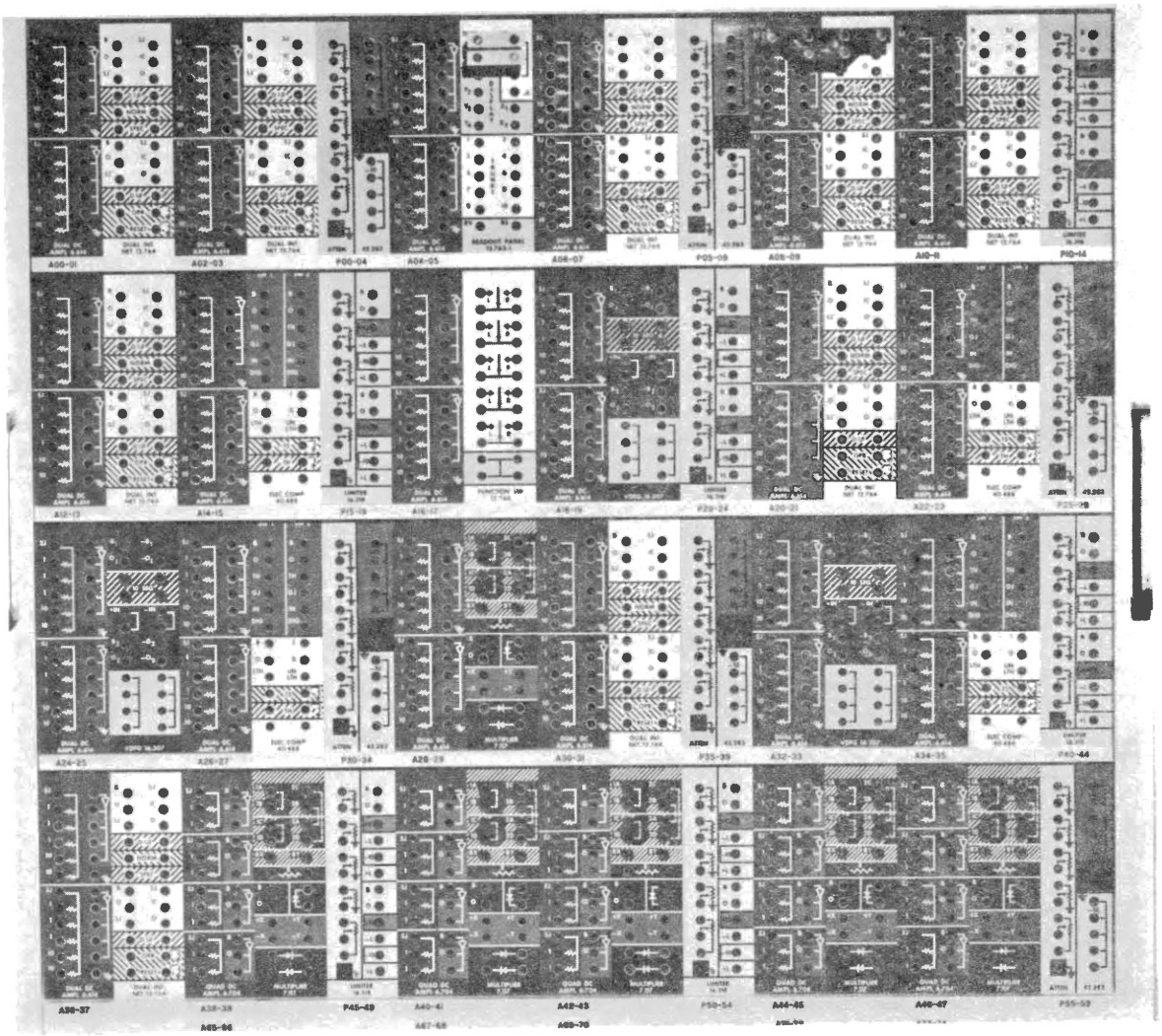

Figure 29. Prepatch Panel for TR-48 Analog Computer

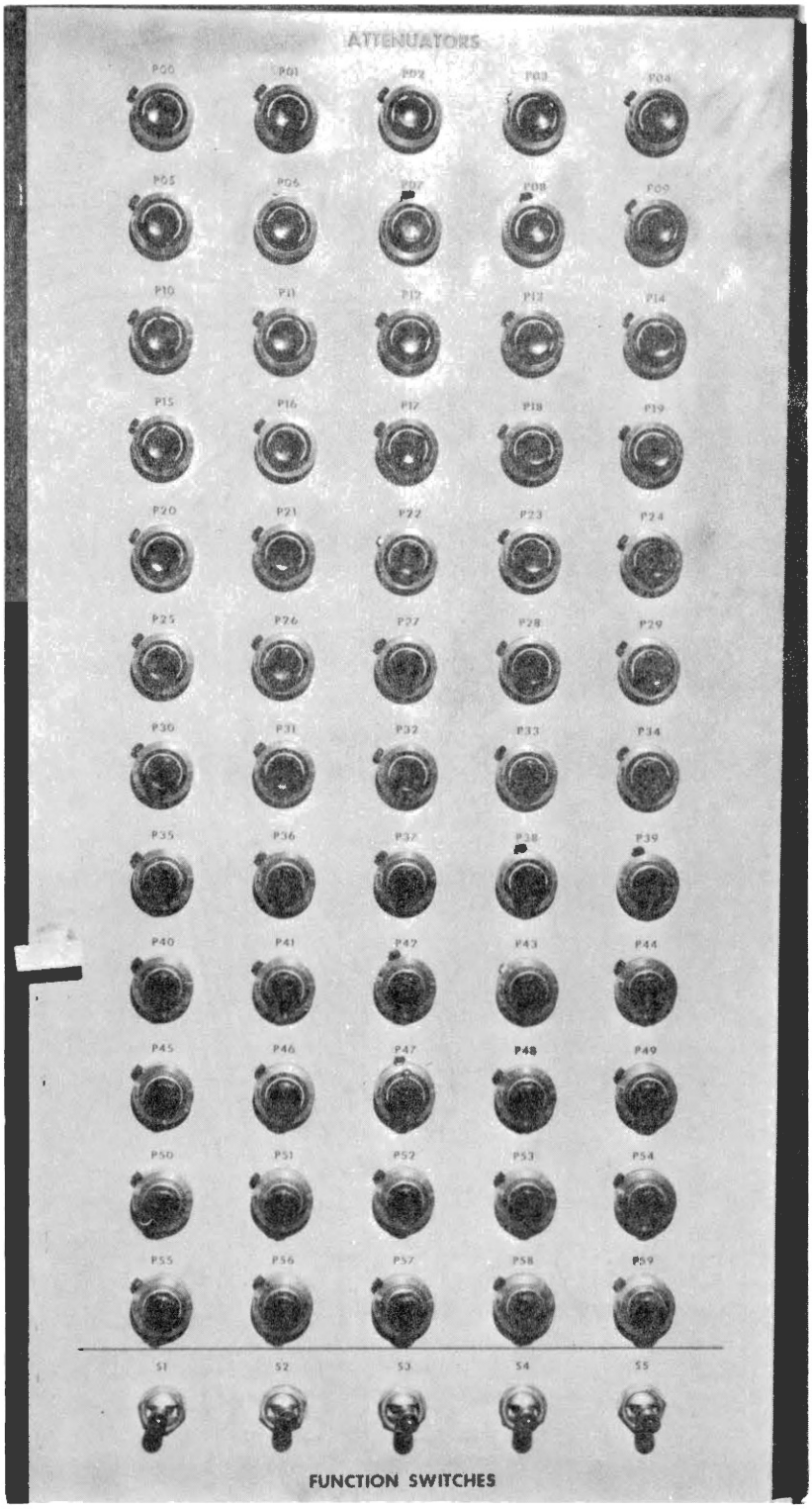

Figure 30. Attenuator and Function Switch Panel for TR-48 Analog Computer

dual connections at each location and, being color coded, allow an easy tracing of "bugs" in the patched panel.

The Attenuator Panel. On this panel are located all the feed control potentiometers and function switches. The potentiometers are numbered and have coarse and fine settings which can be locked-in to help maintain a constant feed to the amplifiers. The potentiometers are integrally connected on the one hand to the display instruments, and on the other hand to the amplifier input and output posts on the patch panel. The maximum input voltage is ten volts, and when capacitors in the integrators display 11.1 volts it means that the capacity has been fully saturated or perhaps the capacitor is damaged. A permanent damage to a module can be checked by wiring the integrator harboring the capacitor to integrate at a low rate of integration. If the voltmeter shows instant saturation, the capacitor is damaged and should not be used in simulation.

Development of Patch Panel

In order to develop a patch panel various modules on the prepatch panel have to be systematically used to obtain the desired results. In Figure 31, a systematic stepwise conversion is presented integrating the flow chart of Figure 26 with electronic hardware. For the sake of convenience, the numbers used to describe the flow chart are the same as used in the hardware description. Thus, step one in Figure 31 corresponds to step one of the flow chart, Figure 27.

In order to perform addition as shown in step one of the flow chart the hardware required is: two potentiometers to feed-in the discrete values, one amplifier, and three resistors. All of these

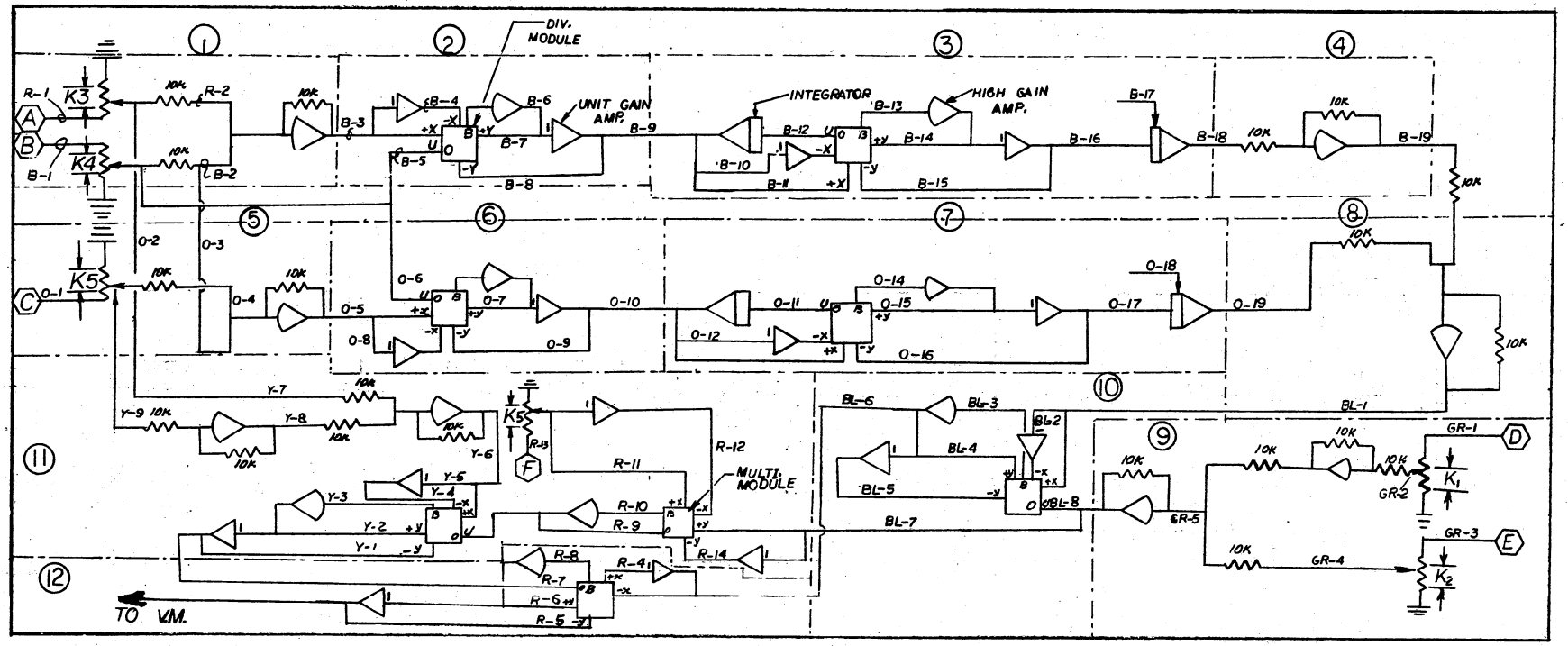

Figure 31. Wiring Diagram for the Electronic Analog

components are shown in the wiring diagram of Figure 31. Ten volts (maximum voltage) from the input port on the patch panel was routed through potentiometer No. 00 to provide one-tenth of the value of time t, (A) to be plugged into the input port of the unit-gain amplifier No. 02 (amplifier No. 01 is damaged). Similarly, potentiometer No. 01 was used to feed in the value of the circulation time (B) into another unit input port of amplifier No. 02. The output from the amplifier -- collected from the output port of the amplifier -- is read on the digital voltmeter to check accuracy of the inputed values. Although the input values were positive the output value (sum of the two input values) is negative (65).

In order to perform the division required in step two of Figure 31, the value for circulation time was read into the potentiometer input port after first routing through the variable resistor. The output port of potentiometer No. 03 was routed to multiplication module No. 1. The output from the unit gain amplifier of step one was fed into another unit-gain amplifier (03), and the output and input from the amplifier routed to ports -x and +x respectively. The output from the multiplier module at ports B and +y, was then routed through a high-gain and a unit-gain amplifier, respectively. The patching was completed by connecting the output from the high-gain amplifier to the port marked +y and from the unit-gain amplifier to the port marked -y. A simplified diagram of this patching is presented in Figure 32-A. It should be noted that the output voltage of the division module is either positive or negative and either value may be used for the input into the next step. The multiplication module is so designed that the

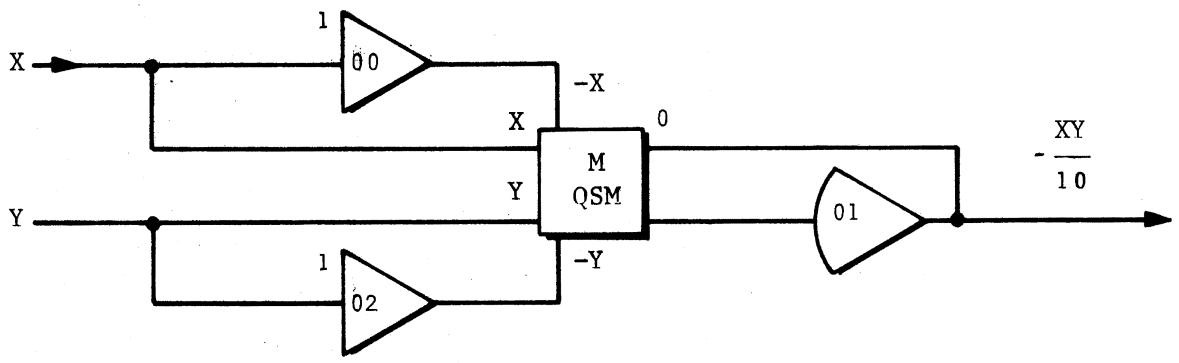

Computer Diagram - A

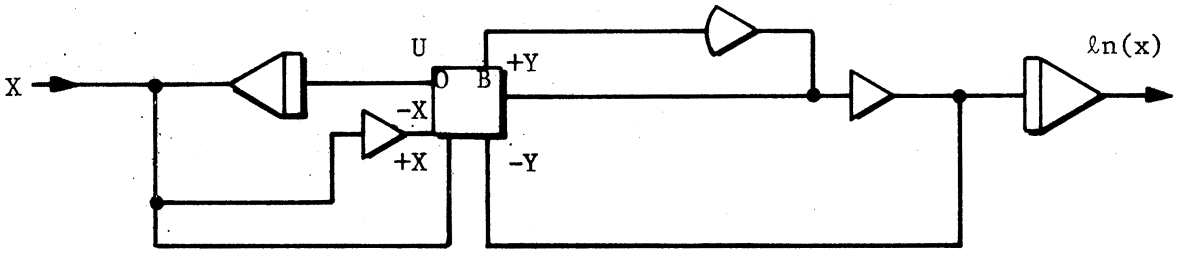

Computer Diagram - B

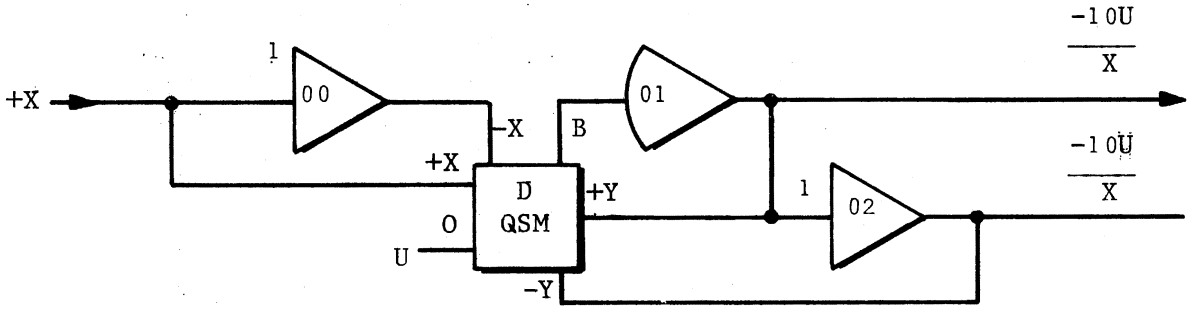

Computer Diagram - C

Figure 32. Component Diagrams for Multiplication, Natural Log and Division Modules

voltage is ten times the actual value for the output, thereby compensating for the fractional input of step one.

The log function generator, as described in step three of the flow chart, is not available on this computer. Therefore, to obtain the logarithmic values for continuous functional feed, the following system of integrators and potentiometers was developed.

Suppose $$y = \ell n\ x \tag{5.1}$$

then $$\dot{y} = \frac{\dot{x}}{x} \tag{5.2}$$

where

y = output value from log function generator

$\dot{y}$ = first derivative of the output value

x = input value into the function generator

$\dot{x}$ = first derivative of the input value

The only known value in Equations 5.1 and 5.2 is the value of x. In order to obtain the first derivative of x, an integrator is used. This value is then divided by the known value of x. The resultant value of $\dot{x}/x$ which is equal to first derivative of y is fed through an integrator to obtain the value of y. A simplified diagram of the log function generator is shown in Figure 32-B. The integrators and amplifiers used for the simulation are labelled on Figure 32-B. Steps five, six, and seven are analogous to steps one, two, and three except that different values for time at steps one and two are used.

In step eight, a subtraction is performed by inverting the output value from the log function generator and making a summation.

In step nine a subtraction is performed by using a summer and an inverter as described in steps four and eight. A division analogous to step two is performed with appropriate numerator and denominator as labelled in Figure 27 to calculate the slope according to the time ratio-temperature semilogarithmic plot of Figure 13.

In step eleven the temperature difference obtained in step nine is multiplied with the discrete input F, ($F = mC_m/4\pi$) where m is the mass of the drilling fluid for unit height and C_m is its specific heat. The input feed F, and output voltage of step nine labelled in Figure 27 and Figure 32-C respectively were plugged into the input ports of the multiplication module. The output from the module at ports "O" and "B" are taken to a high-gain amplifier. As is indicated in Figure 32-C the output voltage of multiplication is negative and the magnitude displayed is one-tenth of the actual value. Step eleven was completed by dividing the output from the multiplication module by the temperature difference obtained by using an inverter and a summer module. The resultant output from step eleven was positive in sign because the negative high-gain amplifier output voltage was selected for feeding into the input port for the division module of step twelve. Step twelve is similar to steps two, six and ten, as described previously except the input voltages are different. Positive voltage from the unit-gain amplifier of the division module used in step twelve was read on the digital voltmeter to obtain values of thermal conductivity.

A complete patch panel showing all the connections described above is presented in Figure 33. In the preparation of this panel it was found that numbered and color coded wires were extremely useful

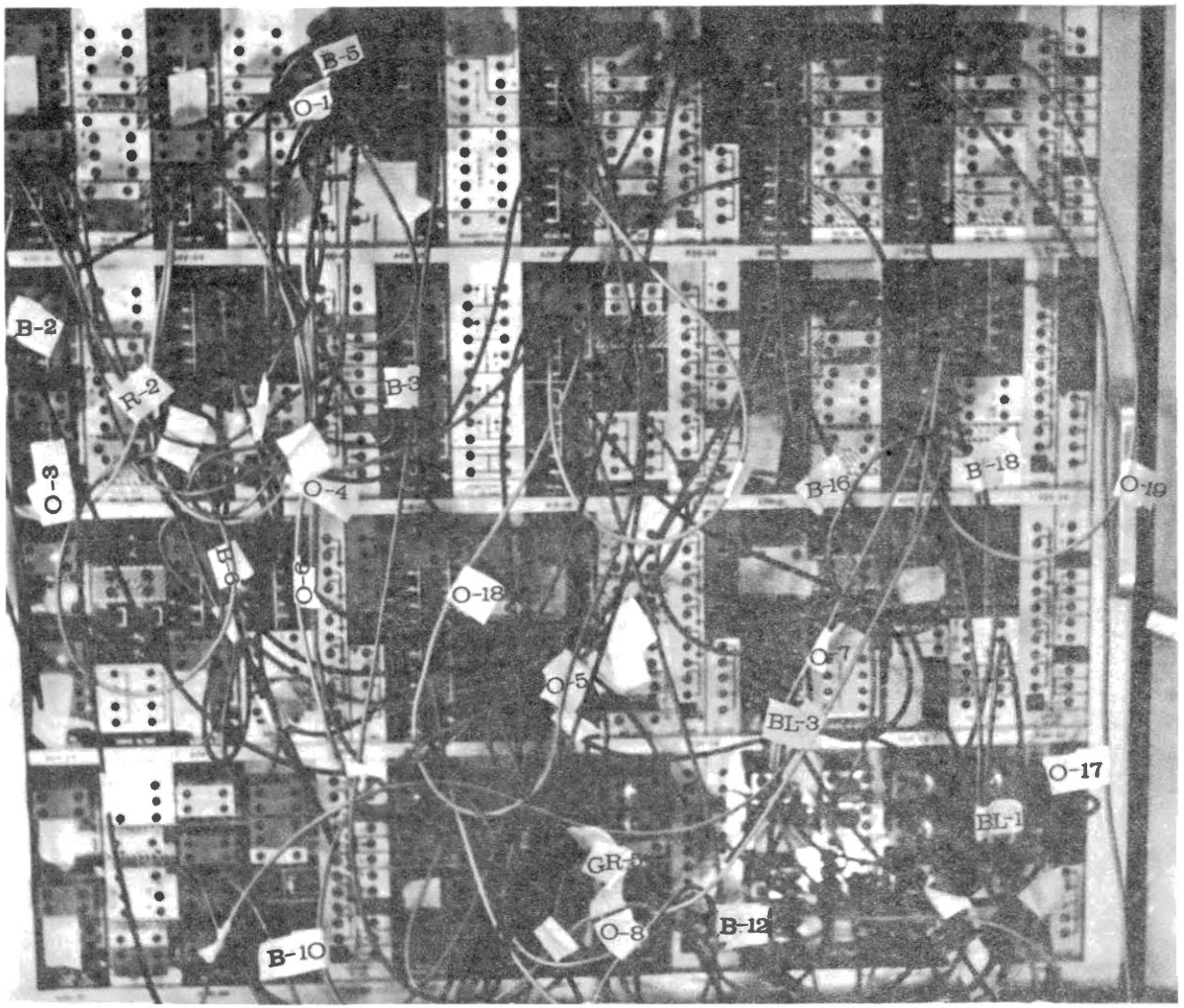

Figure 33. Patched Panel for the Analog Showing Color Codes and Wiring Numbers

in tracing the computational steps. The color coding scheme and numbers used to tag the wires are shown in Figure 31.

As previously mentioned, the objective behind the electronic analog simulation of the mathematical model was not to develop a field module to do the thermal conductivity calculations, but to show the feasibility of such a module. The complexity of the analog as reflected by the variety of individual modules used when translated into dollar values is prohibitive in terms of costs for a field module. However if the situation warrants, a field module can be easily assembled by procuring the hardware shown in Figure 31 and interconnecting as described in this section.

To check accuracy of the electronic analog, sample calculations were made for preselected intervals. In order to perform calculations in one step, eight multiplication modules are needed. However, only four working modules were available on the TR-48 computer, therefore, calculations in step 11 were fed in from computer calculation output directly into the division module of step 12. Input values for A, B, C, D, E, and step 11 are shown in Table III. Because of external resistances from patch cords, bottle plugs, and unaccounted for gains from the high gain-amplifiers used in the analog, the first analog computer thermal conductivity value at 5,000 feet depth was found to be seven percent lower than the calculated value. Subsequent thermal conductivity values were accordingly scaled-up to account for this loss in signal. The results determined by the analog model are presented in Chapter VI along with other results to facilitate comparison between the calculated, experimental, interpolated and analog computer results.

TABLE III

DATA USED IN CALCULATIONS FOR ELECTRONIC ANALOG

No.	Depth	A	B	C	D	E	Step-11	Computed Therm. Cond.	Calc. Therm. Cond.	Scale Factor %	% Error
1	5,000	12.0	4.5	16.0	98.8199	100.2727	60.5812	0.7694	1.0994	7.0	+0.001
2	5,040	12.0	4.5	16.0	98.7389	100.2182	58.5471	0.7416	1.0446	7.0	+1.300
3	5,080	12.0	4.5	16.0	99.2300	100.7527	57.6497	0.7021	1.0031	7.0	+0.010
4	5,120	12.0	4.5	16.0	99.4987	100.9418	44.7876	0.5821	0.8317	7.0	+0.020
5	5,130	12.0	4.5	16.0	99.4732	102.1226	139.3775	0.9960	1.4421	7.0	+1.330
6	5,150	12.0	4.5	16.0	99.5542	101.0610	40.1893	0.7277	1.0359	7.0	-0.410
7	5,200	12.0	4.5	16.0	99.7121	101.1424	31.5897	0.6205	0.8865	7.0	+0.010
8	5,240	12.0	4.5	16.0	99.8484	100.8486	23.6884	0.667	0.9532	7.0	+0.04
9	5,250	12.0	4.5	16.0	99.8614	100.7866	25.207	0.755	1.0949	7.0	+1.50

Summary

In this chapter development of an electronic analog to simulate the mathematical model is presented. A description of the software (symbolic flow diagram of the mathematical model) is presented and a detailed wiring diagram showing the various modules used in the simulation along with the procedure used to patch them together are discussed. Color coded numbered wires were used in patching the prepatch panel. A photograph of the completely patched panel is included. Actual computation of thermal conductivity by the analog is carried out by using discrete input values as defined in Figure 27. The output from the analog is approximately scaled for the first calculation and the difference between the calculated and the simulated values is used to scale up subsequent calculations (as is customary in electronic analog simulation studies).

The discussion and development of the analog presented in this chapter appears to establish the feasibility for development of an electronic tool for field use in conjunction with temperature logging. By using this analog not only temperature but also thermal conductivity of the subsurface rocks may be recorded on the same log. If the density and specific heat are also known, it should be possible to determine the heat flow at any depth in a bore hole.

CHAPTER VI

PRESENTATION AND DISCUSSION OF RESULTS

Introduction

A detailed discussion of the theoretical basis for this study has been presented in Chapters III, IV and V. In this chapter results obtained through programming and electronic simulation of the mathematical models are presented. For ease of discussion, the subject matter is divided into three sections: the first section includes the results of thermal conductivity calculations and development of a nomograph to determine the stabilized temperature; in the second section results from electronic analog computation are presented; and in the last section results of thermal diffusivity calculations are included.

In this discussion of results, as well as in preceeding chapters, a number of terms have been used to describe the sources of origin of thermal conductivity and diffusivity values. In order to avoid further confusing terminology, the adjectives experimental and interpolated are reiterated to describe or compare the reference thermal property data as presented in Chapter IV. The term "calculated" thermal conductivity or diffusivity is used to describe the values obtained through programming of the mathematical models; and the term "computed" is used to describe the thermal conductivity values obtained from the electronic analog simultation. "In situ" and "actual" thermal conductivity

and diffusivity are used synonymously to describe the "apparent" or "true" thermal properties of rocks in their natural habitat.

Thermal Conductivity Calculation

In Chapter III a mathematical model which simulates the physical conditions of heat flow from a formation into a well bore is discussed. As a result of the discussion it is shown that thermal conductivity of a rock can be calculated from the slope of a semilogarithmic graph of time-ratio vs. temperature of the type shown in Figure 13. However, from the same equation which leads to the above conclusion, stabilized formation temperature can be calculated by using appropriate input data. A computer program was developed for this purpose and is presented in Appendix A. The results from the computer program are used to develop a nomograph from which stabilized temperature of a formation can be obtained if initial temperature, circulation time, and buildup time are available. The development of this nomograph is presented next.

Stabilized Formation Temperature Nomograph

In Chapter III, Equation 3.17 describes how the stabilized formation temperature varies as a function of initial temperature, thermal conductivity, buildup and drawdown times and rate of heat flow from the formation into the well bore. Assuming the formation to be sandstone and assuming one hour for circulation time, a plot of initial temperature vs. buildup time for one hour circulation time can be developed for an 8" diameter well bore filled with 10 pounds per gallon weight drilling fluid. A series of graphs for assumed values of circulation times were developed as shown in Figure 34. From the

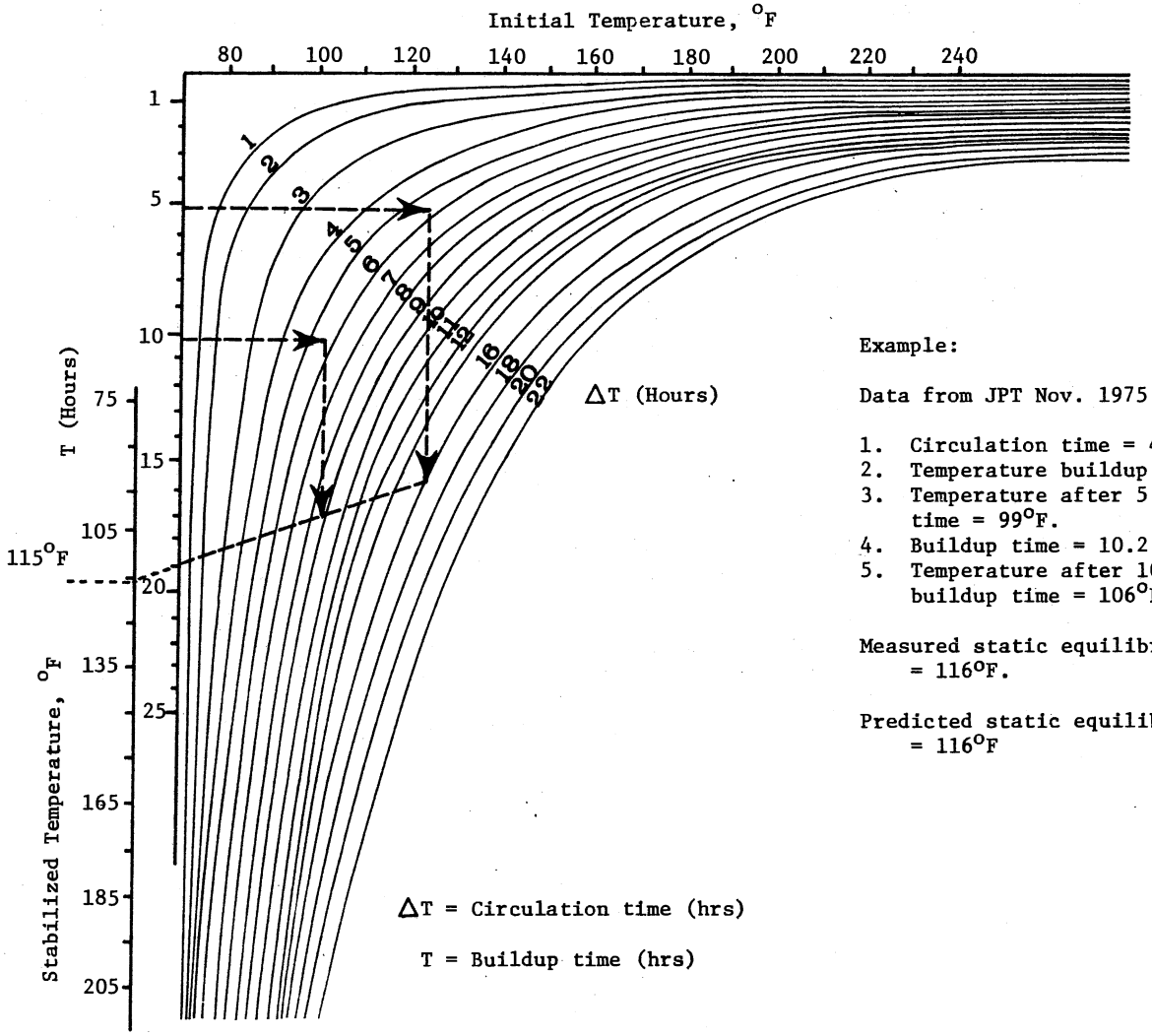

Example:

Data from JPT Nov. 1975 page 1329

1. Circulation time = 4 1/2 hrs.
2. Temperature buildup time = 5.1 hrs.
3. Temperature after 5.1 hr buildup time = 99°F.
4. Buildup time = 10.2 hrs.
5. Temperature after 10.2 hrs of buildup time = 106°F

Measured static equilibrium temperature = 116°F.

Predicted static equilibrium temperature = 116°F

Figure 34. Equilibrium Temperature Nomograph

literature (51) experimental data which described the stabilized formation temperature as a function of buildup time, drawdown times, and initial temperatures was obtained. A scale similar to initial temperature scale was selected for the stabilized temperature and was allowed to slide up and down along the buildup time abscissa until the value of stabilized temperature as shown by the example in Figure 34 could be obtained by using the procedure outlined.

To check this nomograph a number of case studies were located in the literature where initial temperature, final temperature, circulation time and drawdown time were available. Using this data, the stabilized temperature for the formations was calculated using the nomograph. A comparison of the stabilized temperatures determined from the nomograph with the experimentally obtained temperatures is presented in Table IV. The comparison shows that the average error in the stabilized temperature determined through the use of the nomograph is $\pm$ 2%.

Calculated Thermal Conductivity Values

Thermal conductivity values at two-foot intervals over the 250-foot section presented in Figure 20 were calculated using the theoretical basis discussed in Chapter III. The calculated thermal conductivity values are presented in Figure 35 and in Tables VI and VIII of Appendix B. These values were compared to the laboratory derived values presented in Chapter IV and the percentage difference between the two values is plotted in Figure 36. In some cases the calculated values deviate from the experimental ones by as much as thirty-two percent. However, in general, the agreement is within ten to fifteen percent.

TABLE IV

PERFORMANCE OF STABILIZED EQUILIBRIUM FORMATION TEMPERATURE NOMOGRAPH

Ref. No.	Stabilized Formation Temperature Measured	From Nomograph	Percentage Difference
50	116 °F	116°F	±0.00
51	297 °F	300°F	-1.00
45	118 °F	117°F	+0.58
67	150 °F	150°F	±0.00
9	106 °F	108°F	+2.00
9	107.5°F	109°F	+2.00

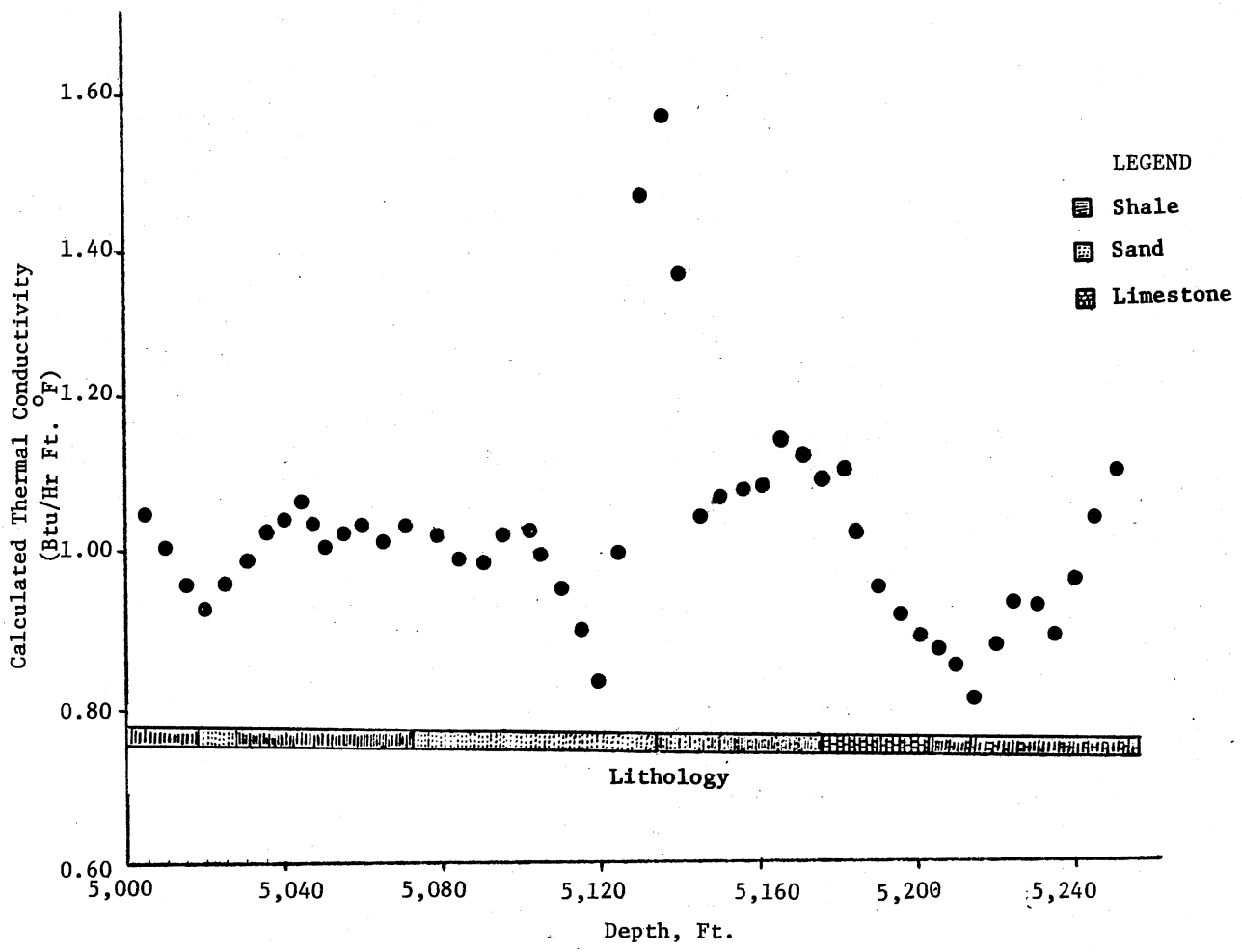

Figure 35. Calculated Thermal Conductivity vs. Depth

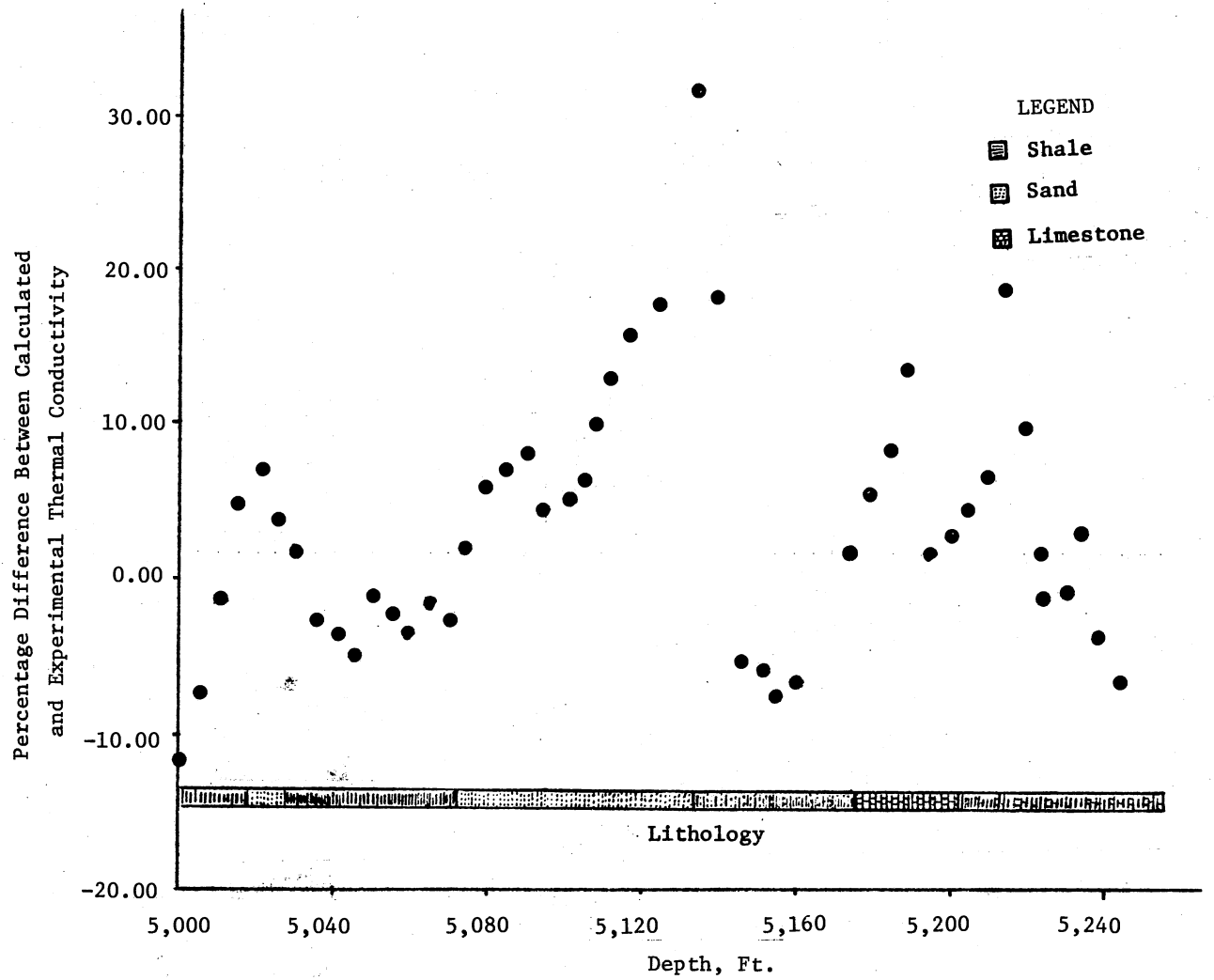

Figure 36. Percentage Difference Between Experimental and Calculated Thermal Conductivity vs. Depth

In those cases where the percentage difference between the calculated and experimental values was unusually large, the corresponding depths were correlated on the SP log. The calculated thermal conductivity values correlate well for formations thicker than twenty-five feet, while the values for formations less than twenty-five feet correlate poorly, indicating that in thin formations the total impact of temperature buildup may not be observed in the well bore because of lateral temperature dissipations.

The calculated thermal conductivity values can be compared with the reference values depending upon if the experimental only or the experimantal and interpolated values are used as a criteria. When the calculated thermal conductivity values are compared with the experimental values over the entire interval, the calculated values are 7.4% higher. However, when comparison is made on the basis of experimental and interpolated thermal conductivity values the calculated values were found to average 10.2% higher.

A number of petrophysical correlations between thermal conductivity and porosity are found in the literature. However, none of these correlations examine the relation between in situ thermal conductivity and in situ porosity. In this study, the calculated thermal conductivity and in situ porosity were both available and therefore a correlation can be attempted.

Relationship Between In Situ Thermal Conductivity and Porosity.

Sommerton et al. (32) report a correlation between thermal conductivity and porosity. The thermal conductivity values for the

interval under study were determined using that correlation and are presented in Figure 37. This data is on the average 15% lower than the calculated thermal conductivity values. Thus the correlation which was determined from experimental thermal conductivity and porosity data gives presumably erroneously low values when applied to the in situ thermal conductivity and porosity values.

The computer program presented in Appendix A was written to develop a correlation between in situ porosity and thermal conductivity through use of s sixth-degree polynomial as was done by Zierfus and Van-Der Vliet (30). Although the sample of data available for the development of the correlation was small it is hoped that, as additional data becomes available the correlation can be further refined (66). The correlation is:

$$K = A + B\phi + C\phi^2 + D\phi^3 + E\phi^4 + F\phi^5 + G\phi^6$$

where

$0 < \phi < 1$

$A = -1.91477$

$B = 7.11759$

$C = -6.696$

$D = -.051025$

$E = 1.549619$

$F = 0.549517$

$G = -0.463172$

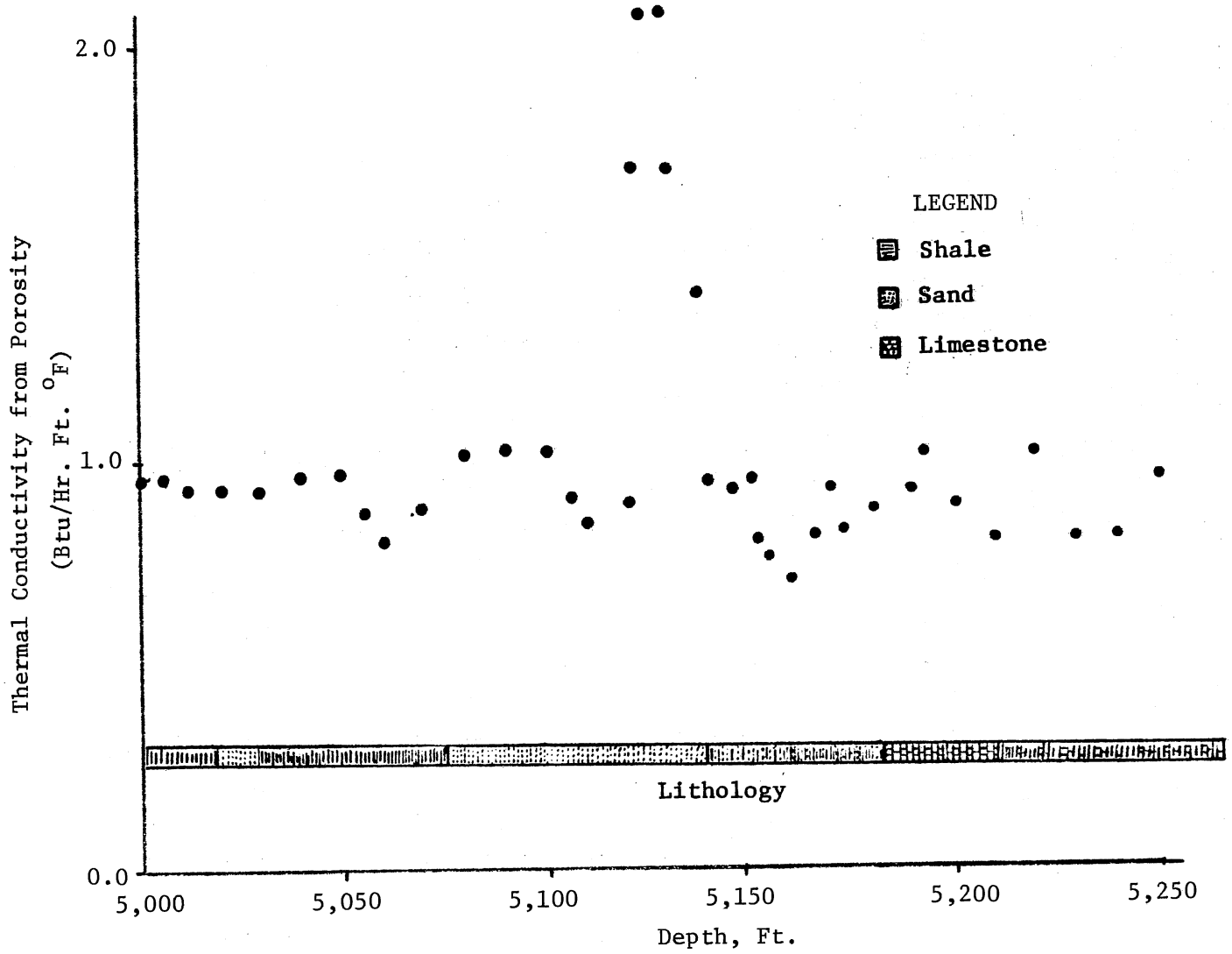

Figure 37. Porosity Derived Thermal Conductivity vs. Depth

Thermal Conductivity Results from Analog Simulation

A detailed discussion of the hardware used to develop the electronic analog was presented in Chapter V. The Electronic Associates Incorporated model No. TR-48 analog computer has six multiplication modules on the prepatch panel. Upon testing these six modules it was found that two were damaged beyond repair and rendered useless. In order to perform the simulation in one step, one multiplication and seven division modules are needed as shown in the wiring diagram of Figure 31. Since the TR-48 contained the largest panel which was readily available, the computations had to be completed in two stages. All the calculations except those of steps ten, eleven and twelve are performed in stage one. The computer modules were then reused to perform the second stage calculation of steps ten, eleven and twelve. Although this two-stage procedure was tedious and time-consuming, it allowed a demonstration of the use of the analog to determine the in situ thermal conductivity.

Nine points along the depth of the well bore at 5,000, 5,040, 5,080, 5,120, 5,130, 5,150, 5,200, 5,240, and 5,250 feet respectively, were chosen for computation of thermal conductivity values. The computations were carried out as described in Chapter V and results of these computations are shown in Figure 38 along with the calculated thermal conductivity values. The calculated thermal conductivity values were found to agree with the computed values within $\pm 1.5\%$.

Results of Thermal Diffusivity Calculations

In Chapter III a method to calculate the thermal diffusivity of

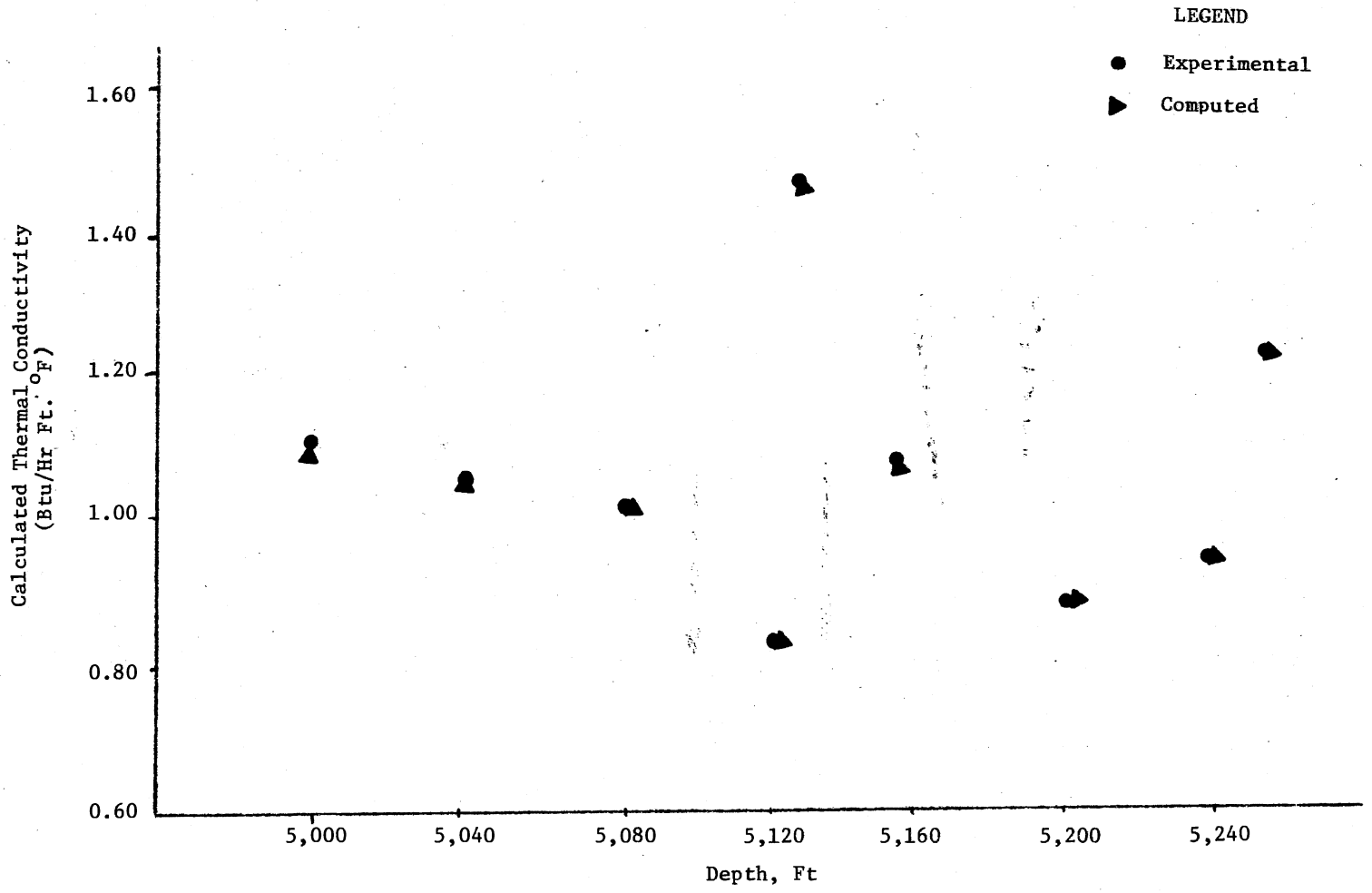

Figure 38. Comparative Plot of Electronic Analog Calculated and Computed Thermal Conductivity Values vs. Depth

a rock by using the in situ time-temperature data was presented. By using this method a series of calculations were performed with the computer program presented in Appendix A. The results of these calculations are presented in Figure 39. From this figure it can be seen that on the average, the calculated thermal diffusivity values are higher than the experimental values. This is further seen in Figure 40 where the percentage difference between the calculated and experimental values is plotted vs. depth. The calculated thermal diffusivity values as shown in Figure 39 can be compared with the reference thermal diffusivity values depending upon if only the experimental or the experimental and interpolated values are used as a criteria. When the calculated thermal diffusivity values are compared with the experimental values over the entire interval, the calculated values on the average are 20.2% higher. When the comparison is made on the basis of experimental and interpolated thermal diffusivity values the calculated values were found to average 25.3% higher.

Summary

This chapter presents results of calculations performed by using the mathematical procedures and electronic analog as developed in Chapters III and IV, respectively. Calculated thermal conductivity and diffusivity values by using the mathematical models are on the average higher than the experimental values. However, the results of electronic analog simulation correlate well with the calculated values. This suggests the possibility of developing a thermal conductivity tool for use in the field. Since in this study in situ thermal conductivity and porosity values were also available, therefore, a petrophysical

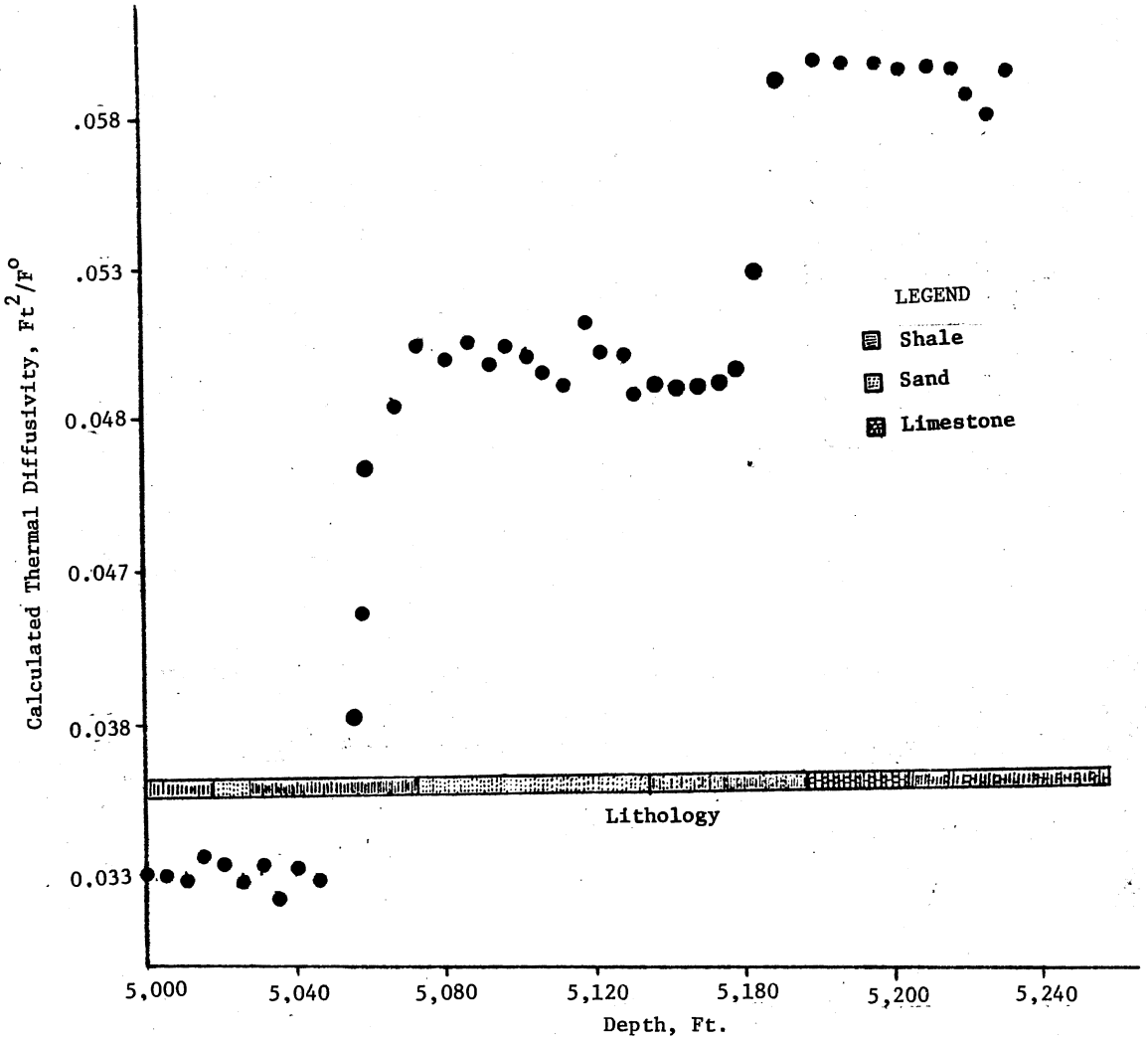

Figure 39. Calculated Thermal Diffusivity vs. Depth

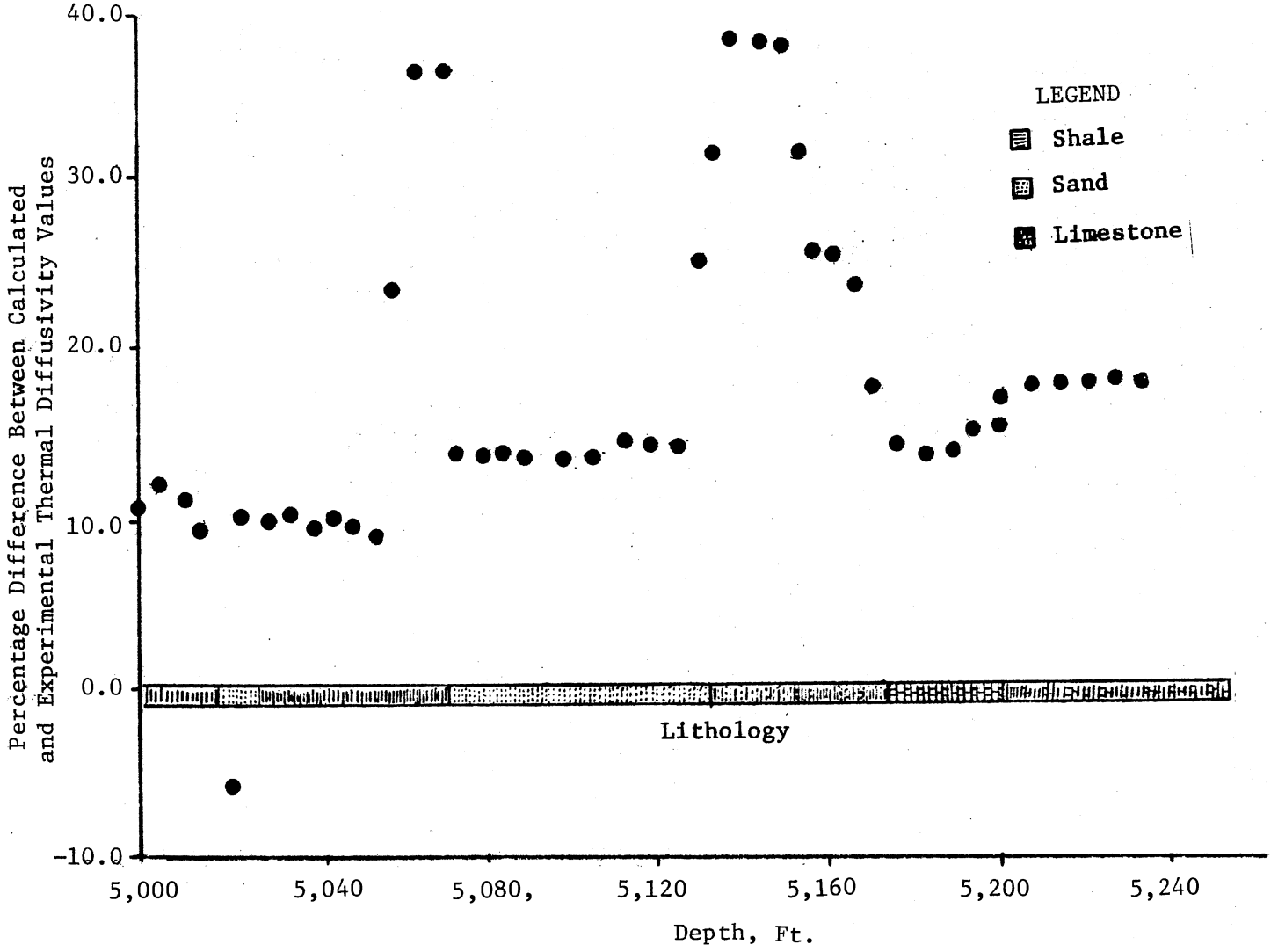

Figure 40. Percentage Difference Between the Calculated and Experimental Thermal Diffusivity Values vs. Depth

correlation using these properties was attempted. Although the data available for the development of this correlation was limited, it is hoped that as more data becomes available this correlation will be further refined.

A nomograph to predict the equilibrium formation temperatures was also presented in this chapter and by using this nomograph a number of calculations were carried out to evaluate its accuracy of prediction. By comparing the predicted equilibrium formation temperature with the experimental values it was shown that the temperature values predicted by the nomograph were within $\pm 2\%$ of the experimental values.

CHAPTER VII

CONCLUSIONS AND RECOMMENDATIONS

Procedures for measurement of thermal conductivity and diffusivity of rocks, both in the laboratory and in the field were critically examined. They have all been found to be time consuming, require elaborate instrumentation and have various inherent drawbacks in determining the "true" thermal properties of massive rock formations.

A mathematical model to determine the thermal properties is presented in this study. This procedure is less time consuming, requires little or no laboratory data in its application, and promises to give more accurate measurements for the thermal properties of rocks in bulk than the methods hitherto encountered.

The method uses the transient temperature buildup in a bore hole to ascertain the thermal properties of rocks, accordingly, it includes measurements under actual field conditions wherein the rock's physical state (density, porosity, pore volume, etc.) is as it actually exists under natural conditions of fluid saturation, temperature and pressure.

Field data were used to test the model. Although the data available were limited, it provided sufficient basis to evaluate the model over a range of field conditions. Thermal property values determined as a result of this method were found to compare favorably with those determined in the laboratory. Although the thermal conductivity values obtained from application of the new method averaged 10.2% higher

than the experimentally derived values, it is shown that such a result is consistent with expectations of in situ measured properties.

An electronic analog of the mathematical model to compute the thermal conductivity of rocks was developed. The output from the analog was found to be consistent with predictions of the mathematical model. Therefore, it demonstrates the field applicability of this method.

Conclusions

From this study it has been found that:

1. "Calculated" thermal conductivity and diffusivity values determined by using in situ time-temperature data as input into the mathematical model are higher than are "experimental" values determined by laboratory measurement. This observation is consistent with the fact that certain physical properties of cores e.g. porosity, bulk volume, fluid saturation, and pressure change as the cores are removed from their natural habitat. Unless the natural environment is duplicated in the laboratory, this change in the physical properties lowers the thermal property values of the cores.

2. Calculated thermal conductivity values of test formations thicker than 25 feet correlated well with experimental measurements, where as formations thinner than 25 feet showed a less favorable correlation. This is as expected since thin formations do not show a proportionate increase in temperature with time partly because of lateral temperature dissipations. As a result, the calculated thermal conductivity values are lower.

3. Thermal conductivity values obtained from empirical porosity correlations were 15% lower than the calculated thermal conductivity values, partly because the petrophysical correlation used to obtain the thermal conductivity values is based upon experimental values. The correlation between calculated thermal conductivity and in situ porosity as developed in this study attempts to correct this situation. However, the sample used for the development of the correlation is small. As more data becomes available, it is hoped that the correlation coefficients will be improved to reflect more realistic response for the correlation.

4. Measurement of stabilized equilibrium formation temperatures is a useful procedure for use in well completion studies and reservoir calculations. The mathematics of this study allows the application of this technique to obtain the equilibrium formation temperature. A nomograph is developed to simplify the application which for a series of test cases is found to give fairly accurate equilibrium temperature predictions.

5. An electronic analog simulation of the mathematical model demonstrates the feasibility of developing a field thermal conductivity tool.

Recommendations

It should be realized that although there are inherent errors in laboratory derived thermal properties, such a data base, nevertheless, provided the best available criteria to evaluate the accuracy of the model described in this study. However, it is recommended that in situ rather than laboratory derived thermal property data be used for

comparison purposes to evaluate the accuracy of the model described in this study.

Temperature variations in bore holes are very sensitive to oil and gas production, water migration, and cementation. Accordingly, it is recommended that any future time-temperature data collection effort should consider these effects.

In this study it was shown that thin formations reflect a disproportionate increase in temperature buildup with time probably because of lateral temperature dissipations in the bore holes. Because of the nature of the lithology of the formations available for this study, this effect of formation thickness on thermal property values has not been thoroughly evaluated. It is recommended that more data be procured to further define this limitation.

REFERENCES

(1) Christopher, H. and H. Armstead. "Geothermal Energy: Review and Development." Paris: Unesco, 1973, 15-18.

(2) Langseth, M. G., Jr. "The Flow of Heat from the Earth and Its Global Distribution at the Surface," AIAA 4th Thermophysics Conference, San Francisco, California, June, 1969.

(3) Levorsen, A. I. Geology of Petroleum. San Francisco: W. H. Freeman Publishing Company, 1967, 1-20.

(4) Werner, H. "Geothermics as a Means of Locating Petroleum Deposits." Petroleum Times London, Vol. 23 (April 10, 1930), 2-20.

(5) Hickel, J. W. "Geothermal Energy." Seattle, Washington: Geothermal Resources Research, Report of Working Congress, held Sept., 1972.

(6) Anderson, J. H. "Geothermal Heat, Our Next Major Source of Power." AIChE 71st National Meeting, Dallas, Texas, February, 1972.

(7) Stewart, R. W. "The Atmosphere and the Ocean." Scientific American, Vol. 221 (Sept., 1969), 76-87.

(8) Pirson, S-J. Handbook of Well Log Analysis. Englewood Cliffs, N. J.: Prentice-Hall, Inc., 1963, 347-350.

(9) Schoeppel, R. J. "A.A.P.G. Geothermal Survey of North America." Final Report. Stillwater: Oklahoma State University August, 1973.

(10) Benfield, A. E. "Terrestrial Heat Flow in Great Britain." Proceedings Royal Society of London, Vol. A, 173 (July, 1939), 428-450.

(11) Beck, A. E., F. M. Angelin and J. H. Sass. "Analysis of Heat Flow Data - In-situ Thermal Conductivity Measurements." Canadian Journal of Earth Sciences, Vol. 8, No. 1 (Jan., 1971), 1-19.

(12) Birch, R. and H. Clark. "The Thermal Conductivity of Rocks and Their Dependence Upon Temperature and Composition." American Journal of Science, Vol. 238, No. 9 (Aug., 1940), 529-635.

(13) Report of the Committee on Underground Temperatures, British Association for the Advancement of Science, 1878. Quoted by Prestaiech, J. Controverted Questions in Geology. London: Macmillan, 1895, 1-100.

(14) Keller, W. D. "Earth Thermal Resistivities at Depths Less Than One Hundred Feet." Bulletin of the American Association of Petroleum Geologists, Vol. 18, No. 1 (Jan., 1934), 39-62.

(15) Lovering, T. S. "Heat Conduction in Dissimilar Rocks and the Use of Thermal Models." Bulletin of the Geological Society of America, Vol. 47 (1935), 87-100.

(16) Lovering, T. S. "Theory of Heat Conduction Applied to Geological Problems." Bulletin of the Geological Society of America. Vol. 46 (1935), 69-94.

(17) Kircheri, A. Mundus Subterraneus, Vol. II (1678), 184-185. Quoted by Birchof, Physical, Chemical and Geological Research on the Internal Heat of the Globe, Vol. 1 London, 1891 Quoted by C. E. Orstrand Van, "Apparatus for the Measurements of Temperatures in Deep Wells by Means of Maximum Recordings Thermometers." Economic Geology, Vol. 19 (1924), 229.

(18) Birch, R. "Flow of Heat in Front Range Colorado." Bulletin of American Geological Society, Vol. 61 (1950), 567-630.

(19) "Symposium on Thermal Conductivity Measurements, and Application of Thermal Insulations." ASTM Technical Publication No. 217 presented at the Philadelphia National Meeting, Philadelphia, Pa., Feb. 6, 1957.

(20) Zierfus, H. "An Apparatus for the Rapid Determination of the Heat Conductivity of Poor Conductors." J. Sci. Inst., 40 (1963), 67-71.

(21) Kunii, O. and J. M. Smith. "Thermal Conduction of Porous Rocks Filled with Stagnant Fluids." Society of Petroleum Engineers Journal, Vol. 1 (1961), 37-42.

(22) Ho, C. Y. and R. E. Taylor. Proceedings of Eighth Conference on Thermal Conductivity. Purdue University, New York: Plenum Press, 1968, 701-771.

(23) Thomas, J., Jr., R. R. Frost and R. D. Harvey. "Thermal Conductivity of Carbonate Rocks." Engineering Geology, Vol. 7, No. 1 (1973), 3-12.

(24) Sass, J. H., et al. "Thermal Conductivity of Rocks from Measurements on Fragments and Its Applications to Determination of Heat Flow." Journal of Geophysical Research, Vol. 76, No. 14 (May, 1971), 3391-3401.

(25) Sass. J. H., et al. "Measurements of Geothermal Flux Through Poorly Consolidated Segments." Earth & Planetary Science Letter, No. 4 (1968), 293-298.

(26) Tye, Roual, Phillip. Thermal Conductivity. New York: Academic Press, 1969, 377-388.

(27) Somerton, W. H. and G. D. Boozer. "Thermal Characteristics of Porous Rocks at Elevated Temperatures." Pet-Trans. AIME, Vol. 219 (1960), 418-422.

(28) Meridith, R. E. "Studies of the Conductivities of Dispersions." (Unpublished Ph.D. Thesis, University of California, Berkley, 1959), 56-133.

(29) Huff, J. R. and J. W. Berg, Jr. "Thermal & Electrical Conductivities of Sandstone Rocks and Ocean Sediments." Geophysics, Vol. 33 (1968), 489-500.

(30) Zierfus, H. and Van-Der Vliet. "Laboratory Measurements of Heat Conductivity of Sedimentary Rocks." Bulletin of the American Association of the Petroleum Geologists, Vol. 40, No. 10 (October, 1956), 2475-2488.

(31) Horai, Ki-Iti and Skiya Uyeda. "Relation Between Thermal Conductivity of Sedimentary Rocks and Water Content." Bulletin of the Earthquake Research Institute, Vol. 38 (1960), 199-206.

(32) Sommerton, W. H. "Some Thermal Characteristics of Porous Rocks." J.P.T., 213 (1958), 375-378.

(33) Diment, W. H. and E. C. Robertson. "Temperature Thermal Conductivity and Heat Flow in a Drilled Hole Near Oak-Ridge, Tennessee," J. Geophys. Res., 68 (1963), 5036-5046.

(34) Shell Science and Technology News Letter No. 14. Rijswick, Holland: Shell Publications, February, 1970, 1-10.

(35) Shao, Ti Hsu. Engineering Heat Transfer. Princeton: D Van Nostrand and Company, 1963, 10-13.

(36) McDonald, et al. "Calculation of the Thermal History of the Earth." Journal of Geophysics Research, Vol. 64, No. 11 (1968), 1967.

(37) Schleirmacher, A.C.E.I. "Aher dle Warmelertung der Gare." Wiederman Ann. Physics, 34 (1888), 625.

(38) Lachernbruch, A. H. "A Probe for Measurement of Thermal Conductivity of Frozen Soils in Place." American Geophysical Union Transactions, (October, 1957), 691-697.

(39) Deustachio, D. and R. E. Schreiner. "A Study of A Transient Method for Measuring Thermal Conductivity." ASHVE, Trans., 58 (1952), 311-346.

(40) Wechslar, A. E. "Development of Thermal Conductivity Probes for Soils and Insulations." Conteract DA-27-021, AMC 25(F), Arthur D. Little, Inc. Technical Report, NASA Publications, 1972.

(41) Von Herzen, R. and A. E. Maxwell. "The Measurement of Thermal Conductivity of Deep Sea Sediments by a Needle Probe Method." Journal of Geo. Res., Vol. 64, No. 10 (1959), 1557-1563.

(42) Jaeger, J. C. "The Measurement of Thermal Conductivity and Diffusivity with Cylinderical Probes." Trans. Amer. Geophys. Un. 39 (1958), pp. 708-710.

(43) De Vries, D. A., et al. "A Non Stationary Method of Determining the Thermal Conductivity of Soils In-situ." Soil Science, 73 (1952), 83-88.

(44) Prats, M. and S. M. O'Brien. "The Thermal Conductivity and Diffusivity of Green River Oil Shales." J.P.T., 1 (Jan. 1975), 97-106.

(45) Morris, Billy P. and R. D. Concanower. "Computers to Enhance the Value of Temperature Logs." SPWLA Proceedings 9th Annual Logging Conference, June, 1968, 1-19.

(46) Edmondson, J. J., et al. "Calculation of Formation Temperature Disturbances Caused by Mud Circulation." J.P.T., 4 (April, 1962), 416-426.

(47) Jaeger, J. C. and J. H. Sass. "A Line Source Method for Measuring the Thermal Conductivity and Diffusivity of Cylindrical Specimens of Rocks and Other Poor Conductors." Brit. J. Appl. Phys., 5 (1964) 1-8.

(48) Ingersoll, L. R. and O. J. Zoebel. Heat Conductions with Engineering and Geological Application. Madison: University of Wisconsin Press, 1947, 148-151.

(49) Carslaw, H. S. and J. C. Jaeger. Conduction of Heat in Solids. Second Edition. London: Oxford University Press. Sec. 10.4(4), 1959.

(50) Matthew, C. S. and D. G. Russell. "Pressure Buildup and Flow Tests in Wells," Monograph Series, Society of Petroleum Engineers of AIME, 1, Dallas (1967) 130.

(51) Timko, D. J. and W. H. Fertl. "How Downhole Temperatures, Pressures, Affect Drilling." World Oil, 174, (Oct. 1972), 73-75.

(52) Dowdle, W. C. and W. M. Cobb. "Static Formation Temperature from Well Logs - An Empirical Method." J.P.T. (Nov. 1975), 1326-1330.

(53) Peacock, R. D. "What You Can Learn from Temperature Logs." Petroleum Engineer, Sept. 1965, 96-103.

(54) Costain, J. R. "Heat Flow and Precision Temperature Measurements in Bore Holes." SPWLA Tenth Annual Logging Symposium, Denver, Colorado, June, 1968, 23-26.

(55) Taylor Instruments Corposition File No. 14-2, New York, 1973.

(56) Bullard, E. C. "The Time Necessary for a Bore Hole to Attain Temperature Equilibrium." R.A.S. Monthly Notices, Geophysics Suppl., 5 (1947), 127-130.

(57) Guyod, Bubert. "Temperature." The Oil Weekly, 124 (Dec., 1946), 26-34.

(58) Cocanower, R. D. Personal Communications, Western Logging Company, December, 1973.

(59) Gouin, Frank. "The Geology of Oil and Gas Fields of Stephens County, Oklahoma." Oklahoma Geological Survey Bulletin 40, Vol. 2 (1926), 26-66.

(60) Mallory, W. W. "Pennsylvanian Stratigraphy and Structure, Velma Field, Stephens County, Oklahoma." Bulletin Amer. Assoc. Petrol. Geol., Vol. 32, No. 10 (1948), 1948-1979.

(61) Rowe, Vance E. "Southwestern Oklahoma Production Reports." Tulsa, Oklahoma: Petroleum Statistical Guide, Inc., 1935-1953.

(62) Wright, Foley. Personal Communications, Atlantic Richfield Corporation, Baton Rouge, Louisiana, March, 1974.

(63) Underwood, W. M., et al. "Thermal Conductivity of Several Plastics, Measured by Unsteady State Methods." Heat Transfer, Chemical Engineering Progress Symposium Series, Vol. 56, No. 30 (1960), 261.

(64) Weyrick, R. C. Fundamentals of Analog Computers. Englewood Cliffs, N. J.: Prentice Hall, 1969, 1-15.

(65) Hartley, G. M. An Introduction to Analog Computers. New York: John Wiley & Sons, 1966, 1-62.

(66) Schoeppel, R. J. "A Proposal to Determine the Thermal Properties of Rocks In Situ." Submitted to National Science Foundation, January, 1976, 1-20.

APPENDIX A

FLOW CHARTS AND PROGRAM LISTINGS

Listing of Main Program

```
1     C------
1     C     +       MAIN PROGRAM                                              +
1     C------
1     C     +                                                                 +
1     C     ++++++++++++++++++++++++++++++++++++++++++++++++++++++++++++++++++
1     C     +                                                                 +
1     C     +                   IN PROGRAM MAIN                               +
1     C     +                                                                 +
1     C     +       T           ARRAY OF TEMPERATURE VALUES IN F              +
1     C     +       TT          ARRAY OF TIME VALUES AT WHICH TEMPERATURE RUNS+
1     C     +                   WERE MADE                                     +
1     C     +                                                                 +
1     C     +                                                                 +
1     C     +       DIF         ARRAY OF EXPERIMENTAL AND INTERPOLATED THERMAL+
1     C     +                   DIFFUSIVITY VALUES IN FT**2/F                 +
1     C     +                                                                 +
1     C     +       CK          ARRAY OF EXPERIMENTAL AND INTERPOLATED THERMAL+
1     C     +                   CONDUCTIVITY IN BTU/HR.FT.F                   +
1     C     +       RHO         DENSITY OF DRILLING FLUID                     +
1     C     +                                                                 +
1     C     +       CM          SPECIFIC HEAT OF DRILLING FLUID               +
1     C     +                                                                 +
1     C     +       RW          RADIUS OF THE WELL BORE                       +
1     C     +                                                                 +
1     C     +       POR         POROSITY AS A FRACTION OF 1.0                 +
1     C     +                                                                 +
1     C     +       DELK        CIRCULATION TIME HRS.                         +
1     C     +                                                                 +
1     C     +       BK          PERCENTAGE ERROR IN CALCULATED THERMAL CONDUCT+
1     C     +                   IVITY                                         +
1     C     +                                                                 +
1     C     +       PK          ARRAY OF  POROSITY OBTAINED THERMAL CONDUCTIVI+
1     C     +                   IVITY                                         +
1     C     +                                                                 +
1     C     +       TK          ARRAY OF PREDICTED THERMAL CONDUCTIVITY       +
1     C     +                                                                 +
1     C     +       FIC         ARRAY OF CAKCULATED THERMAL DIFFUSIVITY       +
1     C     +                                                                 +
1     C     +       ERR         ARRAY OF PERCENTAGE ERROR IN CALCULARED THERM +
1     C     +                   DIFFUSIVITY AS COMPARED WITH THE EXPERIMENTAL +
1     C     +                   AND INTERPOLATED THERMAL DIFFUSIVITY VALUES.  +
1     C     +                                                                 +
1     C     +       DEAT        RATE OF HEAT FLOW                             +
1     C     +                                                                 +
1     C     +                                                                 +
1     C     ++++++++++++++++++++++++++++++++++++++++++++++++++++++++++++++++++
1     C
1     C
1           DIMENSION T(8,130),TT(8),D(130),DID(130),DET(7),TEE(8),DEP(130),
2          APOR(130),AK(8,130),DIF(130),TME(130),DK(130),
3          AERR(130),WP(10),DEL(8,130),FID(32)
4          A,PK(10,130),TEMNOR(8,130),CP(8),P(8),V(8),RP(8),FIC(130)
5          A,Y(8),X(8),CC(10),DEAT(8)
6          A,SL(130),CK(130),ARATE(130),TK(130),SFT(130)
```

Continued on Page 132

Listing of Main Program Continued from Page 131

```
      A,BK(130),PDP(130),DCP(130),RW(130)
C-----
C-----
      CALL PLOTS
      MY=126
      NX=7
C
      DO 201 M=1,MY
C-----
      READ(5,101) DEP(M),(T(N,M),N=1,NX),DIF(M),POR(M)
  101 FORMAT(F6.1,2F8.4,5(1X,F8.4),F5.1,1X,F4.2)
  201 CONTINUE
C-----
      DO 203 M=1,MY
      READ(5,105) CK(M),RW(M)
  105 FORMAT(2F15.6)
  203 CONTINUE
C-----
C
      READ(5,103)(TT(K),K=1,7),RHO,CM
  103 FORMAT(7F6.3,2F6.3)
C
      DO214 M=1,MY
      DO213 K=1,7
      DELK=4.5
      RP(K)=TT(K)+DELK
      CP(K)=DELK/RP(K)
      P(K)=ALOG(CP(K))
      X(K)=P(K)
      Y(K)=T(K,M)
  213 CONTINUE
C-----
      CALL CURVFT(X,Y,7,1,C,ESQRMN)
C-----
      CALL THECON(M,T,TT,RHO,CM,RW,C,TK,DEAT)
  214 CONTINUE
C-----
      DO 312 M=1,MY
      BK(M)=((CK(M)-TK(M))/CK(M))*100.0
  312 CONTINUE
      DO 991 MM=1,MY
      X(MM)=TK(MM)
      Y(MM)=POR(MM)
  991 CONTINUE
      CALL DOOF(X,Y,126,6,WP,ESQRMN)
      WRITE(6,990) WP
  990 FORMAT(7F15.6)
      CALL PORK(POR,PK)
C-----
      CALL ANORM(T,DEP,TEMNOR)
C-----
      DO 321 M=1,MY
      DO 196 L=1,7
      X(L)=TT(L)
```

Continued on Page 133

Listing of Main Program Continued from Page 132

```
49          Y(L)=T(L,M)
50        196 CONTINUE
51      C
51          CALL CURVFT(X,Y,7,1,C,ESQRMN)
52          DO 199 N=1,6
53          X(N)=DEAT(N)
54          Y(N)=TT(N)
55        199 CONTINUE
56          CALL CURVFT(X,Y,6,3,CC,ESQRMN)
57          CALL CIFF(M,RW,DIF,C,CC,FIC,ERR)
58      C-----
58        321 CONTINUE
59      C-----
59      C-----
59          WRITE(6,118)
60        118 FORMAT(1H1)
61          WRITE(6,108)
62        108 FORMAT(1H,'WELL BORE DEPTH',3X,'EXP. TH. COND.',2X,'CALC. TH. COND
63           A.',1X,'PERCENT ERROR',1X,'EXP. TH. DIFF.',1X,'CALC. TH. DIFF.',1X,
64           A'PERCENT ERROR')
65          WRITE(6,119) (DEP(M),CK(M),TK(M),BK(M),DIF(M),FIC(M),ERR(M),M=1,MY
66      C
66        119 FORMAT(1XF15.1,2F15.4,F15.2,2F15.4,F15.2)
67          WRITE(6,519)
68        519 FORMAT(1H1)
69          WRITE(6,520)
70        520 FORMAT(1H,'DEPTH',5X,'NORM.TEMP.',4X,'POROSITY',4X,'SH.TH.COND.'
71           A,4X,'SD.TH.COND.',5X,'LM.TH.COND.')
72          WRITE(6,521)(DEP(M),TEMNOR(3,M),POR(M),PK(2,M),PK(3,M),PK(10,M),M=
73      C
73        521 FORMAT(1XF6.1,F15.3,F10.2,3F15.3)
74          STOP
75          END
```

Listing of Main Program Concluded

Flow Chart of Main Program
This program controls input, output and sets up subroutines.

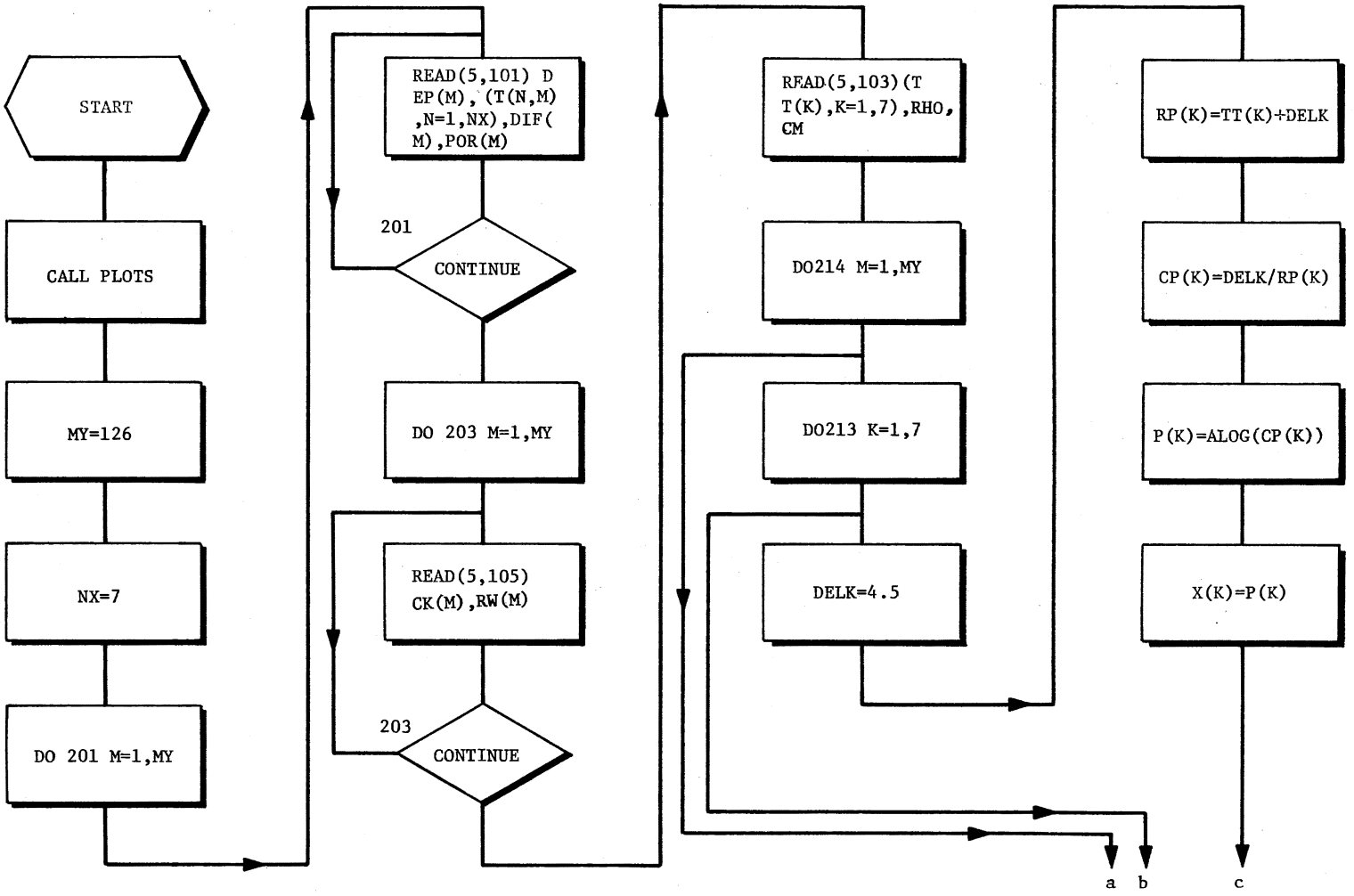

Continued on Page 135

Flow Chart of Main Program Continued from Page 134

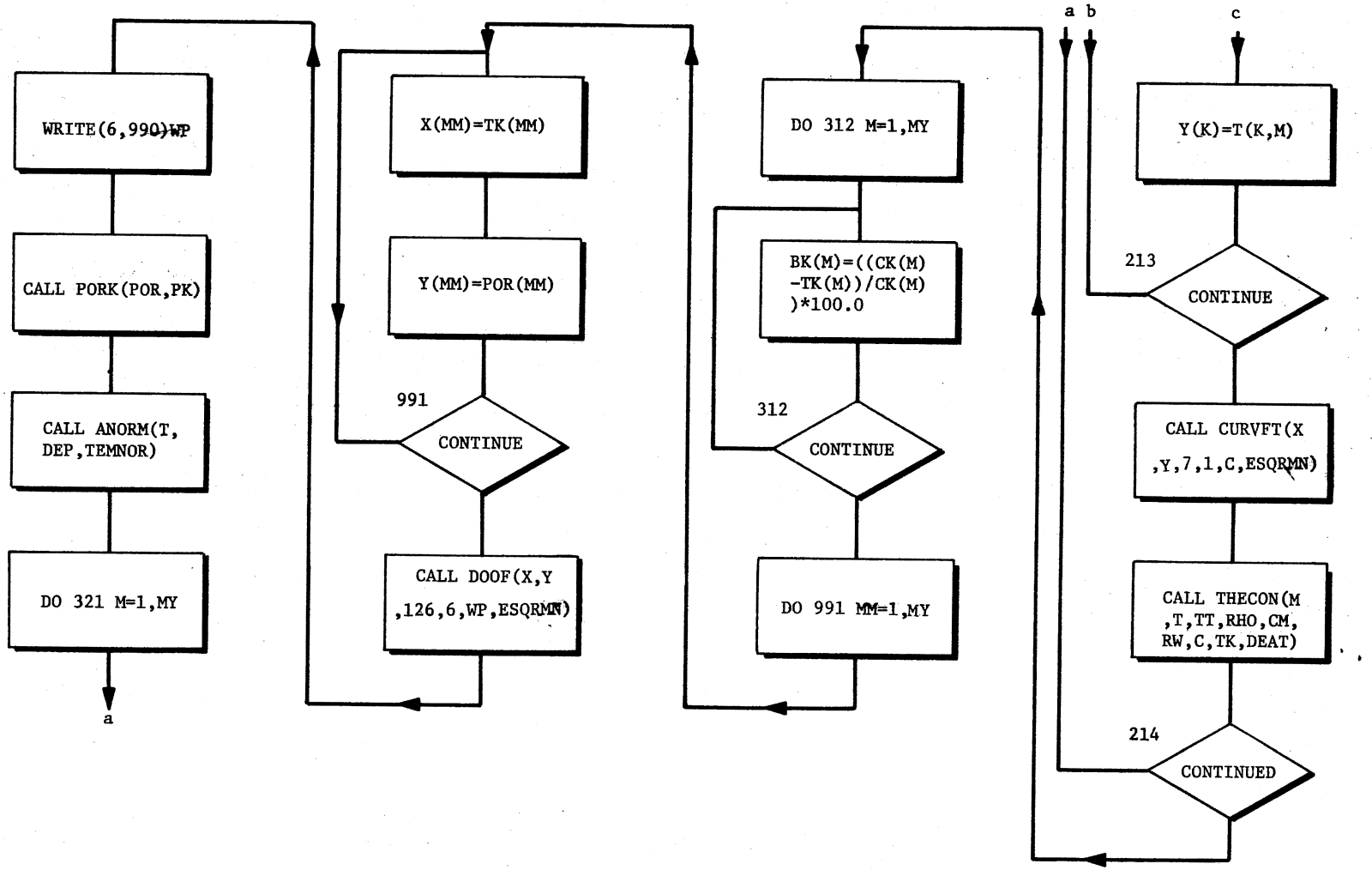

Continued on Page 136

Flow Chart of Main Program Continued from Page 135

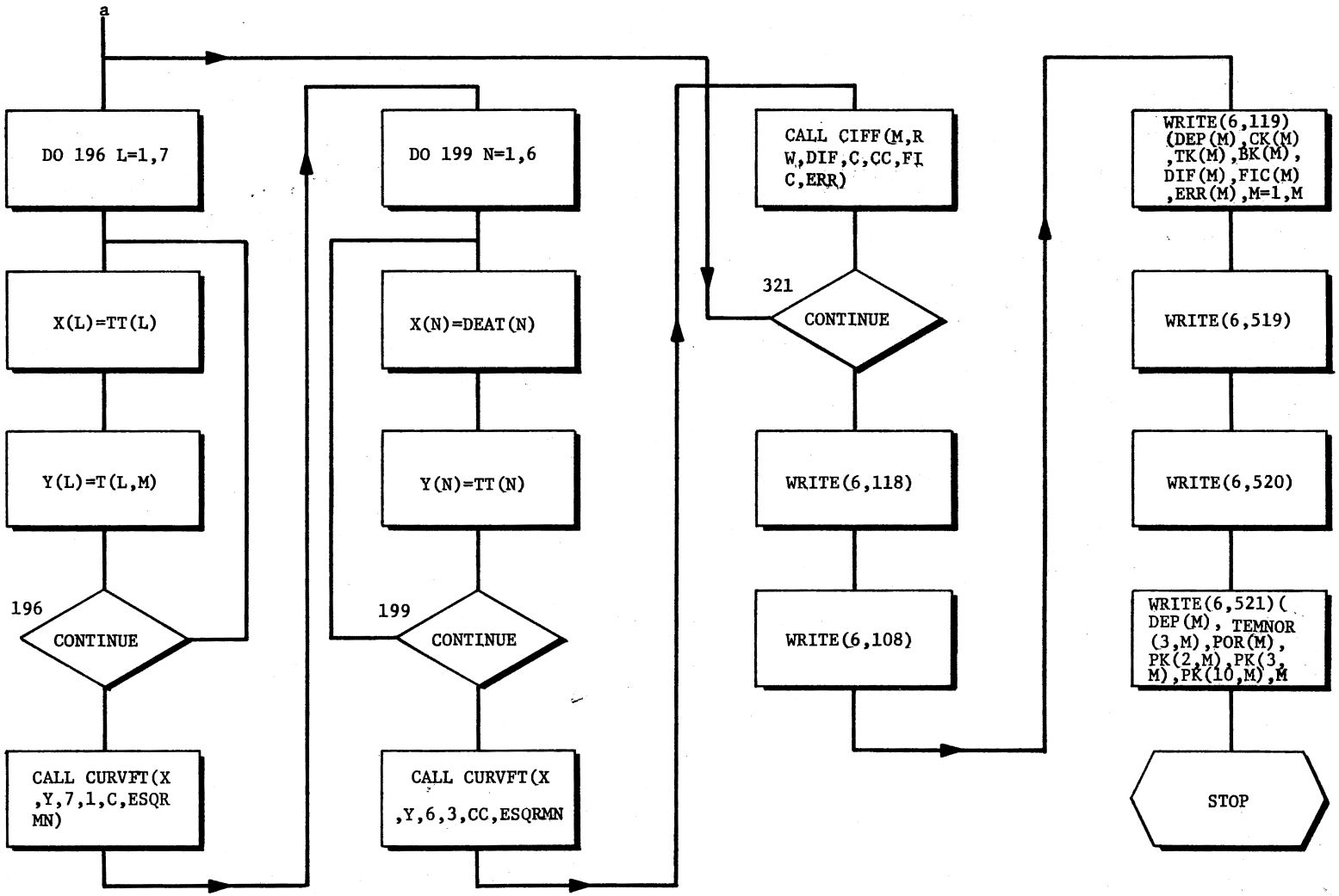

Flow Chart of Main Program Concluded

Listing of Subroutine COOK

```
1     C     +       SUBROUTINE COOK -CALCOM PLOTTER                          +
1     C------
1           SUBROUTINE COOK(DEP,CK)
2     C------
2     C     ++++++++++++++++++++++++++++++++++++++++++++++++++++++++++++++++++
2     C     +
2     C     +                                                                +
2     C      +                CALLING REQUIREMENTS                          +
2     C     +                                                                +
2     C     +       XARRAY     ARRAY OF VALUES ALONG THE X- DIRECTION        +
2     C     +
2     C     +       YARRAY     ARRAY OF VALUES ALONG THE Y-DIRECTION         +
2     C     +                                                                +
2     C     +       DEP        WELL BORE DEPTH ALONG THE X-DIRECTION         +
2     C     +                                                                +
2     C     +       CK         ARRAY OF THERMAL CONDUCTIVITY VALUES ALONG THE+
2     C     +                  Y-DIRECTION                                   +
2     C     +                                                                +
2     C     +                                                                +
2     C     ++++++++++++++++++++++++++++++++++++++++++++++++++++++++++++++++++
2           DIMENSION DEP(130),DIF(130),XARRAY(128),YARRAY(128)
3          A,CK(130)
4     C     SET ORIGIN TO RIGNT HAND OF THE DRUM
4     C------
4           CALL PLOTC(0.,-11.0,-3)
5     C      REORIGIN TO CENTER | AXIS ON THE PAGE
5     C------
5           CALL PLOTC(0.,2.5,-3)
6     C------
6     C     GENERATE DATA POINTS TO BE PLOTTED
6     C------
6           DO 218 M=1,126
7           XARRAY(M)=DEP(M)
8           YARRAY(M)=CK(M)
9       218 CONTINUE
10    C------
10    C SCALE THE VALUES AND DRAW THE LINE
10    C------
10          CALL SCALE(XARRAY,10.0,126,1)
11          CALL AXIS(0.0,0.0,'DEPTH FEET',-10,10.0,0.0,XARRAY(127),XARRAY(128
12    C-----
12          CALL SCALE(YARRAY,6.0,126,1)
13          CALL AXIS(0.0,0.0,'THERM.COND.BTU/HR.FT.F',22,6.0,90.0,YARRAY(127)
14    C
14    C     PLOT AXIS
14          CALL LINE(XARRAY,YARRAY,126,1,1,3)
15          RETURN
16          END
```

Listing of Subroutine COOK Concluded

Flow Chart of Subroutine COOK
This subroutine does plotting.

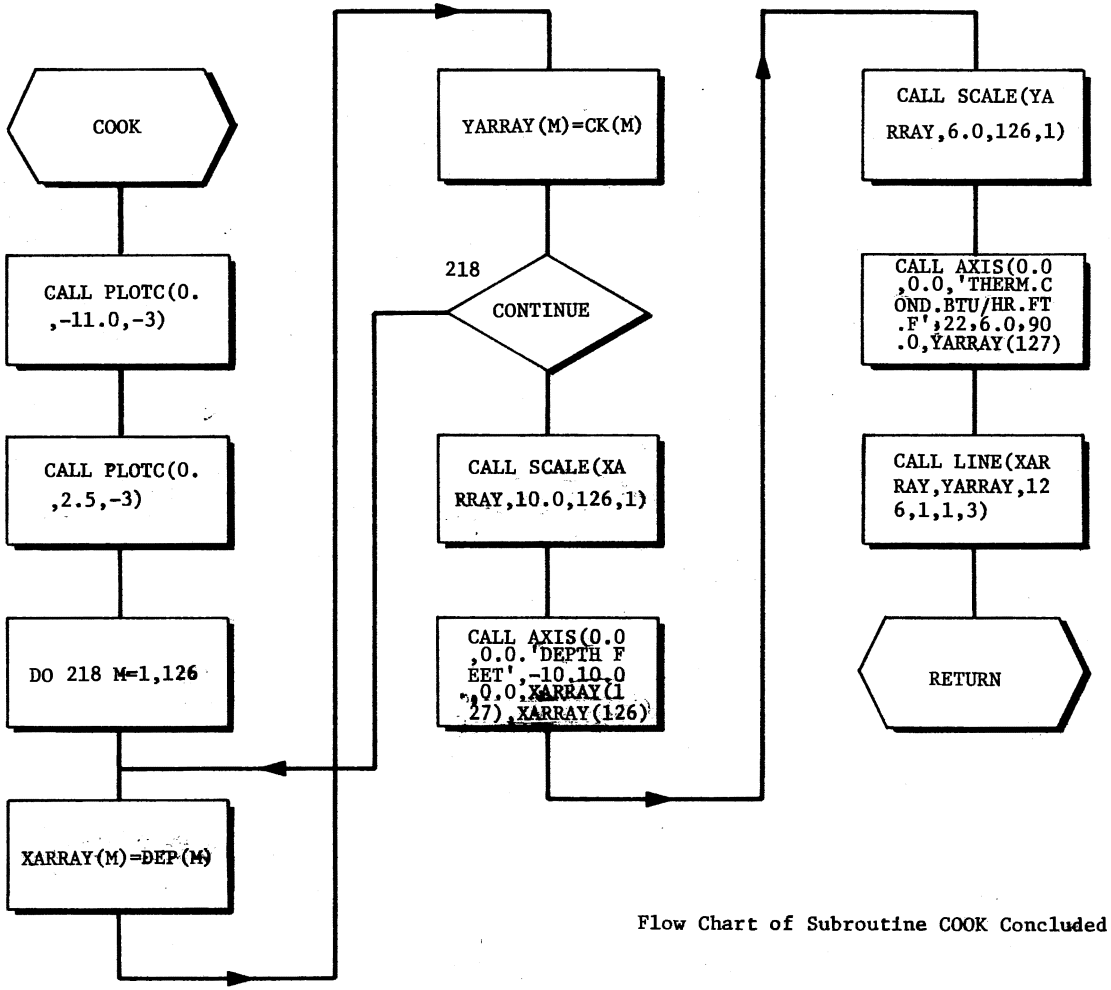

Flow Chart of Subroutine COOK Concluded

Listing of Subroutine CURVFT

```
C     +       SUBROUTINE CURVFT - LEAST SQUARES METHOD                  +
C-----
      SUBROUTINE CURVFT(X,Y,N,NDEGX,C,ESQRMN)
C-----
C     ++++++++++++++++++++++++++++++++++++++++++++++++++++++++++++++++++
C     +                                                                 +
C     +       CALLING REQUIREMENTS                                      +
C     +                                                                 +
C     +       X          ARRAY OF VALUES OF INDEPENDENT VARIABLE        +
C     +       Y          ARRAY OF VALUES OF DEPENDENT VARIABLE          +
C     +       N          DIMENSION OF X OR Y                            +
C     +       NDEGX      MAXIMUM DEGREE OF POLYNOMIAL IN X              +
C     +       C          RESULTING COEFFICIENT VECTOR FOR A FUNCTIONAL  +
C     +                  RELATION OF THE FORM Y = SUM( C(I)*(X**(I-1))  +
C     +                                           I                     +
C     +       ESQRMN     MINIMUM SQUARED ERROR FOUND                    +
C     +                                                                 +
C     +       SUBPROGRAM REQUIREMENT                                    +
C     +       SIMQ       TO SOLVE LINEAR SIMULTANEOUS EQUATIONS (SSP)   +
C     +       PVAL       TO EVALUATE A POLYNOMIAL AT THE POINT X(SSP)   +
C     +                                                                 +
C     ++++++++++++++++++++++++++++++++++++++++++++++++++++++++++++++++++
C-----
      DIMENSION X(8),Y(8),C(10
     *                       ),XKPNM1(21),A(121)
C-----
      NXP1 = NDEGX + 1
      NXT2 = NDEGX*2
      LENTHA = NXP1*NXP1
C-----
      DO 10 IC=1,NXP1
   10 C(IC) = 0.0
      DO 11 IA=1,LENTHA
   11 A(IA) = 0.0
C-----
      DO 100 K=1,N
      XKPNM1(1) = 1.0
      IF(NXT2.EQ.0) GO TO 21
      DO 20 IX=1,NXT2
   20 XKPNM1(IX+1) = XKPNM1(IX)*X(K)
C-----
   21 DO 100 IP=1,NXP1
      IARG = IP - NXP1
      DO 30 I=1,NXP1
      IARG = IARG + NXP1
   30 A(IARG) = A(IARG) + XKPNM1(IP+I-1)
  100 C(IP) = C(IP) + Y(K)*XKPNM1(IP)
C-----
      IF(NXP1.GT.1) GO TO 41
      C(1) = C(1)/A(1)
      GO TO 42
   41 CALL SIMQ(A,C,NXP1,0)
C-----
   42 ESQRMN = 0.0
```

Continued on Page 140

Listing of Subroutine CURVFT Continued from Page 139

```
27          DO 40 K=1,N
28          CALL PVAL(YK,X(K),C,NXP1)
29       40 ESQRMN= ESQRMN + (Y(K) -YK)*(Y(K)-YK)
30          RETURN
31          END
```

Listing of Subroutine CURVFT Concluded

Flow Chart of Subroutine CURVFT
This subroutine smooths out the experimental data.

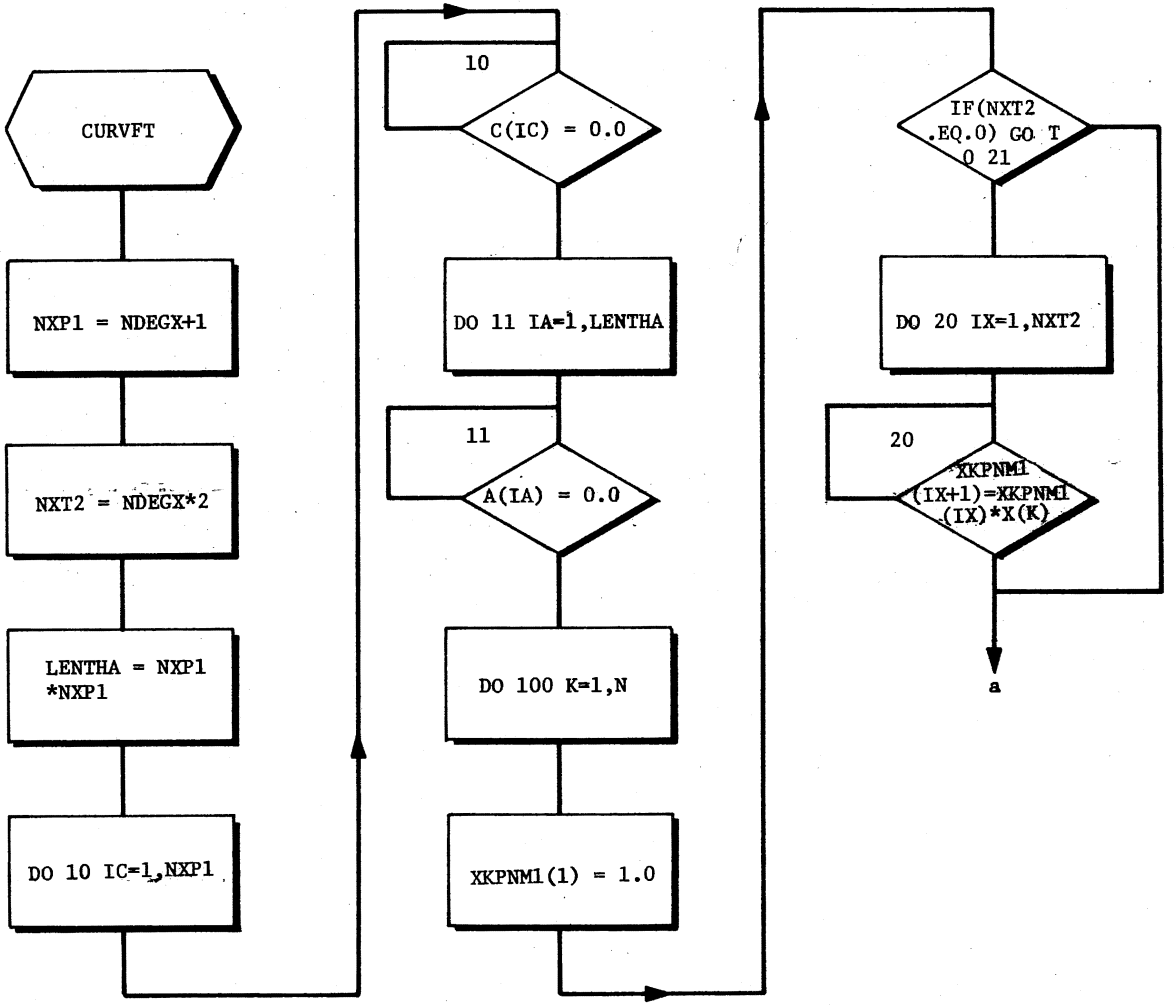

Continued on Page 142

Flow Chart of Subroutine CURVFT Continued from Page 141

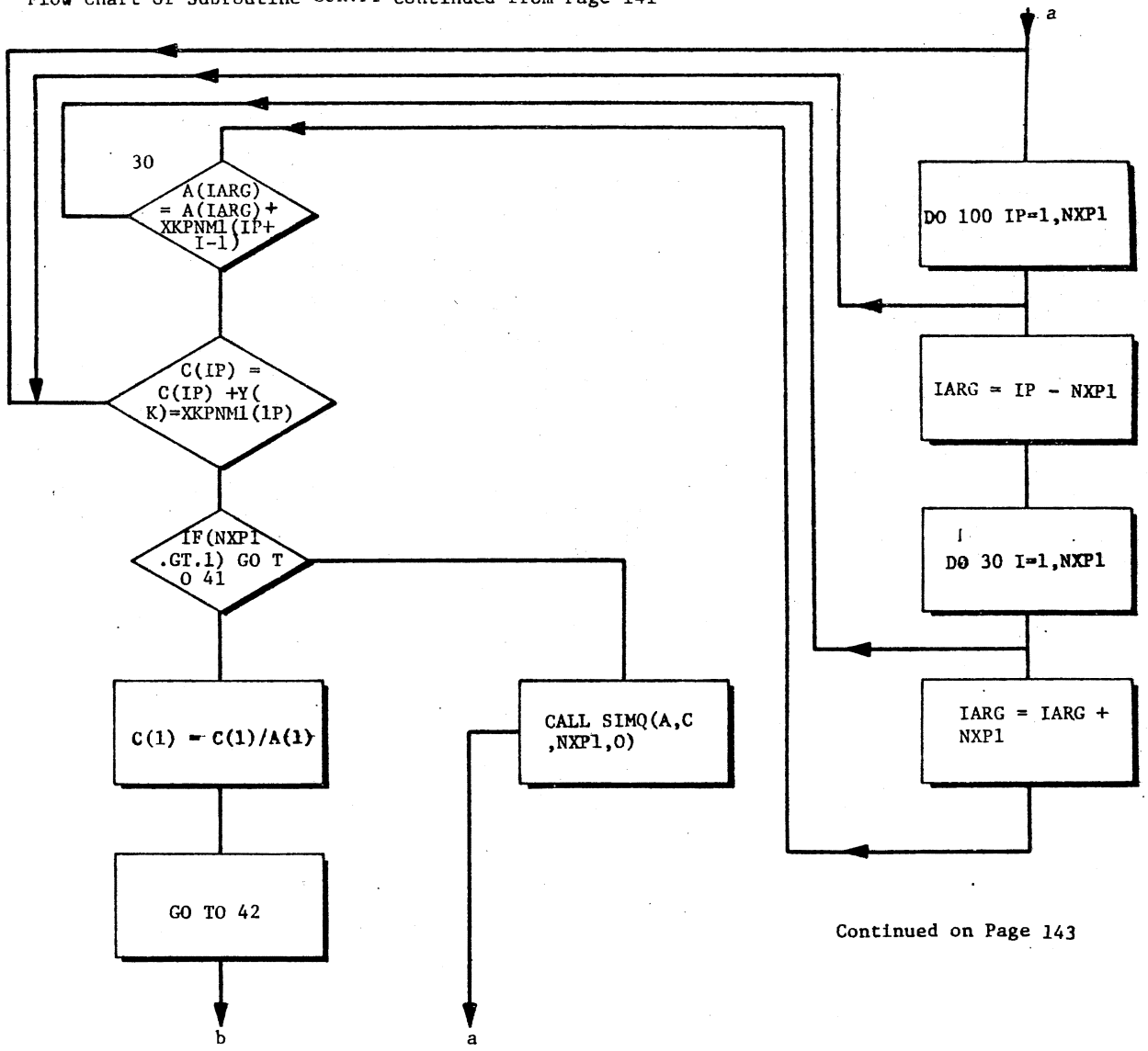

Continued on Page 143

Flow Chart of Subroutine CURVFT Continued from Page 142

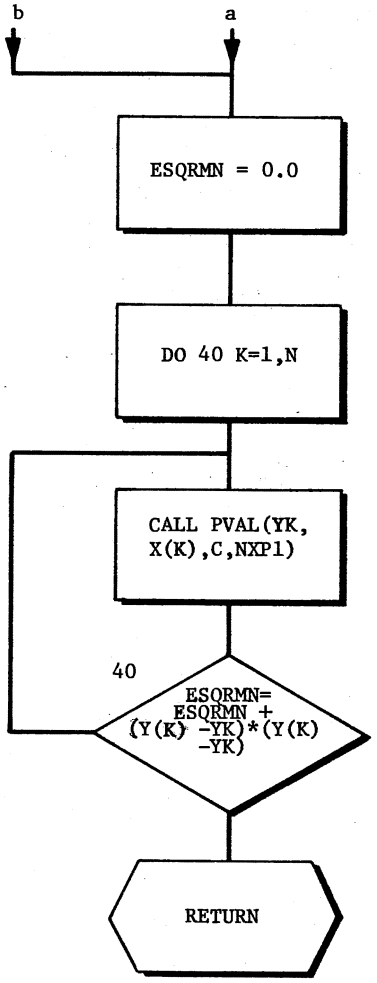

Flow Chart of Surbroutine CURVFT Concluded

Listing of Subroutine THECON

```
1     C      +       SUBROUTINE THECON TO PREDICT THERMAL COND. VALUES
1     C------
1           SUBROUTINE THECON(M,T,TT,RHO,CM,RW,C,TK,DEAT)
2     C------
2     C     ++++++++++++++++++++++++++++++++++++++++++++++++++++++++++++++++++++
2     C     +                                                                  +
2     C      +                    CALLING REQUIREMENTS                       +
2     C     +                                                                  +
2     C     +        M           CALCULATION COUNTER                         +
2     C     +                                                                  +
2     C     +        TT          ARRAY OF TIME FOR TEMPERATURE RUNS          +
2     C     +                                                                  +
2     C     +        RHO         DENSITY OF DRILLING FLUID                   +
2     C     +                                                                  +
2     C     +        CM          SPECIFIC HEAT OF DRILLING FLUID             +
2     C     +                                                                  +
2     C     +        RW          RADIUS OF THE WELL BORE                     +
2     C     +                                                                  +
2     C     +        C           CURVE FIT COEFFICIENTS                      +
2     C     +                                                                  +
2     C     +        TK          CALCULATED THERMAL CONDUCTIVITY             +
2     C     +                                                                  +
2     C     +                                                                  +
2     C     +        DEP         DEPTH OF WELL BORE IN FEET                  +
2     C     +                                                                  +
2     C     +        CK          ARRAY OF EXPERIMENTAL AND INTERPOLATED THERMAL+
2     C     +                                                                  +
2     C     +                    CONDUCTIVITY VALUES IN BTU/HR.FT.F          +
2     C     ++++++++++++++++++++++++++++++++++++++++++++++++++++++++++++++++++++
2           DIMENSION C(3),Y(130),TME(7),DEL(8,130),HEAT(7),TT(8),T(8,130)
3          A,ARATE(130),TK(130),SFT(130),SLP(130),DEAT(8),RW(130)
4           X=0.5
5           Y(M)=C(2)*X+C(1)
6           SLP(M)=(Y(M)-C(1))/(0.5)
7     C    --------INITIALIZE
7           DO 4 N=1,6
8           TME(N)=0.0
9           DEL(N,M)=0.0
10         4 CONTINUE
11    C-----
11          LN=6
12          DO5 N=1,LN
13          QU=RHO*CM
14          TME(N)=TT(N+1)-TT(N)
15          DEL(N,M)=T(N+1,M)-(T(N,M))
16          HEAT(N)=(DEL(N,M)*QU)/(TME(N))
17          DEAT(N)=QU*HEAT(N)*(RW(M)**2)
18         5 CONTINUE
19    C-----
19          THEAT=HEAT(1)+HEAT(2)+HEAT(3)+HEAT(4)+HEAT(5)+HEAT(6)
20          ARATE(M)=((THEAT)*(-1.0))/6.0
21          TK(M)=(ARATE(M)*(RW(M)**2)/(SLP(M)*4.0)
22          RETURN
23          END
```

Listing of Subroutine THECON Concluded

Flow Chart of Subroutine THECON
This subroutine calculates thermal conductivity.

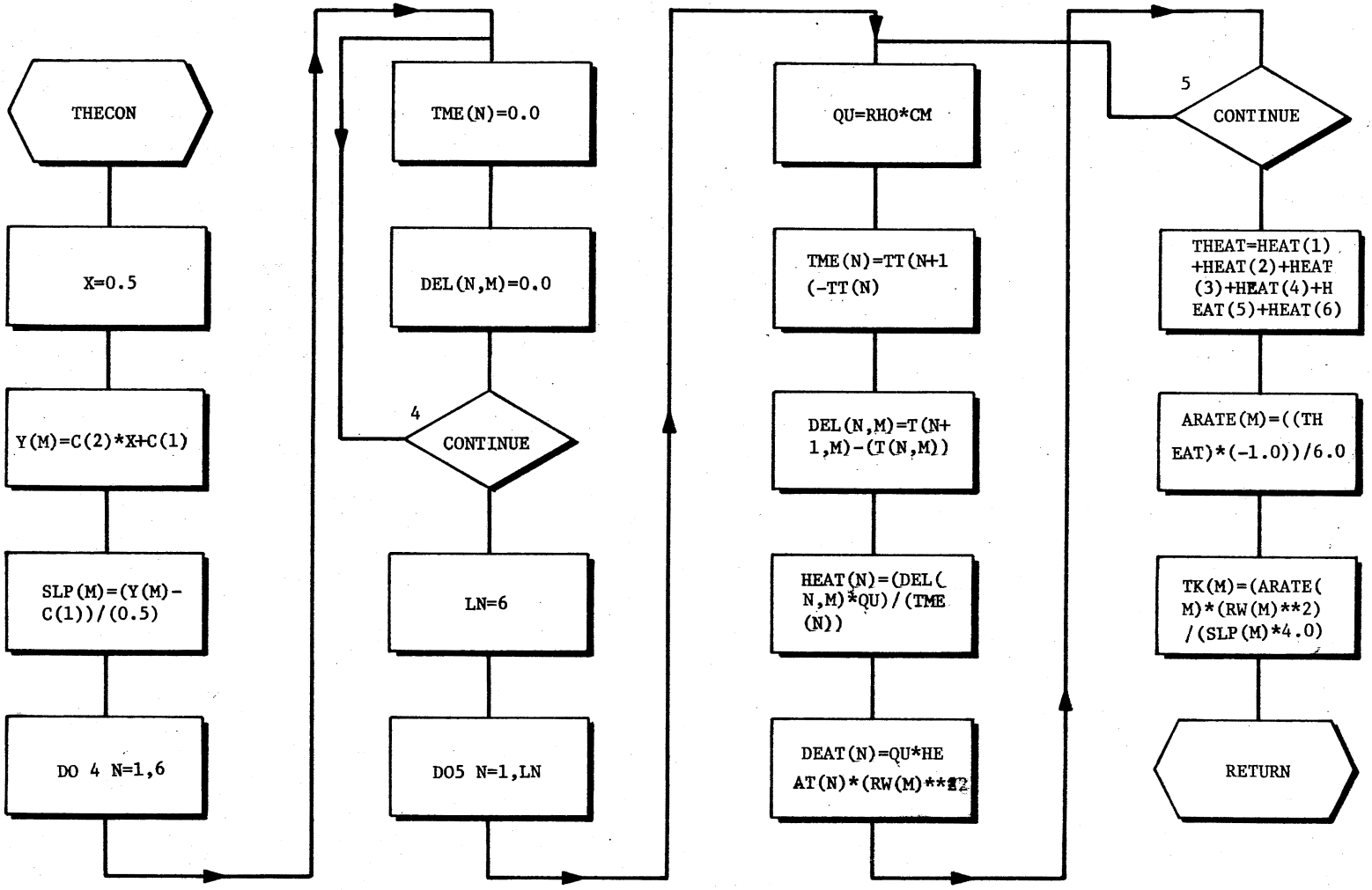

Flow Chart of Subroutine THECON Concluded

Listing of Subroutine DOOF

```
1          SUBROUTINE DOOF(X,Y,N,NDEGX,C,ESQRMN)
2     C-----
2     C     ++++++++++++++++++++++++++++++++++++++++++++++++++++++++++++++++
2     C     +       SUBROUTINE CURVFT - LEAST SQUARES METHOD                 +
2     C     +                                                                +
2     C     +       CALLING REQUIREMENTS                                     +
2     C     +                                                                +
2     C     +       X          ARRAY OF VALUES OF INDEPENDENT VARIABLE       +
2     C     +       Y          ARRAY OF VALUES OF DEPENDENT VARIABLE         +
2     C     +       N          DIMENSION OF X OR Y                           +
2     C     +       NDEGX      MAXIMUM DEGREE OF POLYNOMIAL IN X             +
2     C     +       C          RESULTING COEFFICIENT VECTOR FOR A FUNCTIONAL +
2     C     +                  RELATION OF THE FORM Y = SUM( C(I)*(X**(I-1)) +
2     C     +                                           I                    +
2     C     +       ESQRMN     MINIMUM SQUARED ERROR FOUND                   +
2     C     +                                                                +
2     C     +       SUBPROGRAM REQUIREMENT                                   +
2     C     +       SIMQ       TO SOLVE LINEAR SIMULTANEOUS EQUATIONS (SSP)  +
2     C     +       PVAL       TO EVALUATE A POLYNOMIAL AT THE POINT X(SSP)  +
2     C     +                                                                +
2     C     ++++++++++++++++++++++++++++++++++++++++++++++++++++++++++++++++
2     C-----
2          DIMENSION X(130),Y(130),C(10),XKPNM1(130),A(130)
3     C-----
3          NXP1 = NDEGX + 1
4          NXT2 = NDEGX*2
5          LENTHA = NXP1*NXP1
6     C-----
6          DO 10 IC=1,NXP1
7       10 C(IC) = 0.0
8          DO 11 IA=1,LENTHA
9       11 A(IA) = 0.0
10    C-----
10         DO 100 K=1,N
11         XKPNM1(1) = 1.0
12         IF(NXT2.EQ.0) GO TO 21
13         DO 20 IX=1,NXT2
14      20 XKPNM1(IX+1) = XKPNM1(IX)*X(K)
15    C-----
15      21 DO 100 IP=1,NXP1
16         IARG = IP - NXP1
17         DO 30 I=1,NXP1
18         IARG = IARG + NXP1
19      30 A(IARG) = A(IARG) + XKPNM1(IP+I-1)
20     100 C(IP) = C(IP) + Y(K)*XKPNM1(IP)
21    C-----
21         IF(NXP1.GT.1) GO TO 41
22         C(1) = C(1)/A(1)
23         GO TO 42
24      41 CALL SIMQ(A,C,NXP1,0)
25    C-----
25      42 ESQRMN = 0.0
26         DO 40 K=1,N
27         CALL PVAL(YK,X(K),C,NXP1)
```

Continued on Page 147

Listing of Subroutine DOOF Continued from Page 146

```
28          40 ESQRMN= ESQRMN + (Y(K) -YK)*(Y(K)-YK)
29             RETURN
3C             END
```

Listing of Subroutine DOOF Concluded

Flow Chart of Subroutine DOOF
This subroutine developes a correlation between porosity and thermal conductivity.

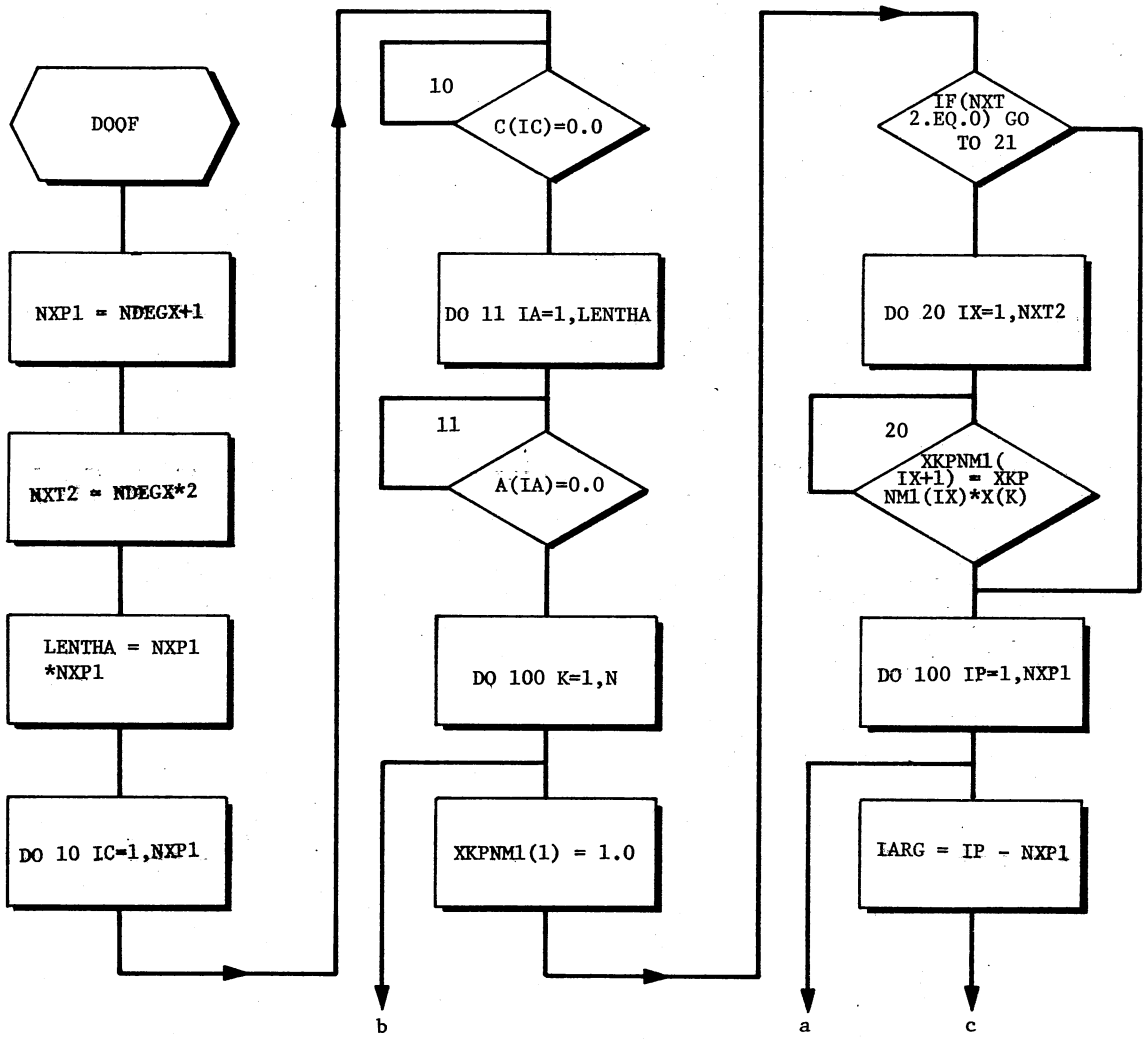

Continued on Page 149

Flow Chart of Subroutine DOOF Continued from Page 148

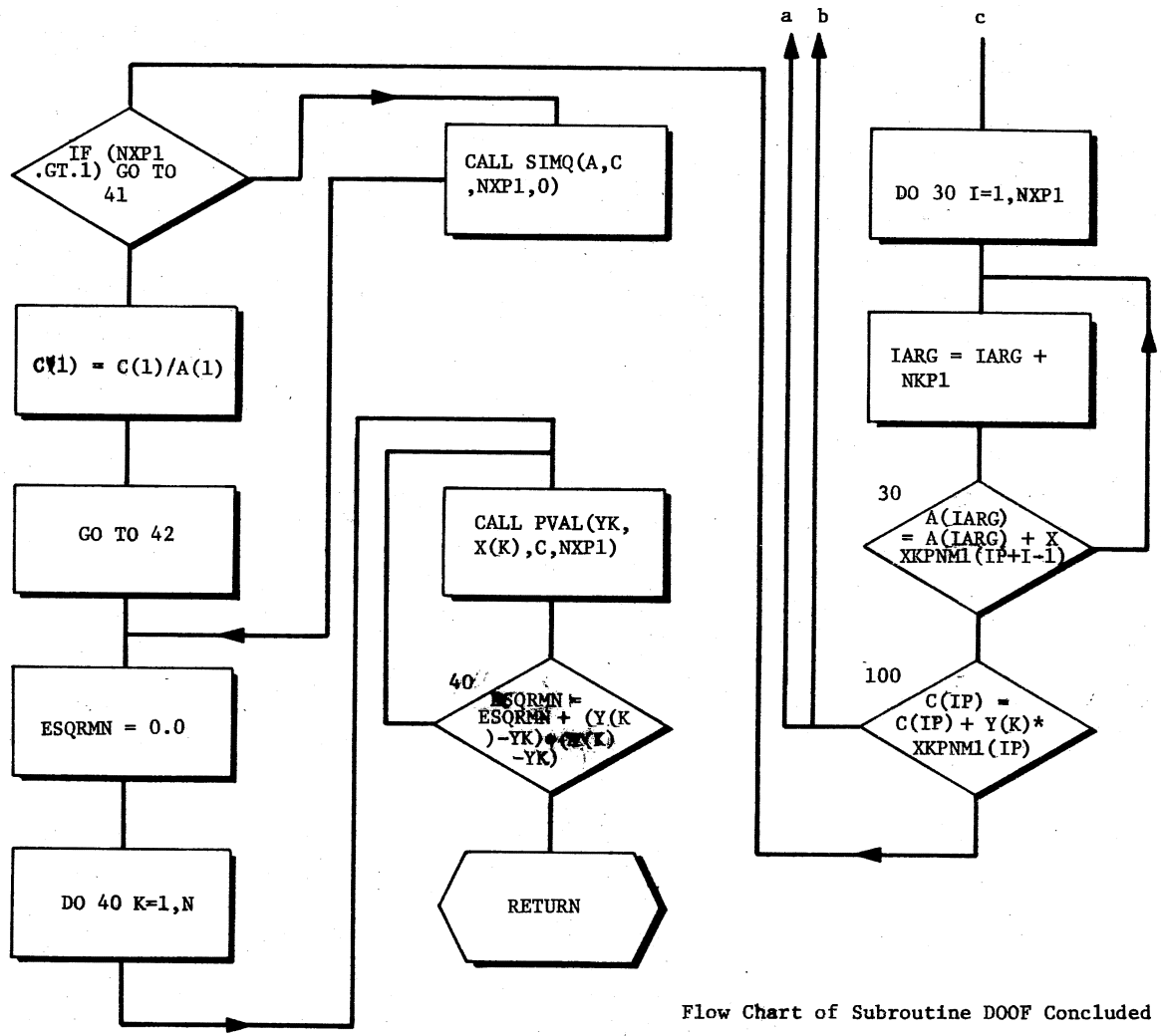

Flow Chart of Subroutine DOOF Concluded

Listing of Subroutine PORK

```
1     C     +       SUBROUTINE PORK-THERMAL CONDUCTIVITY FROM POROSITY       +
1     C------
1           SUBROUTINE PORK(POR,PK)
2     C------
2     C     ++++++++++++++++++++++++++++++++++++++++++++++++++++++++++++++++++
2     C     +                                                                +
2     C     +                                                                +
2     C     +                    CALLING REQUIREMENTS                        +
2     C     +                                                                +
2     C     +       POR          POROSITY AS A FRACTION OF 1.0               +
2     C     +       PK           POROSITY DERIVED THERMAL CONDUCTIVITY       +
2     C     +                                                                +
2     C     +       AIN          ARRAY OF ROCK MATRIX THERMAL CONDUCTIVITY   +
2     C     +                                                                +
2     C     +                                                                +
2     C     ++++++++++++++++++++++++++++++++++++++++++++++++++++++++++++++++++
2     C
2     C
2     C-----
2           DIMENSION AIN(10),ZINC(130),PK(10,130)
3          A,POR(130)
4     C
4     C
4     C
4           DATA AIN/1.0,1.2,1.4,1.6,1.8,2.0,2.2,2.4,2.6,2.8/
5            RT=0.1
6           C=0.999
7           DO 1 MK=1,126
8     C-----
8           ZINC(MK)=C*POR(MK)
9           DO 1 I=1,10
10    C-----
10          PK(I,MK)=AIN(I)*(((RT/AIN(I)))**ZINC(MK))
11    C
11       1 CONTINUE
12    C
12          RETURN
13          END
```

Listing of Subroutine PORK Concluded

Flow Chart of Subroutine PORK
This subroutine calculates thermal conductivity from porosity.

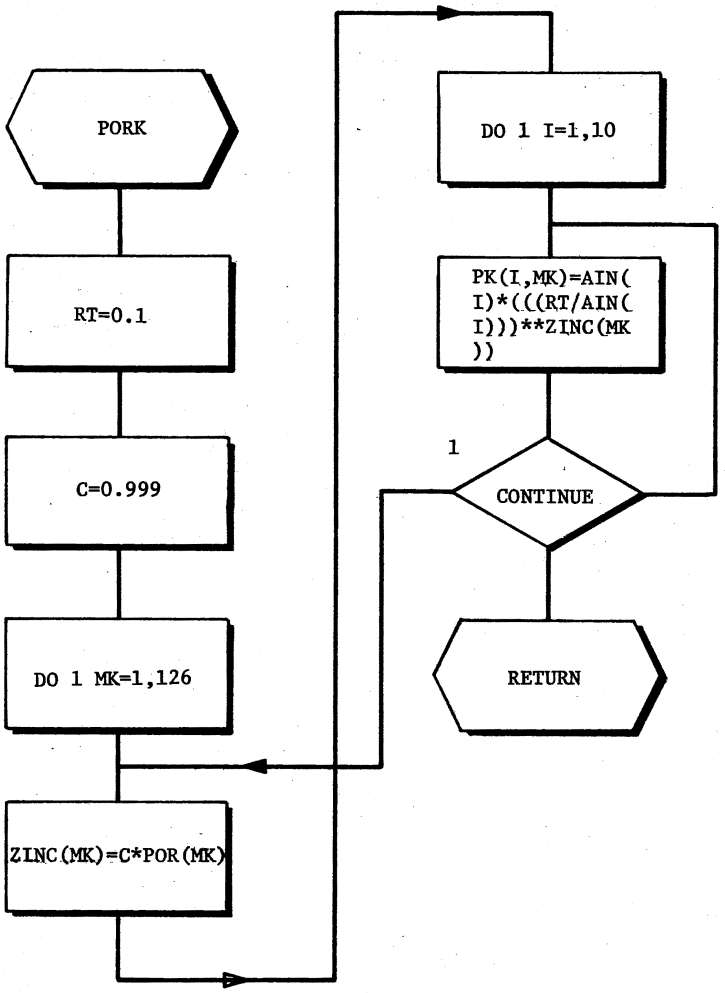

Flow Chart of Subroutine PORK Concluded

Listing of Subroutine ANORM

```
1     C      +        SUBROUTINE ANORM-NORMALIZED TEMPERATURE                +
1     C------
1           SUBROUTINE ANORM(T,DEP,TEMNOR)
2     C------
2     C     ++++++++++++++++++++++++++++++++++++++++++++++++++++++++++++++++++
2     C     +                                                                 +
2     C     +                    CALLING REQUIREMENTS                         +
2     C     +                                                                 +
2     C     +        ATM         ATMOSPHERIC TEMPERATURE                      +
2     C     +                                                                 +
2     C     +        T           WELL BORE TEMPERATURE                        +
2     C     +                                                                 +
2     C     +        DEP         WELL BORE DEPTH                              +
2     C     +                                                                 +
2     C     +        TEMNOR      NORMALIZED TEMPERATURE                       +
2     C     +                                                                 +
2     C     +                                                                 +
2     C     ++++++++++++++++++++++++++++++++++++++++++++++++++++++++++++++++++
2     C-----
2     C-----
2     C-----
2           DIMENSION T(8,130),DEP(130),TEMNOR(8,130),ABT(130)
3     C
3           DO 121 M=1,126
4           ATM=70.0
5           DO 121 I=1,7
6     C-----
6     C-----
6           ABT(M)=(DEP(M)*0.007)+ATM
7           TEMNOR(I,M)=T(I,M)-ABT(M)
8     C-----
8       121 CONTINUE
9     C-----
9     C-----
9           RETURN
10          END
```

Listing of Subroutine ANORM Concluded

Flow Chart of Subroutine ANORM
This subroutine calculates normalized temperatures.

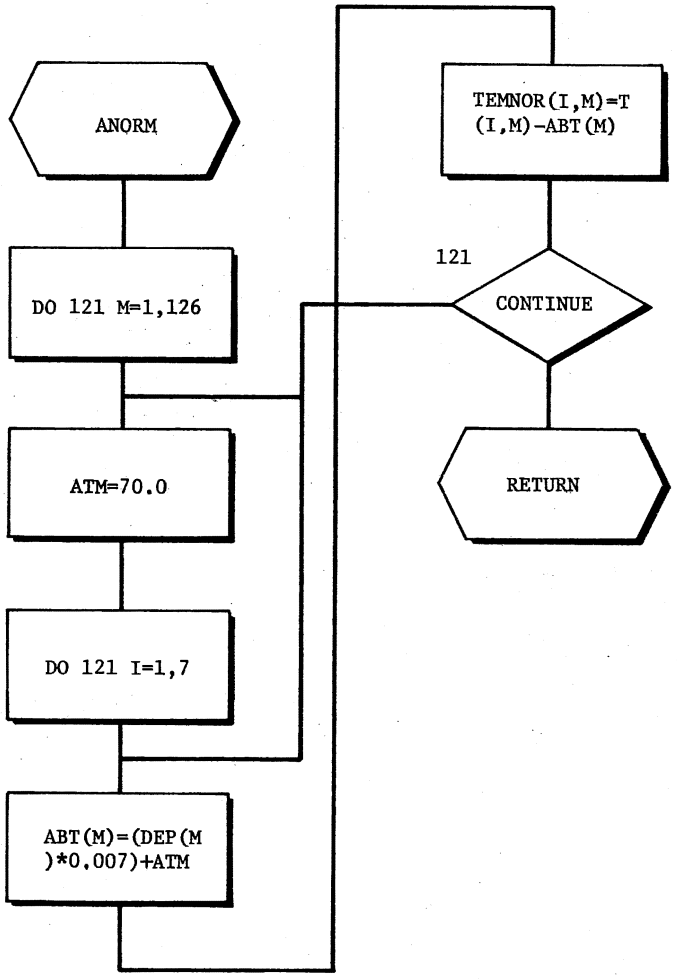

Flow Chart of Subroutine ANORM Concluded

Listing of Subroutine CIFF

```
1     C     +       SUBROUTINE CIFF-THERMAL DIFF. METHOD                  +
1     C------
1           SUBROUTINE CIFF(M,RW,DIF,C,CC,FIC,ERR)
2     C------
2     C     ++++++++++++++++++++++++++++++++++++++++++++++++++++++++++++++++
2     C     +                                                              +
2     C     +                    CALLING REQUIREMENTS                      +
2     C     +                                                              +
2     C     +       M            CALCULATION COUNTER                       +
2     C     +                                                              +
2     C     +       RW           WELL BORE RADIUS                          +
2     C     +                                                              +
2     C     +       DIF          EXPERIMENTAL THERMAL DIFFUSIVITY          +
2     C     +                                                              +
2     C     +       C            CURVE FIT COEFFICIENT                     +
2     C     +                                                              +
2     C     +       FIC          CALCULATED THERMAL DIFFUSIVITY            +
2     C     +                                                              +
2     C     +       ERR          PERCENTAGE ERROR                          +
2     C     +                                                              +
2     C     +       ADM          CONVERGENCE CRITERIA                      +
2     C     +                                                              +
2     C     +       DEAT         RATE OF HEAT FLOW                         +
2     C     +                                                              +
2     C     +                                                              +
2     C     ++++++++++++++++++++++++++++++++++++++++++++++++++++++++++++++++
2     C-----
2     C-----
2     C-----
2           DIMENSION C(3),DIF(130),FIC(130),TL(130),BM(130),AM(130),DR(130),
3          A,TK(130),B(130),AB(130),ERR(130),RW(130),DS(130),AD(130),CC(10)
4     C-----
4     C-----
4           X1=16.0
5           TK(M)=C(2)*X1+C(1)
6           X2=12.0
7           TL(M)=C(2)*X2+C(1)
8           B(M)=TL(M)/TK(M)
9           AM(M)=DIF(M)
10    C-----
10          N=0
11    C-----
11    C-----
11      142 BD=(48.0)*(AM(M))
12          DB= (RW(M)**2)/BD
13          DI= ((DB)**2)/4.0
14           DJ=((DB)**3)/18.0
15          DK=((DB)**4)/96.0
16          DY=(DB)/1.33333
17          DY1=((DY)**2)/4.0
18          DY2=((DY)**3)/18.0
19          DY3=((DY)**4)/96.0
20    C-----
20    C-----
```

Continued on Page 155

Listing of Subroutine CIFF Continued from Page 154

```
20          ZV=ALOG(DB)
21          ZK=ALOG(DY)
22      C-----
22          DR(M)=0.057722+ZV-DB+DI-DJ+DK
23          DS(M)=0.57722+ZK-DY+DY1-DY2+DY3
24          CB=CC(4)*(X1)**3+CC(3)*(X1)**2+CC(2)*X1+CC(1)
25          DB=CC(4)*(X2)**3+CC(3)*(X2)**2+CC(2)*X2+CC(1)
26          QB=CB/DB
27          AB(M)=(DR(M)/DS(M))*QB
28          AD(M)=ABS(B(M)-AB(M))
29          N=N+1
30          IF(AD(M).LE.0.001) GO TO 181
31          IF(N.GT.50) GO TO 181
32      C-----
32      C-----
32          IF(AD(M).GT.0.001) GO TO 171
33        171 AM(M)=AM(M)+0.011
34          GO TO 142
35      C-----
35      C-----
35        181 CONTINUE
36          FIC(M)=AM(M)
37           GO TO 143
38        143 ERR(M)=((FIC(M)-DIF(M))/(FIC(M)))*100.0
39          RETURN
40          END
```

Listing of Subroutine CIFF Concluded

Flow Chart of Subroutine CIFF
This subroutine calculates thermal diffusivity.

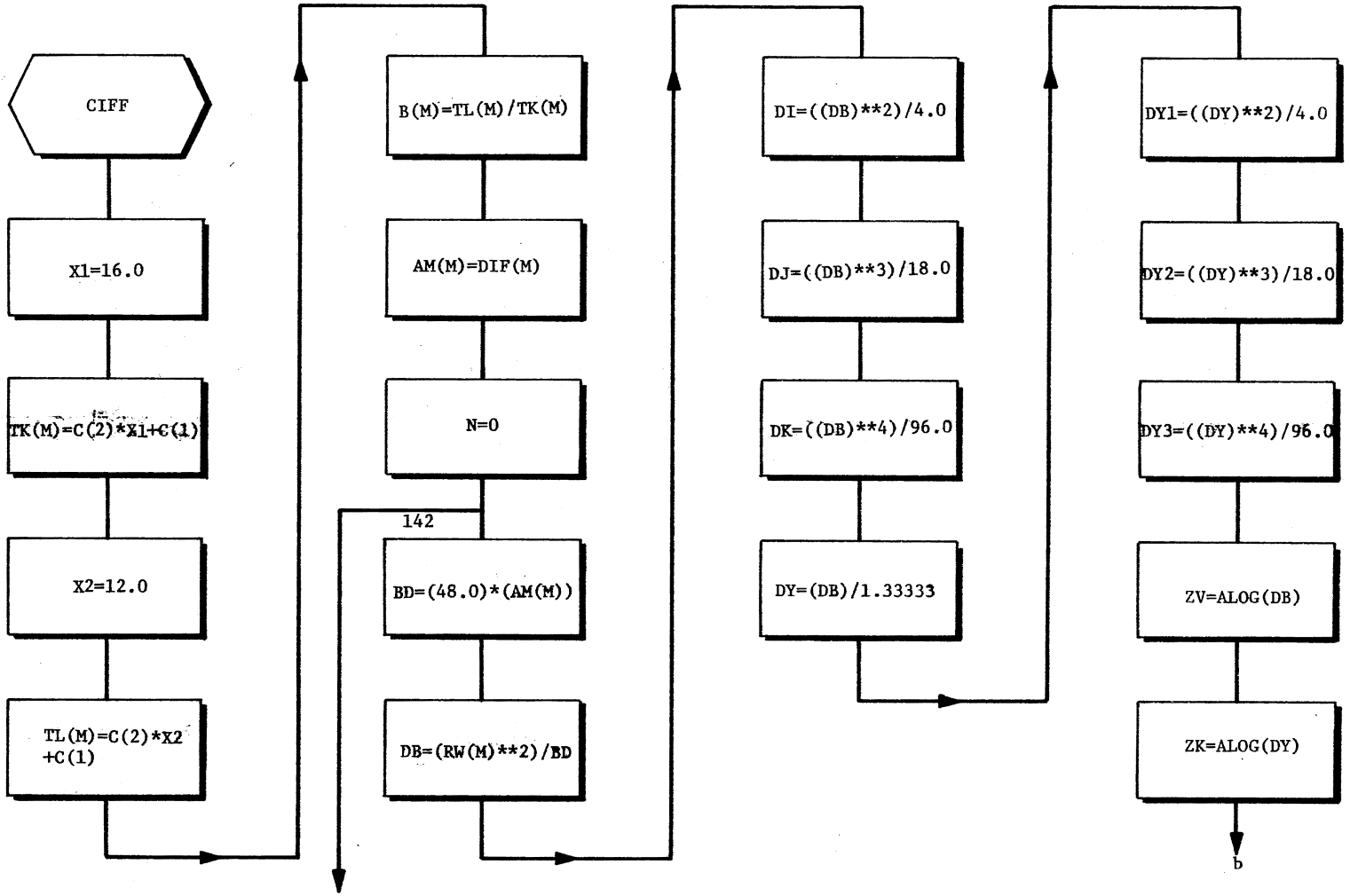

Continued on Page 157

Flow Chart of Subroutine CIFF Continued from Page 156

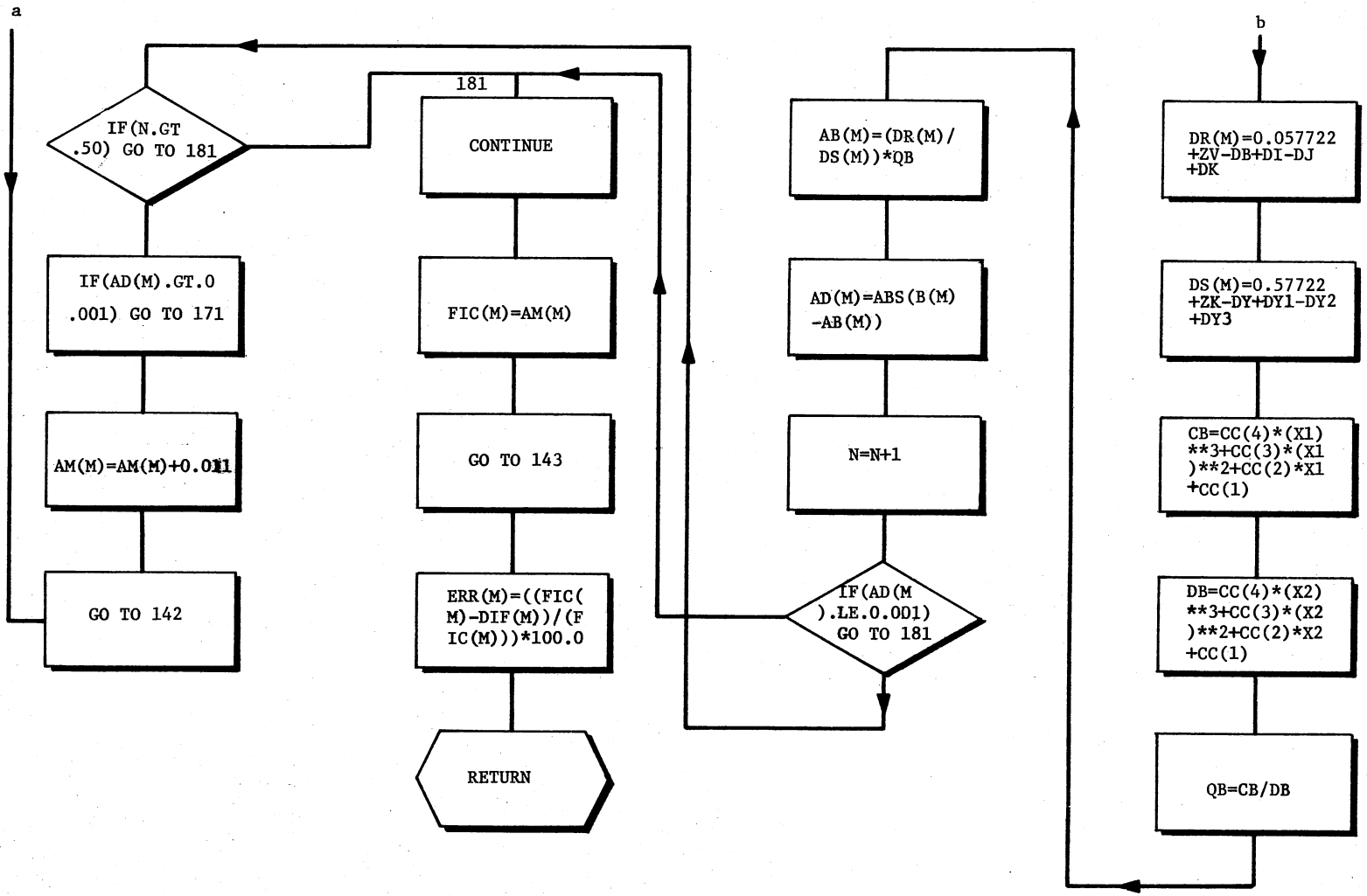

Flow Chart of Subroutine CIFF Concluded

Listing of Subroutine ICSICU

```
1     C     +       SUBROUTINE ICSICU (F,X,N,C,WK,IER)
1     C------
1           SUBROUTINE ICSICU(F,X,N,C,WK,IER)
2     C------
2     C     ++++++++++++++++++++++++++++++++++++++++++++++++++++++++++++++++++++
2     C     +                                                                  +
2     C     +                                                                  +
2     C     +       CALLING REQUIREMENTS
2     C     +                                                                  +
2     C     +                                                                  +
2     C     +FUNCTIONCUBIC SPLINE ONE DIMENTIONAL COEFFICIENT CALCULATOR       +
2     C     +       WITH UNEQUALLY SPACED DATA                                 +
2     C     +       F           VECTOR OF UNEQALLY SPACED FUNCTIONAL VALUES    +
2     C     +       X           VECTOR OF ABSCISSA                             +
2     C     +       N           NUMBER OF DATA POINTS                          +
2     C     +       C           OUT PUT MATRIX OF SPLINE COEFFICIENTS          +
2     C     +       WK          WORK AREA DIMENSION                            +
2     C     +       IER         ERROR PARAMETER                                +
2     C     +                                                                  +
2     C     ++++++++++++++++++++++++++++++++++++++++++++++++++++++++++++++++++++
2           DIMENSION           F(8),C(3,6),WK(72),X(8)
3     C*    DOUBLE PRECISION    F,X,C,WK,EPSLN,OMEGA,W,SP,SPP,SPPP
3     C1    DATA                EPSLN,OMEGA/1.D-14,1.0717967697244908D0/
3           DATA                EPSLN,OMEGA/1.E-5,1.071797/
4           NM1 = N-1
5           NT=5*N
6           I2 = NM1
7           I3 = I2+NM1
8           I4 = I3+NM1
9           I5 = I4+NM1
10          I6 = I5 + NM1
11          I7 = I6+N
12          IER = 0
13    C                                       COMPUTE THE DELTA X AND DELTA F
13          DO 5 I=1,NM1
14             J2 = I2+I
15             WK(I) = X(I+1)-X(I)
16             WK(J2) = (F(I+1)-F(I))/WK(I)
17        5 CONTINUE
18          DO 10 I=2,NM1
19             J2 = I2+I
20             J3 = I3+I
21             J4 = I4+I
22             J5 = I5+I
23             J6 = I6+I
24             J7 = I7+I
25             WK(J3) = WK(I-1)+WK(I)
26             WK(J4) = .5*WK(I-1)/WK(J3)
27             WK(J5) = (WK(J2)-WK(J2-1))/WK(J3)
28             WK(J6) = 2.*WK(J5)
29             WK(J7) = 3.*WK(J5)
30        10 CONTINUE
31          WK(I6+1) = 0.
32          J6 = I6+N
```

Continued on Page 159

Listing of Subroutine ICSICU Continued from Page 158

```
33          WK(J6) = 0.
34          KCOUNT = 0
35       15 ETA = 0.
36          KCOUNT = KCOUNT + 1
37          IF (KCOUNT.GT.NT) GO TO 35
38    C                                     ITERATION TO DETERMINE THE SECOND
38    C                                        DERIVATIVE
38          DO 25 I=2,NM1
39             J4 = I4+I
40             J6 = I6+I
41             J7 = I7+I
42             W = (WK(J7)-WK(J4)*WK(J6-1)-(.5-WK(J4))*WK(J6+1)-WK(J6))*OMEGA
43    C*       IF(DABS(W).LE.ETA) GO TO 20
43    C2       ETA=DABS(W)
43             IF (ABS(W).LE.ETA) GO TO 20
44             ETA = ABS(W)
45       20    WK(J6) = WK(J6)+W
46       25 CONTINUE
47          IF (ETA.GE.EPSLN) GO TO 15
48          DO 30 I=1,NM1
49             J2 = I2+I
50             J6 = I6+I
51             SPP = WK(J6)
52             SPPP = (WK(J6+1)-SPP)/WK(I)
53             SP = WK(J2)-WK(I)*(SPP+SPP+WK(J6+1))/6.
54    C                                     COMPUTE THE COEFFICIENTS FROM THE
54    C                                     FIRST, SECOND, AND THIRD DERIVATIVES
54             C(3,I) = SPPP/6.
55             C(2,I) = .5*SPP
56             C(1,I) = SP
57       30 CONTINUE
58          GO TO 9005
59       35 IER = 129
60     9000 CONTINUE
61          CALL UERTST (IER,6HICSICU)
62     9005 RETURN
63          END

 1    C      SUBROUTINE UERTST (IER,NAME)
 1    C
 1    C
 1    C    FUNCTION              - ERROR MESSAGE GENERATION
 1    C    PARAMETERS    IER     - ERROR PARAMETER. TYPE + N  WHERE
 1    C                              TYPE= 128 IMPLIES TERMINAL ERROR
 1    C                                    64 IMPLIES WARNING WITH FIX
 1    C                                    32 IMPLIES WARNING
 1    C                              N    = ERROR CODE RELEVANT TO CALLING ROUTINE
 1    C                  NAME    - INPUT VECTOR CONTAINING THE NAME OF THE
 1    C                              CALLING ROUTINE AS A SIX CHARACTER LITERAL
 1    C                              STRING.
 1    C-----------------------------------------------------------------------
 1    C
 1          SUBROUTINE UERTST(IER,NAME)
 2    C
 2          DIMENSION           ITYP(5,4),IBIT(4)
```

Continued on Page 160

Listing of Subroutine ICSICU Continued from Page 159

```
      INTEGER*2          NAME(3)
      INTEGER            WARN,WARF,TERM,PRINTR
      EQUIVALENCE        (IBIT(1),WARN),(IBIT(2),WARF),(IBIT(3),TERM)
      DATA     ITYP      /'WARN','ING ','    ','    ','    ',
     *                    'WARN','ING(','WITH',' FIX',')   ',
     *                    'TERM','INAL','    ','    ','    ',
     *                    'NON-','DEFI','NED ','    ','    '/,
     *         IBIT      / 32,64,128,0/
      DATA     PRINTR    / 6/
      IER2=IER
      IF (IER2 .GE. WARN) GO TO 5
C                                      NON-DEFINED
      IER1=4
      GO TO 20
    5 IF (IER2 .LT. TERM) GO TO 10
C                                      TERMINAL
      IER1=3
      GO TO 20
   10 IF (IER2 .LT. WARF) GO TO 15
C                                      WARNING(WITH FIX)
      IER1=2
      GO TO 20
C                                      WARNING
   15 IER1=1
C                                      EXTRACT 'N'
   20 IER2=IER2-IBIT(IER1)
C                                      PRINT ERROR MESSAGE
      WRITE (PRINTR,25) (ITYP(I,IER1),I=1,5),NAME,IER2,IER
   25 FORMAT(' *** I M S L(UERTST) ***  ',5A4,4X,3A2,4X,I2,
     *   ' (IER = ',I3,')')
      RETURN
      END
```

Listing of Subroutine ICSICU Concluded

Flow Chart of Subroutine ICSICU
This cubic spline subroutine does interpolation.

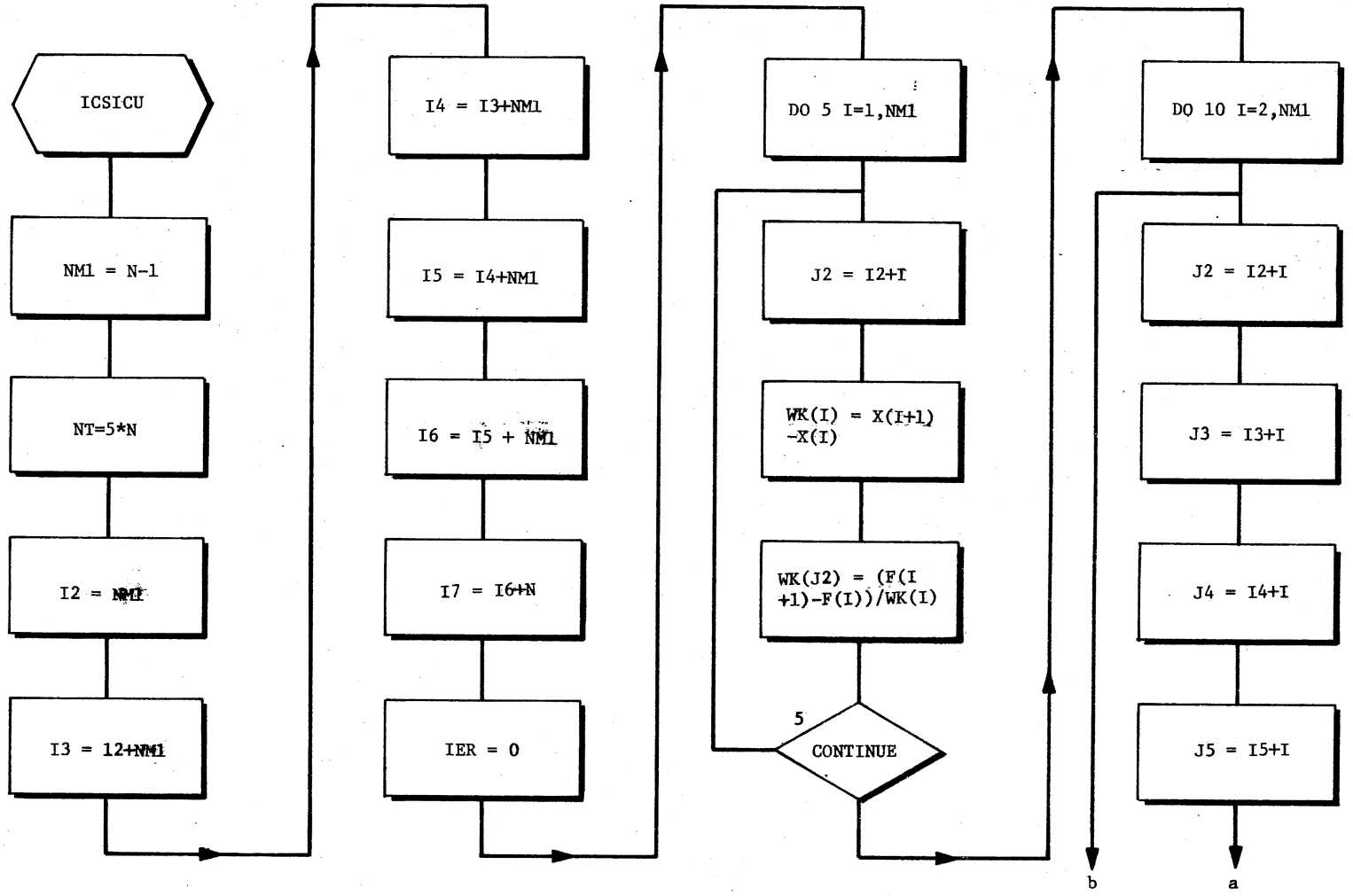

Continued on Page 162

Flow Chart of Subroutine ICSICU Continued from Page 161

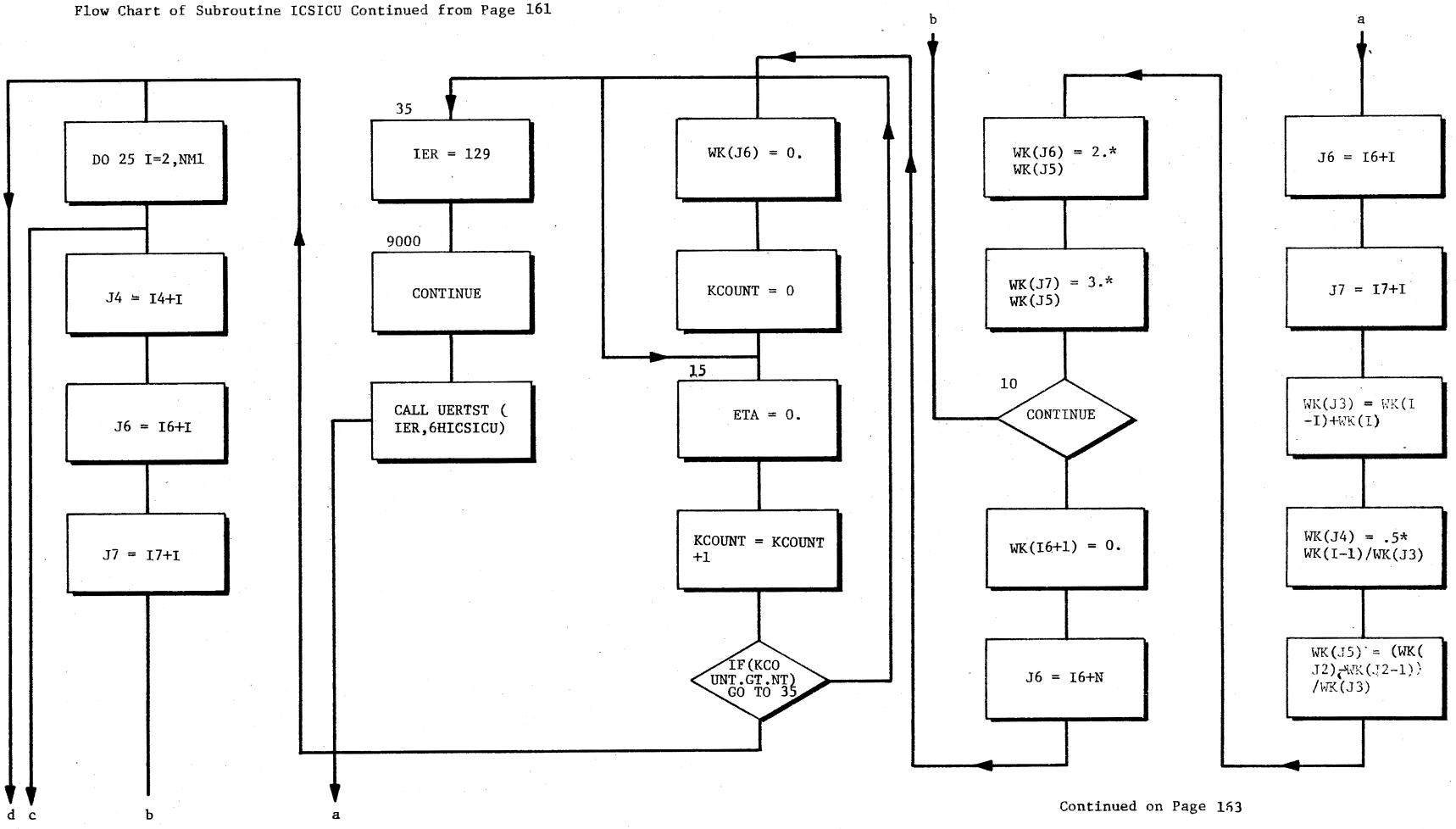

Continued on Page 163

Flow Chart of Subroutine ICSICU Continued from Page 162

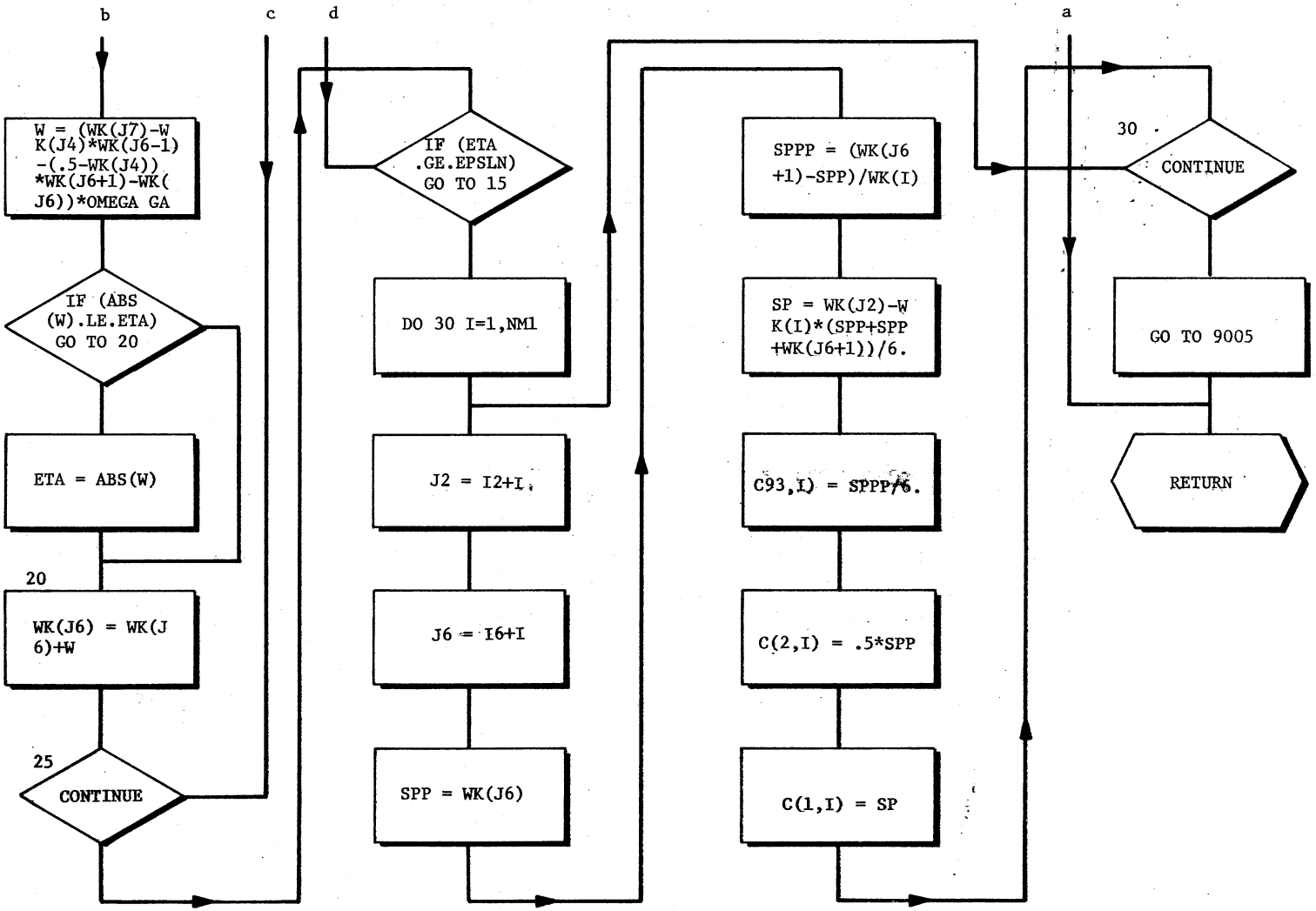

Flow Chart of Subroutine ICSICU Concluded

Flow Chart for Subroutine UERTST
This subroutine is a functional subroutine for ICSICU.

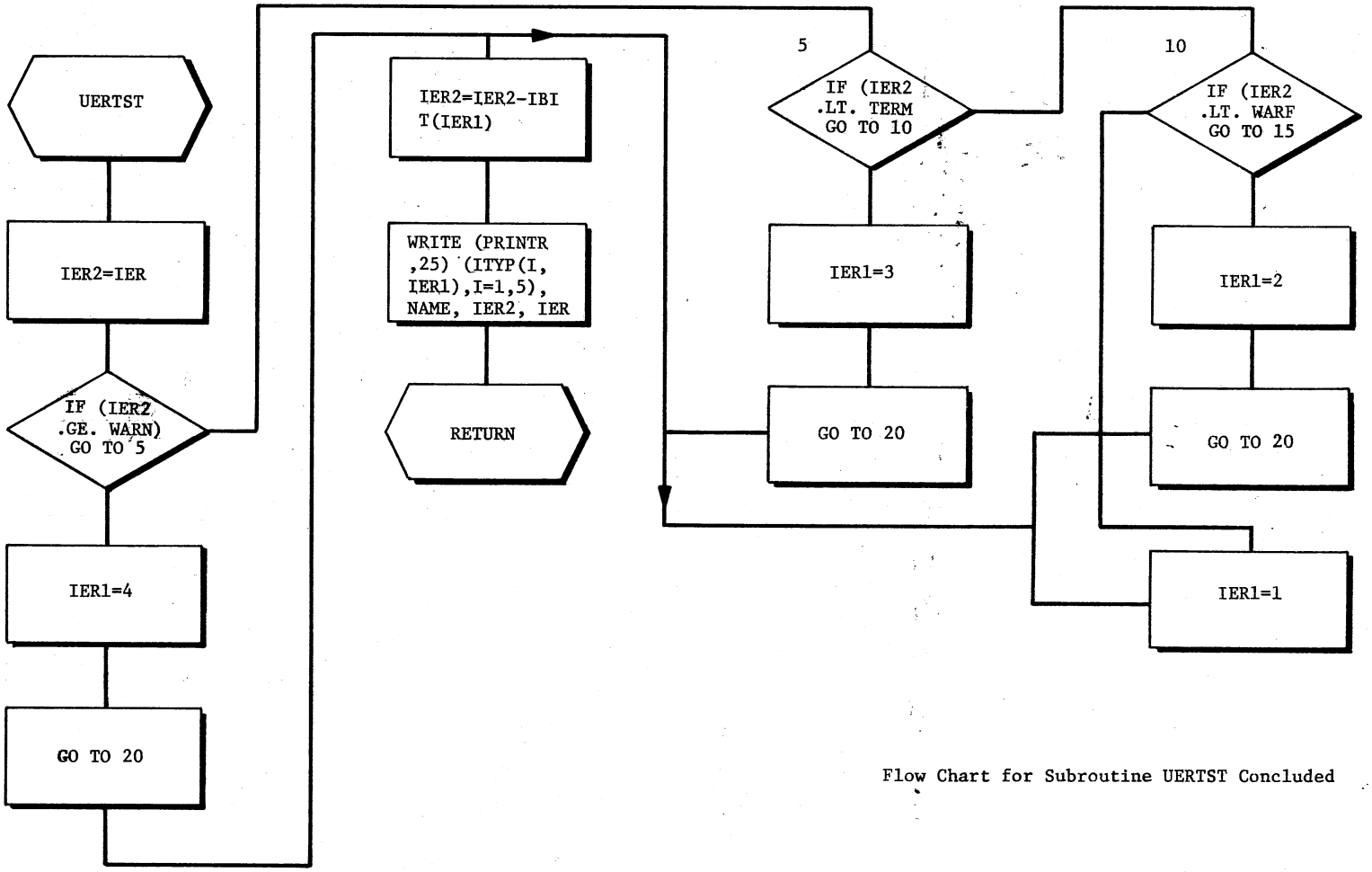

Flow Chart for Subroutine UERTST Concluded

Listing of Program SFTN

```
1     C------
1     C              PROGRAM SFTN-STABILILIZED FORMATION TEMPERATURE
1     C------
1     C     ++++++++++++++++++++++++++++++++++++++++++++++++++++++++++++++++
1     C     +                                                              +
1     C     +       IDG         INTEGER INDICATOR(1-WATER BASE ,0-OIL BASE MUD+
1     C     +                                                              +
1     C     +       NOM         INTEGER INDICATOR(0-SAND,1-SHALE,2-LIMESTONE) +
1     C     +                                                              +
1     C     +       TS          STABILIZED FORMATION TEMPERATURE            +
1     C     +       CM          SPECIFIC HEAT OF MUD                        +
1     C     +                                                              +
1     C     +       DM          DENSITY OF MUD                              +
1     C     +       THERMAL CONDUCTIVITY OF FORMATION                       +
1     C     +                                                              +
1     C     +       POR         POROSITY                                    +
1     C     +                                                              +
1     C     ++++++++++++++++++++++++++++++++++++++++++++++++++++++++++++++++
1     C
1     C
1           DIMENSION TS(20,20)
2           READ(5,2) BB,POR,DM,NOM,IDG
3         2 FORMAT(3F10.6,2I2)
4           TT=1.0
5           T1=60.0
6           TDEL=1.0
7           TS(1,1)=62.0
8           DO 17 KK=1,20
9           TDEL=TDEL+KK
10          DO 11 NN=1,20
11          TT=TT+NN
12          T1=T1+(10.0*NN)
13          DTT=TT-1.0
14          D1=TS(KK,NN)-T1
15          CALL MUD(DM,IDG,CM)
16          PM=((DM*62.5)/8.33)*((BB/24.0)**2)*3.1415
17          Q=(PM*CM*D1)/DTT
18    C
18          CALL COND(POR,T1,NOM,C)
19    C
19          CALL UNSTE(KK,NN,Q,C,TDEL,TT,TS)
20       11 CONTINUE
21          WRITE(6,51) TDEL,TT,(TS(KK,NN),NN=1,20)
22       51 FORMAT(3F10.6)
23       17 CONTINUE
24          STOP
25          END
```

Listing of Program SFTN Concluded

Flow Chart for Program SFTN
This program calculates stabilized formation temperature.

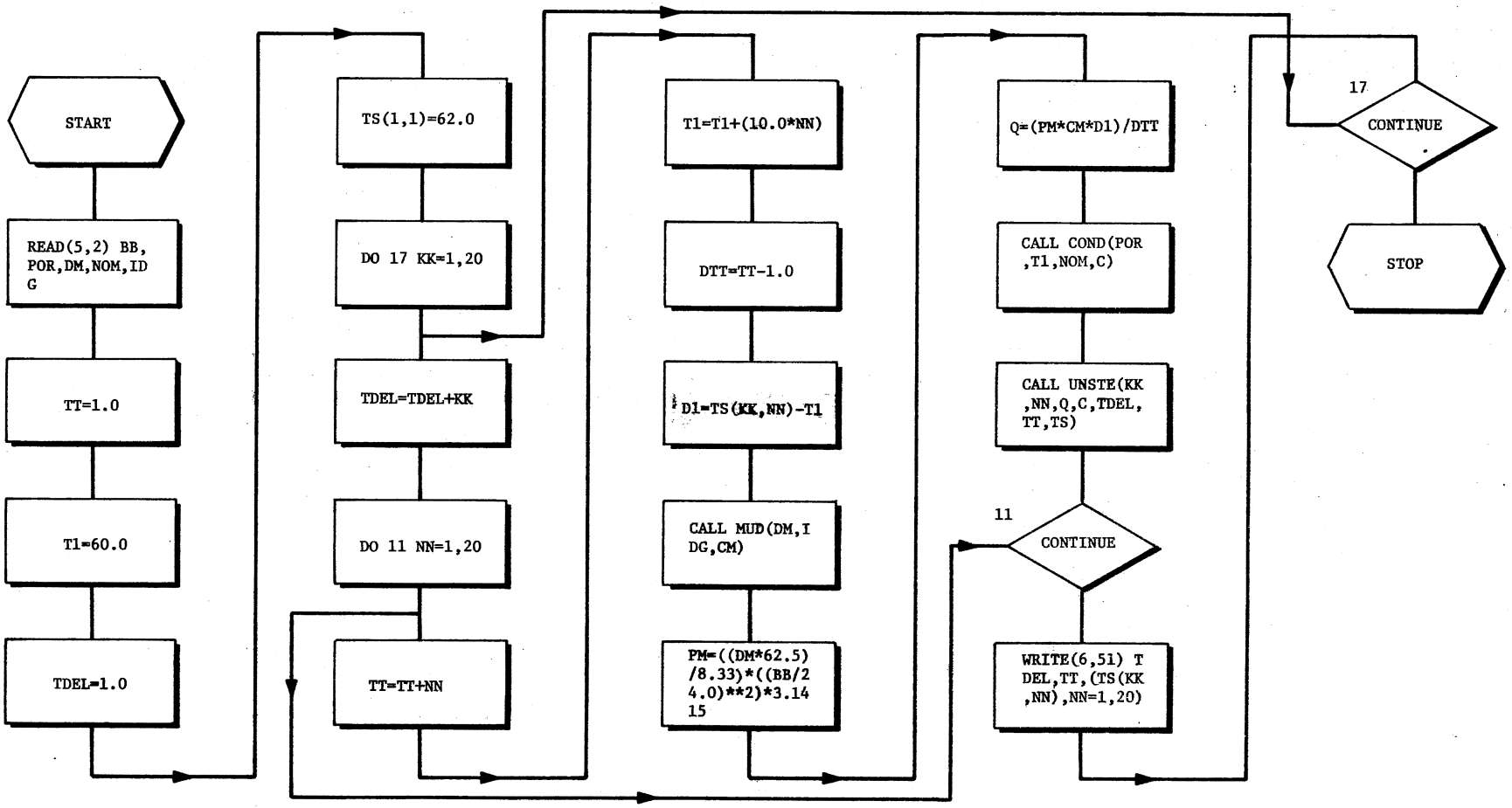

Flow Chart for Program SFTN Condluded

Listing for Subroutines UNSTE, MUD and COND

```
      SUBROUTINE UNSTE(KK,NN,Q,C,T1,TDEL,TT,TS)
      DIMENSION TS(20,20)
      AS=Q/(12.566*C)
      AB=ALOG((TT+TDEL)/(TDEL))
      TS(KK,NN)=T1+(AB*AS)
      RETURN
      END

      SUBROUTINE COND(POR,T1,NOM,C)
       POR=POR*100.
      IF (NOM) 11,31,41
C     THERMAL CONDUCTIVITY OF SHALE
   11 PK=1.0+(70.5-POR)/83.3
      RATIO=-0.5116E-03*T1+0.132E 01-0.312E C3/T1+0.948/T1**2-0.112E 08/
     AT1**3+0.461E 09/T1**4
       C=PK*RATIO
        RETURN
C      THERMAL CONDUCTIVITY OF SAND
   31 PK=1.+(42.5-POR)/40.0
      RATIO=0.119E-02*T1-0.121E 01+0.895E 03/T1-0.149E 06/T1**2+0.111E 0
     A8/T1**3-0.3035E 09/T1**4
       C=PK*RATIO
       RETURN
C       THERMAL CONDUCTIVITY OF LIME STONE
   41 PK=1.+(67.5-POR)/44.7
      RATIO=-0.483E-03*T1+0.138E 01-0.386E 03/T1+0.104E 06/T1**2-0.111E
     A08/T1**3+0.414E 09/T1**4
       C=PK*RATIO
        RETURN
      END

       SUBROUTINE MUD(DM,IDG,CM)
       IF(IDG.EQ.1) GO TO 81
      IF(IDG.EQ.0) GO TO 91
C      IDG IS SPECIFIED AS ONE FOR  WATER BASE MUD
C     IDG EQUAL TO ZERO  IS SPECIFIED FOR OIL BASE DRILLING  MUD.
   81  CM=-0.0746*(DM-9.0)+0.964
       RETURN
   91 CM=-0.045*(DM-8.0)+0.641
       RETURN
      END
```

Listing for Subroutines UNSTE, MUD and COND
Concluded

Flow Chart for Subroutines UNSTE, MUD and COND.
These surbroutines calculate stabilized temperature, specific heat of drilling fluid and thermal conductivity of rocks respectively.

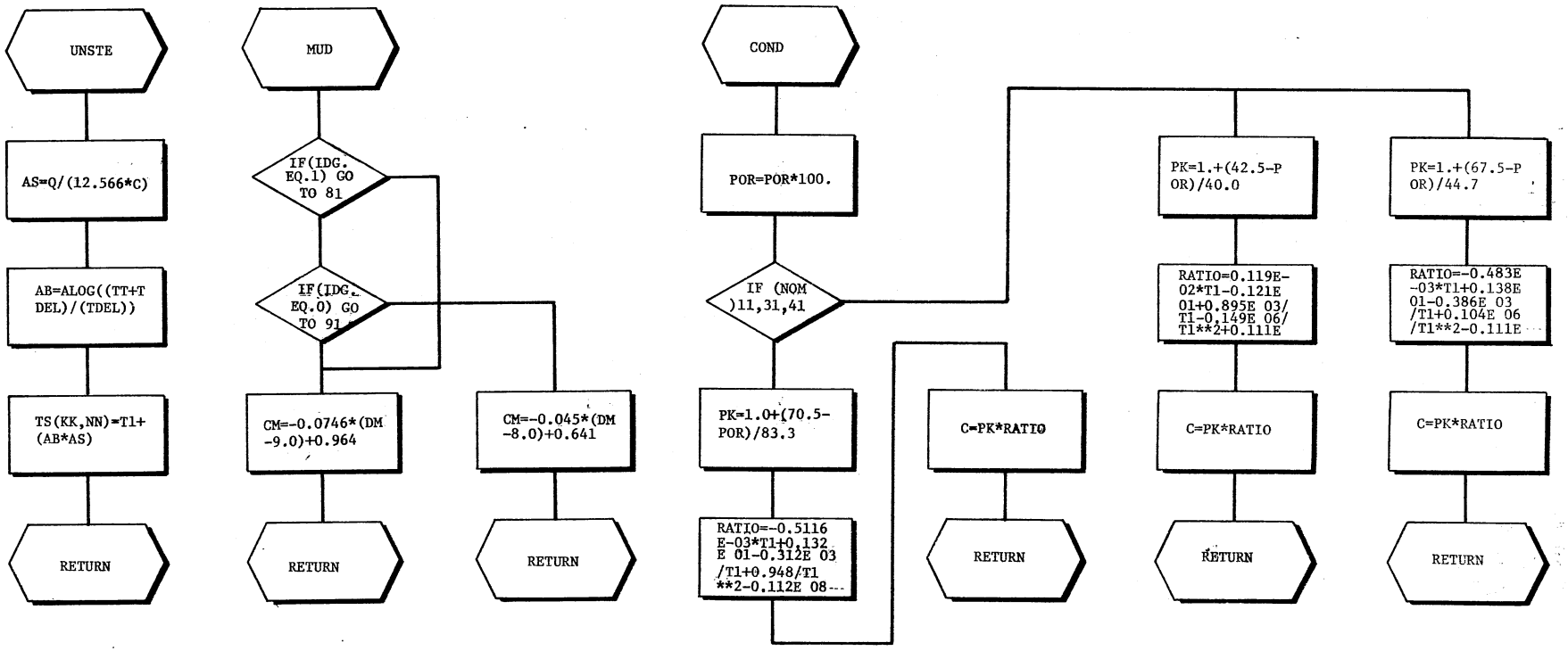

Flow Chart for Subroutines UNSTE, MUD, and COND Concluded

APPENDIX B

COMPUTED RESULTS

TABLE V

SEQUENTIAL DESCRIPTION OF THERMAL CONDUCTIVITY CALCULATIONS

Step #	Function of the Step	Description of the Step	Computer Symbol	Units	Program Used
1	Specify Interval	Well Bore Depth	DEP(M)	FT	MAIN
2	Specify Temperature	Buildup Temperature, at Times 1,2,3,...	T(M,N)	^{o}F	MAIN
3	Specify Time Interval	Buildup Times 1,2,3,...	TT(N)	HRS	MAIN
4	Specify Circulation Time	Drawdown Time	DELK	HRS	MAIN
5	Specify Mud Parameters	Specific Heat Density	RHO CM	LBS/FT^3 BTU/#	MAIN MAIN
6	Specify Well Bore Parameters	Radius of Well Bore	RW(M)	FT	MAIN
7	Calculate Time Ratio	Circulation Time Divided by Circulation Plus Buildup Time	RP(K)	--	MAIN
8	Calculate	Log of Log of Circulation Time Ratio	P(K)	--	MAIN

TABLE V (Continued)

Step #	Function of the Step	Description of the Step	Computer Symbol	Units	Program Used
9	Smooth	Least Squares Fit of PK(K) and TT(N)	X(K) Y(K)	-- ^{o}F	CURVFT
10	Calculate	Slope	SLP(M)	--	THECON
11	Calculate	Rate of Heat Flow for Times 1,-6	HEAT(N)	BTU/HR	THECON
12	Calculate	Average Rate of Heat Flow	ARATE(M)	BTU/HR	THECON
13	Calculate	Thermal Conductivity	TK(M)	BTU/HR-FT^{o}F	THECON

TABLE VI

COMPUTED RESULTS I

Well Bore Depth Ft.	Experimental and Interpolated Thermal Conductivity Btu/Hr-Ft-^{o}F	Calculated Conductivity Btu/Hr-Ft-^{o}F	Percentage Error
5000.0	0.9811	1.0994	-12.05
5002.0	0.9811	1.0854	-10.63
5004.0	0.9811	1.0647	- 8.52
5006.0	0.9811	1.0417	- 6.17
5008.0	0.9811	1.0949	- 2.42
5010.0	0.9811	1.0011	- 2.03
5012.0	0.9914	0.9805	1.11
5014.0	0.9924	0.9346	5.83
5016.0	1.0121	0.9504	6.10
5018.0	1.0121	0.9265	8.46
5020.0	1.0121	0.9200	9.10
5022.0	0.9932	0.9208	7.29
5024.0	0.9932	0.9382	5.54
5026.0	0.9932	0.9580	3.54
5028.0	0.9932	0.9613	3.21
5030.0	0.9932	0.9738	1.95
5032.0	0.9932	0.9923	0.10
5034.0	0.9932	1.0198	- 2.68
5036.0	0.9932	1.0157	- 2.27
5038.0	0.9934	1.0205	- 2.73
5040.0	0.9935	1.0446	- 5.14

TABLE VI (Continued)

Well Bore Depth Ft.	Experimental and Interpolated Thermal Conductivity Btu/Hr-Ft-^{o}F	Calculated Conductivity Btu/Hr-Ft-^{o}F	Percentage Error
5042.0	0.9934	1.0344	- 4.13
5044.0	0.9934	1.0579	- 6.49
5046.0	0.9934	1.0608	- 6.78
5048.0	0.9934	1.0195	- 2.63
5050.0	0.9941	1.0005	- 0.64
5052.0	0.9932	1.0168	- 2.38
5054.0	0.9932	1.0116	- 1.85
5056.0	0.9933	1.0125	- 1.93
5058.0	0.9932	1.0257	- 3.27
5060.0	0.9934	1.0374	- 4.43
5062.0	0.9936	1.0068	- 1.33
5064.0	0.9944	1.0046	- 1.03
5066.0	0.9946	1.0154	- 2.09
5068.0	0.9966	1.0224	- 2.58
5070.0	0.9986	1.0253	- 2.67
5072.0	1.0432	1.0309	1.18
5074.0	1.0532	1.0279	2.40
5076.0	1.0632	1.0241	3.67
5078.0	1.0731	1.0222	4.74
5080.0	1.0773	1.0031	6.89
5082.0	1.0774	0.9973	7.43
5084.0	1.0773	0.9941	7.72
5086.0	1.0773	0.9648	10.45

TABLE VI (Continued)

Well Bore Depth Ft.	Experimental and Interpolated Thermal Conductivity Btu/Hr-Ft-^{o}F	Calculated Conductivity Btu/Hr-Ft-^{o}F	Percentage Error
5088.0	1.0774	0.9706	9.92
5090.0	1.0774	0.9683	10.12
5092.0	1.0776	1.0040	6.83
5094.0	1.0776	1.0328	4.15
5096.0	1.0776	1.0094	6.33
5098.0	1.0775	1.0171	5.60
5100.0	1.0776	1.0241	4.96
5102.0	1.0778	1.0214	5.24
5104.0	1.0779	1.0107	6.23
5106.0	1.0776	0.9774	9.29
5108.0	1.0778	0.9543	11.46
5110.0	1.0779	0.9450	12.33
5112.0	1.0779	0.9258	14.11
5114.0	1.0732	0.9103	15.18
5116.0	1.0713	0.8742	18.40
5118.0	1.0211	0.8542	16.34
5120.0	1.0200	0.8234	19.27
5122.0	1.0111	0.8317	17.74
5124.0	1.0000	0.8283	17.17
5126.0	2.1132	1.4515	31.31
5128.0	2.1132	1.4430	31.72
5130.0	2.1130	1.4421	31.75
5132.0	2.1140	1.4445	31.67

TABLE VI (Continued)

Well Bore Depth Ft.	Experimental and Interpolated Thermal Conductivity Btu/Hr-Ft-^{o}F	Calculated Conductivity Btu/Hr-Ft-^{o}F	Percentage Error
5134.0	2.1160	1.4382	32.03
5136.0	2.1130	1.7247	18.38
5138.0	2.1140	1.7247	18.42
5140.0	2.1110	1.7247	18.30
5142.0	0.9998	1.0793	- 7.95
5144.0	0.9914	1.0474	- 5.65
5146.0	0.9918	1.0359	- 4.44
5148.0	0.9913	1.0446	- 5.38
5150.0	0.9914	1.0652	- 7.45
5152.0	0.9916	1.0336	- 4.24
5154.0	0.9918	1.0669	- 7.57
5156.0	0.9928	1.0736	- 8.14
5158.0	0.9931	1.0559	- 6.32
5160.0	0.9941	1.0799	- 8.63
5162.0	0.9961	1.1095	-11.38
5164.0	0.9862	1.1298	-14.57
5166.0	0.9913	1.1432	-15.32
5168.0	0.9914	1.1288	-13.86
5170.0	0.9814	1.1292	-15.06
5172.0	0.9916	1.0905	- 9.97
5174.0	1.1832	1.0848	8.31
5176.0	1.1632	1.0820	6.98
5178.0	111632	1.0986	5.55

TABLE VI (Continued)

Well Bore Depth Ft.	Experimental and Interpolated Thermal Conductivity Btu/Hr-Ft-°F	Calculated Conductivity Btu/Hr-Ft-°F	Percentage Error
5180.0	1.1632	1.0936	5.99
5182.0	1.1632	1.0677	8.21
5184.0	1.1120	1.0267	7.67
5186.0	1.1130	0.9747	12.43
5188.0	1.1140	0.9617	13.67
5190.0	1.1120	0.9426	15.23
5192.0	1.1130	0.9397	15.57
5194.0	0.9123	0.9200	- 0.84
5196.0	0.9123	0.9020	1.13
5198.0	0.9123	0.8865	2.83
5200.0	0.9123	0.8854	2.95
5202.0	0.9123	0.8686	4.79
5204.0	0.9123	0.8681	4.85
5206.0	0.9123	0.8684	4.81
5208.0	0.9123	0.8529	6.51
5210.0	0.9123	0.8417	7.74
5212.0	0.9123	0.8130	10.89
5214.0	1.0420	0.8094	22.33
5216.0	1.0430	0.7963	23.65
5218.0	0.9123	0.8144	10.74
5220.0	0.9123	0.8704	4.59
5222.0	0.9123	0.9163	- 0.43
5224.0	0.9123	0.9288	- 1.80

TABLE VI (Continued)

Well Bore Depth Ft.	Experimental and Interpolated Thermal Conductivity Btu/Hr-Ft-^{o}F	Calculated Conductivity Btu/Hr-Ft-^{o}F	Percentage Error
5226.0	0.9123	0.9524	- 4.39
5228.0	0.9123	0.9600	- 5.22
5230.0	0.9123	0.9098	0.27
5232.0	0.9123	0.8855	2.94
5234.0	0.9123	0.8799	3.55
5236.0	0.9123	0.8869	2.78
5240.0	0.9123	0.9532	- 4.48
5242.0	0.9123	1.0566	-15.81
5244.0	0.9123	1.0244	-12.28
5246.0	0.9123	1.0949	-20.01
5248.0	0.9123	1.0949	-20.01
5250.0	0.9123	1.0949	-20.01

TABLE VII

SEQUENTIAL DESCRIPTION OF THERMAL DIFFUSIVITY CALCULATIONS

Step #	Function of the Step	Description of the Step	Computer Symbol	Units	Program Used
1	Specify Temperatures	Buildup Temperatures at Times, 1,2,3,...	T(M,N)	^{o}F	MAIN
2	Specify Time Interval	Buildup Times 1,2,3,...	TT(N)	HRS	MAIN
3	Specify Interval	Well Bore Depth	DEP(M)	FT	MAIN
4	Specify Well Bore Parameter	Radius of Well Bore	RW(M)	FT	MAIN
5	Smooth	Temperature vs Time	X(L) Y(L)	HRS ^{o}F	CURVFT
6	Calculate	Rate of Heat Flow	DEAT(M)	BTU/HR	THECON
7	Smooth	Rate of Heat Flow	X(N) Y(N)	BTU/HR HRS	CURVFT CURVFT
8	Specify	Time	X1	HRS	CIFF

TABLE VII (Continued)

Step #	Function of the Step	Description of the Step	Computer Symbol	Units	Program Used
9	Calculate	Value of E_t Function at Time - X_1	DR(M)	--	CIFF
10	Calculate	Value of E_t Function at Time - X_2	DS(M)	--	CIFF
11	Calculate	Temperature Ratio	B(M)	--	CIFF
12	Calculate	Rate of Heat Flow at Times X_1 and X_2	CB DB	BTU/HR	CIFF
13	Establish	Convergence Criteria	AD(M)	--	CIFF
14	Calculate	Thermal Diffusivity	CIF(M)	$FT^2/^oF$	CIFF

TABLE VIII

COMPUTED RESULTS II

Well Bore Depth Ft.	Experimental and Interpolated Thermal Diffusivity $Ft^2/^oF$	Calculated Thermal Diffusivity $Ft^2/^oF$	Percentage Error	Porosity Derived Thermal Conductivuty Btu/Hr-Ft-^oF		
				Thermal Conductivity as 100% Shale	Thermal Conductivity as 100% Sand	Thermal Conductivity as 100% Limestone
5000.0	0.0295	0.0330	10.69	0.960	1.104	2.075
5002.0	0.0290	0.0330	12.13	0.960	1.104	2.075
5004.0	0.0292	0.0330	11.55	0.960	1.104	2.075
5006.0	0.0295	0.0330	10.69	0.960	1.104	2.075
5008.0	0.2093	0.0330	11.27	0.936	1.075	2.007
5010.0	0.0295	0.0330	10.69	0.891	1.020	1.878
5012.0	0.0300	0.0331	9.26	0.891	1.020	1.878
5014.0	0.0295	0.0330	10.69	0.936	1.076	2.007
5016.0	0.0375	0.0335	-11.98	0.960	1.104	2.075
5018.0	0.0375	0.0335	-11.98	0.936	1.076	2.007
5020.0	0.0375	0.0335	-11.98	0.936	1.076	2.007
5022.0	0.0297	0.0330	10.12	0.913	1.048	1.941
5024.0	0.0297	0.0330	10.12	0.936	1.076	2.007
5026.0	0.0297	0.0330	10.12	0.936	1.076	2.007
5028.0	0.0297	0.0330	10.12	0.936	1.076	2.007
5030.0	0.0298	0.0330	9.83	0.936	1.076	2.007
5032.0	0.0297	0.0330	10.12	0.960	1.104	2.075
5034.0	0.0297	0.0330	10.12	0.960	1.104	2.075
5036.0	0.0298	0.0330	9.83	0.960	1.104	2.075
5038.0	0.0299	0.0331	9.54	0.960	1.104	2.075
5040.0	0.0298	0.0330	9.83	0.936	1.076	2.007
5042.0	0.0298	0.0330	9.83	0.936	1.076	2.007

TABLE VIII (Continued)

Well Bore Depth Ft.	Experimental and Interpolated Thermal Diffusivity $Ft^2/^oF$	Calculated Thermal Diffusivity $Ft^2/^oF$	Percentage Error	Porosity Derived Thermal Conductivity Btu/Hr-Ft-^oF		
				Thermal Conductivity as 100% Shale	Thermal Conductivity as 100% Sand	Thermal Conductivity as 100% Limestone
5044.0	0.0298	0.0330	9.83	0.936	1.076	2.007
5046.0	0.0298	0.0330	9.83	0.984	1.134	2.145
5048.0	0.0298	0.0330	9.83	0.960	1.104	2.075
5050.0	0.0296	0.0330	10.40	0.807	0.918	1.644
5052.0	0.0300	0.0331	9.26	0.768	0.871	1.538
5054.0	0.0305	0.0331	7.82	0.891	1.020	1.878
5056.0	0.0310	0.0331	6.39	0.936	1.076	2.007
5058.0	0.0315	0.0494	36.27	0.807	0.918	1.644
5060.0	0.0315	0.0494	36.27	0.936	1.076	2.007
5062.0	0.0315	0.0494	36.27	0.936	1.076	2.007
5064.0	0.0315	0.0494	36.27	0.807	0.918	1.644
5066.0	0.0315	0.0494	36.27	0.891	1.020	1.878
5068.0	0.0315	0.0494	36.27	0.936	1.076	2.007
5070.0	0.0315	0.0494	36.27	0.891	1.020	1.878
5072.0	0.0435	0.0504	13.77	0.891	1.020	1.878
5074.0	0.0435	0.504	13.77	1.034	1.195	2.293
5076.0	0.0435	0.504	13.77	1.087	1.260	2.451
5078.0	0.0435	0.0504	13.77	0.936	1.076	2.007
5080.0	0.0435	0.0504	13.77	0.984	1.134	2.145
5082.0	0.0435	0.0504	13.77	0.936	1.076	2.007
5084.0	0.0435	0.0504	13.77	0.936	1.076	2.007
5086.0	0.0435	0.0504	13.77	0.936	1.076	2.007
5088.0	0.0435	0.0504	13.77	0.891	1.020	1.878

TABLE VIII (Continued)

Well Bore Depth Ft.	Experimental and Interpolated Thermal Diffusivity $Ft^2/^oF$	Calculated Thermal Diffusivity $Ft^2/^oF$	Percentage Error	Porosity Derived Thermal Conductivity Btu/Hr-Ft-^oF		
				Thermal Conductivity as 100% Shale	Thermal Conductivity as 100% Sand	Thermal Conductivity as 100% Limestone
5090.0	0.0435	0.0504	13.77	0.936	1.076	2.007
5092.0	0.0435	0.0504	13.77	0.827	0.943	1.699
5094.0	0.0435	0.0504	13.77	0.848	0.968	1.757
5096.0	0.0435	0.0504	13.77	0.848	0.968	1.757
5098.0	0.0435	0.0504	13.77	0.936	1.076	2.007
5100.0	0.0435	0.0504	13.77	0.936	1.076	2.007
5102.0	0.0435	0.0504	13.77	0.960	1.104	2.075
5104.0	0.0435	0.0504	13.77	0.891	1.020	1.878
5106.0	0.0435	0.0504	13.77	0.891	1.020	1.878
5108.0	0.0430	0.0504	14.69	0.749	0.848	1.488
5110.0	0.0430	0.0504	14.69	0.768	0.871	1.538
5112.0	0.0431	0.0504	14.51	0.891	1.020	1.878
5114.0	0.0431	0.0504	14.51	0.891	1.020	1.878
5116.0	0.0431	0.0504	14.51	0.827	0.943	1.699
5118.0	0.0431	0.0504	14.51	0.891	1.020	1.878
5120.0	0.0431	0.0504	14.51	0.936	1.076	2.007
5122.0	0.0431	0.0504	14.51	1.034	1.195	2.293
5124.0	0.0431	0.0504	14.51	0.984	1.134	2.145
5126.0	0.0431	0.0504	14.51	0.891	1.020	1.878
5128.0	0.0380	0.0500	23.97	0.848	0.968	1.757
5130.0	0.0360	0.0498	27.73	0.730	0.826	1.439
5132.0	0.0340	0.0496	31.51	0.730	0.826	1.439
5134.0	0.0305	0.0493	38.19	0.730	0.826	1.439

TABLE VIII (Continued)

Well Bore Depth Ft.	Experimental and Interpolated Thermal Diffusivity $Ft^2/^oF$	Calculated Thermal Diffusivity $Ft^2/^oF$	Percentage Error	Porosity Derived Thermal Conductivity Btu/Hr-Ft-^oF		
				Thermal Conductivity as 100% Shale	Thermal Conductivity as 100% Sand	Thermal Conductivity as 100% Limestone
5136.0	0.0305	0.0493	38.19	0.730	0.826	1.439
5138.0	0.0305	0.0493	38.19	0.730	0.826	1.439
5140.0	0.0305	0.0493	38.19	0.695	0.784	1.346
5142.0	0.0305	0.0493	38.19	0.695	0.784	1.346
5144.0	0.0305	0.0493	38.19	0.848	0.968	1.757
5146.0	0.0305	0.0493	38.19	0.848	0.968	1.757
5148.0	0.0305	0.0493	38.19	0.730	0.826	1.439
5150.0	0.0315	0.0494	36.27	0.730	0.826	1.439
5152.0	0.0340	0.0496	31.51	0.807	0.918	1.644
5154.0	0.0360	0.0498	27.73	0.807	0.918	1.644
5156.0	0.0370	0.0499	25.84	0.730	0.826	1.439
5158.0	0.0380	0.0500	23.97	0.936	1.076	2.007
5160.0	0.0390	0.0501	22.10	0.936	1.076	2.007
5162.0	0.0410	0.0591	30.63	0.768	0.871	1.538
5164.0	0.0421	0.0592	28.90	1.034	1.195	2.293
5166.0	0.0460	0.0596	22.82	0.695	0.784	1.346
5168.0	0.0480	0.0598	19.73	0.730	0.826	1.439
5170.0	0.0480	0.0598	19.73	0.730	0.826	1.439
5172.0	0.0500	0.0600	16.67	0.730	0.826	1.439
5174.0	0.0510	0.0601	15.14	0.661	0.744	1.259
5176.0	0.0515	0.0601	14.38	0.661	0.744	1.259
5178.0	0.0520	0.0602	13.62	0.768	0.871	1.538
5180.0	0.0520	0.0602	13.62	0.848	0.968	1.757

TABLE VIII (Continued)

Well Bore Depth Ft.	Experimental and Interpolated Thermal Diffusivity $Ft^2/^oF$	Calculated Thermal Diffusivity $Ft^2/^oF$	Percentage Error	Porosity Derived Thermal Conductivity Btu/Hr-Ft-^oF		
				Thermal Conductivity as 100% Shale	Thermal Conductivity as 100% Sand	Thermal Conductivity as 100% Limestone
5182.0	0.0520	0.0602	13.62	0.768	0.871	1.538
5184.0	0.0520	0.0602	13.62	0.848	0.968	1.757
5186.0	0.0520	0.0602	13.62	0.768	0.871	1.538
5188.0	0.0520	0.0602	13.62	0.807	0.918	1.644
5190.0	0.0520	0.0602	13.62	0.827	0.943	1.699
5192.0	0.0510	0.0601	15.14	0.936	1.076	2.007
5194.0	0.0510	0.0601	15.14	0.984	1.134	2.145
5196.0	0.0500	0.0600	16.67	0.891	1.020	1.878
5198.0	0.0510	0.0601	15.14	0.827	0.943	1.699
5200.0	0.0500	0.0600	16.67	0.848	0.968	1.757
5202.0	0.0490	0.0599	18.20	0.807	0.918	1.644
5204.0	0.0495	0.0599	17.43	0.848	0.868	1.757
5206.0	0.0490	0.0599	18.20	0.848	0.968	1.757
5208.0	0.0495	010599	17.43	0.807	0.918	1.644
5210.0	0.0495	0.0599	17.43	0.768	0.871	1.538
5212.0	0.0492	0.0599	17.89	0.730	0.826	1.439
5214.0	0.0492	0.0599	17.89	0.768	0.871	1.538
5216.0	0.0490	0.0599	18.20	0.891	1.020	1.878
5218.0	0.0490	0.0599	18.20	1.087	1.260	2.451
5220.0	0.0490	0.0599	18.20	0.936	1.076	2.007
5222.0	0.0490	0.0599	18.20	0.848	0.968	1.757
5224.0	0.0490	0.0599	18.20	0.730	0.826	1.439
5226.0	0.0490	0.0599	18.20	0.848	0.968	1.757

TABLE VIII (Continued)

Well Bore Depth Ft.	Experimental and Interpolated Thermal Diffusivity $Ft^2/^oF$	Calculated Thermal Diffusivity $Ft^2/^oF$	Percentage Error	Porosity Derived Thermal Conductivity Btu/Hr-Ft-^oF		
				Thermal Conductivity as 100% Shale	Thermal Conductivity as 100% Sand	Thermal Conductivity as 100% Limestone
5228.0	0.0490	0.0599	18.20	0.807	0.918	1.644
5230.0	0.0490	0.0599	18.20	0.807	0.918	1.644
5232.0	0.0490	0.0599	18.20	0.848	0.968	1.757
5234.0	0.0490	0.0599	18.20	0.730	0.826	1.439
5236.0	0.0490	0.0599	18.20	0.807	0.918	1.644
5238.0	0.0490	0.0599	18.20	0.629	0.705	1.178
5240.0	0.0490	0.0599	18.20	0.730	0.826	1.439
5242.0	0.0490	0.0599	18.20	0.807	0.918	1.644
5244.0	0.0490	0.0599	18.20	0.807	0.918	1.644
5246.0	0.0500	0.0600	16.67	0.984	1.134	2.145
5248.0	0.0500	0.0600	16.67	0.960	1.104	2.075
5250.0	0.0500	0.0600	16.67	0.960	1.104	2.075

VITA

Ata-ur-Rehman Choudhary

Candidate for the Degree of

Doctor of Philosophy

Thesis: AN APPROACH TO DETERMINE THE THERMAL CONDUCTIVITY AND DIFFUSIVITY OF A ROCK IN SITU

Major Field: Mechanical Engineering

Biographical:

Personal Data: Born at Rupar, Pakistan, January 20, 1941, the son of Mr. and Mrs. Choudhary Abdur-Rehman.

Education: Passed the high school examination from M.B. High School M.B.Din in 1958 with a first class in middle and high school examinations and topped the list of successful candidates. Joined University of Karachi in October, 1958, and earned Bachelor of Science and Master of Science degrees in Chemistry in 1962 and 1964 respectively in first division. Received certificate of honorable mention and merit in 1962 and certificate of honorable mention in 1964. Received a Master of Science degree in Petroleum Engineering from University of Texas at Austin in 1969 and completed requirements for the degree of Doctor of Philosophy from Oklahoma State University in December, 1976.

Professional Experience: Quality Control Supervisor for California Texas Oil Company refinery, 1964-1966; Research Assistant, Department of Petroleum Engineering, University of Texas at Austin, 1967-1969; Research Assistant, Department of Electrical Engineering and Mechanical Engineering, Oklahoma State University, 1970-1972; Designer, Midco Control Systems, Houston, Texas, 1972-1973; Mechanical Design Engineer, Riley Stoker Corporation, 1973-1975.